Departement für Pferde
der Vetsuisse-Fakultät Universität Zürich

Direktor: Prof. Dr. med. vet. Anton Fürst, Dipl. ECVS

Center for Applied Biotechnology and Molecular Medicine (CABMM)
and Musculoskeletal Research Unit

Leitung: Prof. Dr. med. vet. Brigitte von Rechenberg, Dipl. ECVS

Arbeit unter wissenschaftlicher Betreuung von PD Dr. med. dent. Stefan Stübinger

Reconstruction of bone defects through local drug delivery from a beta - tricalcium phosphate (β-TCP) bone graft substitute

Inaugural-Dissertation

zur Erlangung der Doktorwürde der
Vetsuisse-Fakultät Universität Zürich

vorgelegt von

Ramon Bucher

Tierarzt
von Escholzmatt-Marbach, Luzern

genehmigt auf Antrag von

PD Dr. med. dent. Stefan Stübinger, Referent

Prof. Dr. Vera Luginbühl, Korreferentin

2014

Departement für Pferde
der Vetsuisse-Fakultät Universität Zürich

Direktor: Prof. Dr. med. vet. Anton Fürst, Dipl. ECVS

Center for Applied Biotechnology and Molecular Medicine (CABMM)
and Musculoskeletal Research Unit

Leitung: Prof. Dr. med. vet. Brigitte von Rechenberg, Dipl. ECVS

Arbeit unter wissenschaftlicher Betreuung von PD Dr. med. dent. Stefan Stübinger

Reconstruction of bone defects through local drug delivery from a beta - tricalcium phosphate (β-TCP) bone graft substitute

Inaugural-Dissertation

zur Erlangung der Doktorwürde der
Vetsuisse-Fakultät Universität Zürich

vorgelegt von

Ramon Bucher

Tierarzt
von Escholzmatt-Marbach, Luzern

genehmigt auf Antrag von

PD Dr. med. dent. Stefan Stübinger, Referent

Prof. Dr. Vera Luginbühl, Korreferentin

2014

My mom and dad,

my godmother and her husband

Zusammenfassung

Die Kieferkammaugmentation mit autologem Knochen (AK) ist eine klinisch erfolgreiche Methode um lokale Kieferkammdefekte (KKD) zu behandeln. Als Ersatz von AK bieten sich derzeit verschiedene Knochenersatzmaterialen wie Verbunde aus β-Tricalciumphosphat mit einer abbaubaren Polymerbeschichtung an, in welche zur lokalen Freisetzung zusätzlich auch Wirkstoffe eingebracht werden können. Ziel dieser Studie war es zu zeigen, dass ein solches Biomaterial als Alternative zu AK in der Augmentation von lateralen KKD eingesetzt werden kann. Dieses wurde deshalb mit Montelukast, Simvastatin und Teriparatid modifiziert und in laterale KKD in 12 Minipigs eingebracht. In der postoperativen Phase, sowie nach 6 Wochen, konnte ein klinisch soweit unauffälliger Wundheilungsverlauf beobachtet werden, wobei sich jedoch auch leichte Entzündungszeichen mit teilweisem Verlust der Abdeckmembran bzw. des Augmentats offenbarten. Qualitative und quantitative histologische Auswertungen zeigten, dass die Beschichtung mit Teriparatid zu einer deutlichen Knochenneubildung führte. Es wurden jedoch keine statistisch signifikanten Unterschiede zwischen den drei modifizierten Beschichtungen beobachtet. Um den Erfolg der drei Modifikationen weitergehend beurteilen zu können sind zusätzliche Versuche mit einer höheren Fallzahl, unterschiedlichen Zeitpunkten und Konzentrationen notwendig. Postoperative Komplikationen könnten möglicherweise durch eine Verbesserung (Refinement) des Tiermodells reduziert werden.

Summary

Lateral or vertical augmentation by use of autologous bone (AB) is a clinically approved method to overcome local alveolar ridge defects. Currently, modification of biomaterials with growth factors or other osteoinductive substances to replace AB grafts is a major issue in dental research. β-tricalcium phosphates (β-TCP) with degradable polymer coatings, that release incorporated substances after implantation, are used as such osteoconductive scaffold and drug-releasing systems in research. The aim of this study was to show that a β-TCP composite may be used as an alternative to AB grafts in mandibular alveolar ridge defects. For this purpose, lateral alveolar crest defects in 12 minipigs were augmented using a β-TCP composite modified with one of three bioactive molecules (montelukast, simvastatin or teriparatide). Overall, the postoperative course proceeded without any major clinical problems, even though some postoperative complications like slight inflammatory reactions or membrane exposures with partial loss of biomaterial occurred. Qualitative and quantitative histological evaluations after 6 weeks revealed that coatings with teriparatide led to a pronounced new bone formation, yet there were no statistically significant differences between coatings. To validate these results, further refinement of the minipig model and testing a larger number of animals, additional timepoints and concentrations is necessary.

1 Introduction

Loss of bone volume in the lower jaw may compromise implant placement for dental rehabilitation of fully or partially edentulous patients. Inadequate volume of alveolar bone, the bone structure supporting the teeth, may result from physiological remodeling after tooth loss, or due to progressed periodontal disease or mechanical trauma[1-3]. Followed by biomechanical anergic state atrophy, the resulting shape of the alveolar ridge may either be compromised in width (horizontal/lateral), height (vertical) or both[4]. This inadequate volume together with a severely resorbed tapered or knife-edge morphology is regarded as contraindication to implant placement, due to increased concomitant soft tissue complications and/or a compromised long-term prognosis[5-7]. For this reason, it has become common practice to augment the deficient alveolar ridge prior to or during implant placement to increase implant stability and sustainability of the procedure. Several approaches have been advocated, which can be chiefly divided into mechanisms of autologous growth (A), biomaterials (B) or tissue engineering (C).

A. Autologous bone growth

Described techniques of using autologous growth to increase bone volume of the mandibular alveolar ridge include: autologous bone grafting by transplantation of bone blocks (onlay) or particulated bone from donor sites of the same patient[8-10]; ridge splitting by creating a vertical intrabony fissure and marginally expanding the cortices during implantation[11,12]; and distraction osteogenesis by gradual separation of bone fragments by traction, resulting in continuous new bone formation between fragments[13,14].

Autologous bone as a graft posesses excellent characteristics, as it is osteoinductive (contains bone-inducing substances), osteoconductive (serves as a scaffold), as well as osteogenic (contains bone-forming cells)[15,16]. Although it is still being considered the gold standard in grafting procedures, its drawbacks

may not be ignored: limited amount of substrate, additional donor site morbidity and increase in surgery time[8,17]. Recent reviews concluded that autologous bone could not demonstrate to promote better bone regeneration as compared with other grafting materials and thus may be inferior to biomaterials due to its exposition of the patient to a higher morbidity[15,18].

B. Biomaterials

Several biomaterials are being used in implant dentistry either as a replacement or as an adjunct to autologous bone in grafting procedures (see Table 1), or in new procedures such as guided bone regeneration (GBR).

Table 1: Current materials used as autologous bone replacements and engineered scaffolds in implant dentistry

	Advantages	Disadvantages
Allograft genetically non-identical donor of the same species (human)	limited osteoinduction due to radiation or other treatment[15] osteoconductive	risk of transmission of disease[19,20] not osteogenic (due to processing)
Xenograft from another species (eg. deproteinized bovine bone)	limited osteoinduction osteoconductive	not osteogenic (due to processing)
Synthetic	osteoconductive[16,21] producible in large quantities pre-shaped/injectable forms possible definable characteristics (eg. porosity)	not osteoinductive[21] not osteogenic large variance in established level of evidence between products[15]
β-tricalcium phosphates (β-TCP)	resorbable[16,22,23]	
Hydroxyapatite (HA)		very slow resorption[23,24] hard structure/brittle[16,24]
Biphasic phosphates (TCP + HA)	combination of both TCP and HA dis-/advantages dependent on HA/TCP ratio[21]	
copolymers, eg: poly(lactic acid) (PLA) poly(glycolic acid) (PGA) poly(lactic-co-glycolide) (PLGA)	resorbable (degradation rate depends on substrate and its composition)[25]	poor osteoconductivity[25] poor mechanical properties

GBR is a concept using barrier membranes to create a secluded space between bone and membrane. Competing soft tissue cells from the mucosa are thereby excluded from the defect healing process. Preference is given to osteoprogenitor cells originating from adjacent bone, which may regenerate the bone defect to a higher degree and volume[5]. Current barrier membranes are biocompatible, occlude cells, maintain space and are easy to use[26]. They may be from natural,

synthetic or other substrates and may either be resorbable or non-resorbable (see Table 2). To further foster three-dimensional bone reconstruction, the space between the barrier membrane and bone is often additionally augmented with biomaterials. Several reviews have strongly suggested the need for more evidence-based studies with regard to the outcome of GBR procedures[18,27]. In this regard especially the need and application of a barrier membrane is a highly controversial issue. One recent systematic review concluded, that although studies may show increased bone volume in comparison to procedures without membranes, there is not enough evidence to support the need of barrier membranes for long-term survival of implants[18]. Overall 1192 studies were initially included in this review, whereupon merely 7 studies finally fulfilled the inclusion criteria of at least 10 consecutively treated patients with a minimum follow-up of 12 months after the start of prosthetic loading.

Table 2: Principle substrates used for clinical or experimental barrier membranes[28]

	Resorbable	**Non-resorbable**
Natural	Collagen Chitosan Chitosan-collagen hybrid	
Synthetic	Alipathic polyesters (PLLA, PLGA, polydioxanone and their co-polymers)	e-PTFE High-density-PTFE
Others		Titanium mesh Titanium reinforced e-PTFE

Socket preservation is a technique to preserve the alveolar ridge after tooth loss, thereby preventing loss of volume due to physiological resorption. Several techniques have been described, including biomaterials as socket grafts or barrier membranes[26,29,30]. Although interventions are more successful in preserving the alveolar ridge dimensions than no treatment, some loss of vestibular bone volume cannot be prevented. Thus, their efficiency and benefit with regard to the final outcome is still under debate[31,32].

C. Tissue engineering

Tissue engineering is the process whereby cells, materials and/or tissue-inducing substances are engineered to regenerate tissues at a particular clinical treatment site[33]. If the chosen approach includes a cell component, stem cells, which are capable of self-renewal and may differentiate into different cell types, may be used[34]. The used material acts as a temporary scaffold providing a three-dimensional environment for both implanted as well as invading cells from the body. Ceramics, polymers (natural or synthetic) or their composites are used as scaffolds (see Table 1). Compounds of the extracellular matrix such as collagens, bone morphogenic proteins (BMPs), transforming growth factor beta (TGF-β) or chondroitin sulfate may be used as bone growth inducing substances[35,36]. Although these molecules have been comprehensively scrutinized in recent years, the signaling pathway upon which they act is not yet fully understood. And in case of BMPs, their safety as potent adjuncts to biomaterials has not been proven yet[37,38].

Although the techniques A - C are already being used successfully to solve the problem of missing bone volume and difficult morphology of the alveolar ridge, their performance in more challenging situations may still be improved. Out of the aforementioned biomaterials, beta-tricalcium phosphate (β-TCP) is a ceramic which is widely used in maxillofacial surgery due to its excellent resorptive and remodeling properties[39-42]. Hydroxyapatite (HA) in comparison is only very slowly resorbable and due to its brittleness is more delicate and challenging for augmentation followed by implant placement[16,22,24]. Biphasic tricalcium phosphates have been developed trying to combine the advantages of both β-TCP and HA in one compound to achieve adequate resorptive properties combined with long-term preservation of augmentation volume[21]. Finding the right substrate morphology to allow body fluid circulation as well as bone-cell colonization to promote osteogenesis has been the topic of many

research groups[22,41,43-45]. In regard to size, granules with sizes especially between 150 - 4000 µm are assessed in preclinical and clinical research[40,45,46]. The morphology of the substrate can be influenced by the sintering and manufacturing process. Porosity is the percentage of void space in the overall material and ranges between 36 % - 70 % depending the product and study[47]. Pore sizes of > 300 µm are recommended to enhance new bone and capillary formation[47]. Several techniques have been described to improve the in vivo performance of β-TCP such as its combination with stem cells to increase its osteogenic capacity[48,49], or with bone growth inducing substances, such as BMPs, TGF-β or platelet-rich plasma[50,51]. Another approach involves composites of polymers and ceramics, combining two materials with different mechanical and resorptive characteristics. The polymer fraction of such biomaterials may be liquefied and re-solidified in situ. Alternatively, it is possible to mold custom shapes based on imprints from the patient[52,53]. Depending on the properties of the polymer it is resorbable between 1 - 15 weeks which makes it a configurable drug delivery system with adaptable releasing properties[25,46,54]. A prolonged release of active substances may allow the graft to maintain its osseoinductive properties for days or weeks, thereby continuing to stimulate bone growth until its complete remodeling and replacement by bone.

Although there is strong evidence that potent growth factors such as BMPs have the ability to induce significant bone growth, their safety has not been proven yet[37,38]. Another approach to improve the performance of biomaterials may be to combine them with already clinically approved and licensed substances, such as the small-molecule drugs montelukast, simvastatin or teriparatide used in this study, which are approved for systemic use in humans and have shown to promote bone growth[55-57]. Unpublished data from an in vitro study could show that the aforementioned bioactive molecules can be incorporated into the PLGA-based polymer-coating of a β-TCP bone grafting

compound. It was further shown that the incorporated substances in the coating were released while incubated in phosphate buffered saline (pH 7.4, 37°C) over a 10 - 60 days period, with 56 - 82 % of active substances being released during that time frame depending the molecule and layering method. There are currently no contraindications described for their use in bone augmentation surgery.

Montelukast is a cysteinyl leukotriene receptor antagonist that is clinically used to improve symptoms and pulmonary function in chronic typical asthma and excercised-induced bronchoconstriction[58,59]. 5-lipoxygenase (5-LO) - a converter of arachidonic acid to leukotrienes in the inflammatory response - negatively regulates fracture healing as seen by the acceleration of fracture healing in 5-LO knockout mice[60]. A specific 5-LO inhibitor also accelerates and enhances fracture-healing in rats[61]. Although 5-LO not only synthesizes cysteinyl leukotrienes but also other leukotrienes, it can be hypothesized that a cysteinyl leukotriene inhibitor such as montelukast may also improve bone healing and growth. In a tibia-fracture model in the rat, montelukast could not improve fracture healing at 3- and 6-week intervals, although positive effects could be seen in the early phases of bone healing[55]. To the author's best knowledge, no clinical trials or studies in large animal models on montelukast and its impact on bone growth and healing have been described in literature up to now.

Simvastatin is an inhibitor of cholesterol synthesis but may increase bone formation by stimulating bone morphogenic protein 2 (BMP-2) gene expression in osteoblasts, inhibiting osteoblast apoptosis and suppressing osteoclastogenesis[62-64]. The bone growth enhancement abilities of the group of statins were first described in mice and rats by topical and oral application and have since then also been shown in numerous other animal models[56,62,63,65]. A large number of observational studies on simvastatin and its influence on fracture risk in older or postmenopausal women and randomized clinical trials

about its role in the treatment of osteoporosis and bone metabolism have been conducted with contradicting results[62].

Teriparatide is a biologically active fragment (amino acid sequence 1 - 34) of the human parathyroid hormone, the major regulator of calcium hemostasis in mammals. Its effect on bone depends on the exposition of the hormone, with systemic continuous exposure having a catabolic and intermittent exposure an anabolic effect on bone remodeling[66]. Studies have shown that teriparatide enhances bone quality in human trials of osteoporotic, postmenopausal women and men suffering from idiopathic osteoporosis[67-71]. In animal studies it has shown to increase bone density in osteopenic ovariectomized rats and in the calvarial defect model[72,73]. It has further shown to increase bone formation in mouse femoral defects and rat tibial fractures[57,74].

The development of a biomaterial that may positively modulate cell signaling, act as a scaffold and deliver substances for bone growth over a longer time period, may allow implant placement despite less than ideal anatomical or biological environments than currently indicated. It was therefore the aim of this study to show that a synthetic β-TCP coated with one of three polymer-based, prolonged drug-releasing systems (montelukast, simvastatin or teriparatide), may be used as an improved alternative to autologous bone grafts in augmentation of the alveolar ridge. The hypothesis of this study was that the biomaterial, used as a graft in a bilateral split-mouth lateral ridge defect model in the minipig, was expected to demonstrate a superior capability to restore bone volume in the atrophic alveolar ridge compared to unmodified PLGA coated β-TCP, autologous bone grafting (positive control) or no treatment (negative control).

2 Material and Methods

2.1 Animals

All experiments were conducted according to the Swiss regulations of animal welfare and the study was approved by the ethical committee and cantonal veterinary office of Zurich, Switzerland (animal experimental permission 177/2012).

Altogether twelve Yucatan miniature pigs (9 female and 3 neutered male) were included in this study. Age of animals was between 2 – 3 years and mean weight was 58.5 ± 7.9 kg at day of first stage surgery. An acclimatization period of at least 30 days per animal allowed adaption to the new husbandry and environment. Animals were clinically examined upon arrival and before surgeries to guarantee that only healthy animals were selected.

2.2 Study Design

To resemble the morphology of human patients disclosing an atrophic alveolar ridge, the premolars (P1) P2 - P4 were extracted in a first step. Additionally, the alveolar ridge was down-leveled by 2 - 3 mm to gain a narrow alveolar ridge. The extraction sockets were allowed to heal for two months. Then, in a split-mouth design, alveolar ridge augmentations of two pre-defined lateral crest defects (1 cm x 1 cm x 0.7 cm) per hemimandible (n=4 per animal) were randomly performed with either a poly(lactic-co-glycolide) (PLGA) coated β-TCP synthetic biomaterial modified with three different drug-releasing systems (montelukast, simvastatin or teriparatide) or the unmodified biomaterial, autologous bone or no augmentation/empty site as control groups (see 7.1 Group Distribution). All defects were covered with a biodegradable membrane (GUIDOR®, Bioresorbable matrix barrier, Sunstar Americas Inc., Chicago, IL, USA) and fixed with biodegradable co-polymer pins (Inion GTR™ Tack kit, Inion Oy, Tampere, Finland).

2.3 Biomaterials

A β-TCP substrate, with beads of 500 - 1000 μm mean diameter and overall porosity of 70%, was either coated with a PLGA (intrinsic viscosity of 32.0 - 44.0 cm^3/g) drug mixture (Montelukast-modified PLGA coated β-TCP, Simvastatin-modified PLGA coated β-TCP) or a layering technique of PLGA and a drug in an aqueous polyvinylpyrrolidone solution (Teriparatide-modified PLGA coated β-TCP). Beads were sterilized, filled in syringes. The syringes were packaged in alupeel bags and the packaged samples were gamma sterilized for use in surgery. In vitro studies showed that 75 - 88 % of embedded molecules could be retrieved after sterilization. Furthermore, unpublished in vitro release studies have shown a delayed release over a 10 - 60 day period with 56 - 82 % of active substances being released during that time frame depending on the group and layering method.

As a control, the same substrate but with an unmodified, pure PLGA polymer coating was used (unmodified PLGA coated β-TCP).

Based on the manufacturer's instructions, all biomaterials were declared stable at room temperature for shipment and application.

2.4 Surgical Procedure

2.4.1 Pre- and Perioperative Management

Animals were fasted 16 - 24 hours before surgery with water available ad libitum. After deep sedation in the stable (azaperone 1 - 2 mg/kg, Stresnil®, Biokema SA, Crissier, Switzerland; atropine 0.01 – 0.04 mg/kg, Atropinsulfat Amino, Amino AG, Neuhof, Switzerland; ketamine 20 - 40 mg/kg, Ketanarkon, Streuli Pharma AG, Uznach, Switzerland; im), the animal was weighed and transported to surgery. An iv catheter was placed in an auricular vein, anesthesia was induced (propofol 1 – 4 mg/kg iv, to effect; Propofol® 1% Fresenius, Fresenius Kabi AG, Stans, Switzerland) and the animal was intubated in sternal recumbency. Carprofen (2 mg/kg BW iv; Rimadyl®, Pfizer AG, Zurich, Switzerland), penicillin (10'000 IU/kg BW iv; Penicillin Natrium

Streuli®, Streuli Pharma AG, Uznach, Switzerland) and methadone (2 mg/kg BW iv; Methadon Streuli®, Streuli Pharma AG, Uznach, Switzerland) were given perioperatively.

Intraoperatively monitored parameters included electrocardiogram, heart rate, pulse rate, arterial blood pressure and oxygen saturation. Anesthesia was maintained via inhalation anesthesia (isoflurane in oxygen; Attane Isoflurane, MINRAD INC., Buffalo, NY, USA) and a CRI of propofol for a balanced protocol.

Right before surgery of each side, the respective mandibular nerve was locally anesthetized with lidocaine 2% (to effect; Lidocain 2 % Streuli, Streuli Pharma AG, Uznach, Switzerland) and/or ropivacaine 0.5% (to effect; NAROPIN Inj Lös 0.5 %, AstraZeneca AG, Zug, Switzerland) at its entry side into the mandible. A peripheral nerve stimulator was used to control the effect (Innervator®, Fisher & Paykel Healthcare, Melbourne, Australia). Adrenaline in a sterile solution (Adrenaline, diluted to 1:20'000 - 1:200'000; ADRENALIN Amino Inj Lös, Amino AG, Neuhof, Switzerland) was injected in the local mucosa to reduce bleeding.

2.4.2 Teeth Extraction (first stage surgery)

The animal was placed in lateral recumbency and the mouth was kept open with a mouth gag. The head was positioned using a moldable surgery cushion.

Adhering to the surgical principle of adequate access, sulcular incisions were performed around the premolars. Additionally, a mesial vertical releasing incision was performed to allow a careful elevation of a full thickness flap. The buccal wall was partially or completely removed by a standard dental drill (iChiropro, Bien-Air Dental SA, Biel, Switzerland) to simplify tooth extraction. Standard dental instruments (forceps, elevators) were used to loosen and extract teeth. Root remnants were either removed with special root elevators or were drilled out with the same dental drill under adequate irrigation. Extraction sockets were cleaned. The lingual soft tissue was loosened from the

bone plate and the mucoperiosteal flap was gently retracted with an elevator. Afterwards, the alveolar bone crest was down-leveled for 1 to 2 mm and sharp bony edges were smoothened.

The buccal and lingual mucoperiosteal flaps were repositioned and closed using single sutures (Vicryl® 2/0, Ethicon, New Jersey, NY, USA). The animal was then turned to the other side and the surgical procedure was repeated in an identical manner on the other side of the mandible.

2.4.3 Augmentation (second stage surgery)

Animal placement and repositioning were analogous to the procedure of the first stage surgery. The alveolar ridge was accessed through a full-thickness flap using a slightly lingual, mid-crestal incision in combination with two vertical releasing-incisions at its mesial and distal end. The flap was then elevated and held back using special retraction hooks.

Two parallel alveolar defects of approximate size 1 cm x 1 cm x 0.7 cm were created (see Figure 1 - 3) on each side of the mandible at the vestibular part of the alveolar ridge (4 defects per animal, 2 per hemimandible/side of the mandible) using a piezosurgery device (Piezosurgery®, Mectron Srl, Carasco, Italy). A small titanium pin (Geistlich Pharma AG, Wolhusen, Switzerland) was fixed at the tip of the bony bridge between the two defects to mark their location (see Figure 1). The defects were then filled or left empty according to the distribution plan (see Table 3):

- Augmentation with modified or unmodified PLGA coated β-TCP - The biomaterial was mixed with blood from the same animal in the provided syringe before application, was applied and then slightly condensed
- Augmentation with autologous bone - Extracted bone from both alveolar ridge defects was particulated and reused as particulated bone graft to augment the autologous defect site of the same side of the mandible
- No augmentation/empty sites - Defect sites were left empty

A synthetic, resorbable poly-D, L-lactide and poly-L-lactide, and acetyl-tributylcitrate membrane (GUIDOR® Bioresorbable Matrix Barrier, Sunstar, Chicago, United States) was placed over each defect (see Figure 4). The membrane was apically fixed with pins made of biodegradable co-polymers composed of L-lactic, D-lactic, glycolic acid and trimethylene carbonate (Inion GTR™ Tack kit, Inion Oy, Tampere, Finland). Finally, slight periosteal releasing incisions were performed and mucoperiosteal flaps were closed tension-free with single sutures (Vicryl® 2/0, Ethicon, New Jersey, NY, USA; see Figure 5).

2.4.4 Postoperative Management

After surgery, the animal was transported back to the stable and extubated upon return of the gagging reflex. Veterinary staff then monitored the animal until full consciousness had returned and the animal was considered stable. Analgesics (methadone 1-3 mg/kg BW im or iv, every 4h; or buprenorphine 0.015 mg/kg BW im or iv, every 8h; Temgesic®, Reckitt Benckiser AG, Wallisellen, Switzerland) were given postoperatively and as deemed necessary according to pain assessment.

Amoxicillin was given depending the weight of the animal (40 - 63 kg BW: 500 mg, 63 - 75 kg BW: 750 mg; BID po; Synulox®, Pfizer AG, Zurich, Switzerland). Anorexic animals were given enrofloxacin (2.5 mg/kg BW SID im; Baytril®, Bayer HealthCare, Leverkusen, Germany) or benzylpenicillin (15'000 IU/kg BW, im; Procacillin, MSD Animal Health, Lucerne, Switzerland) until acceptance of oral medication. No clinical signs of infection, such as prolonged reduced behavior/appetite or hyperthermia, were reported postoperatively. Carprofen (2 - 4 mg/kg BW SID po, iv or im) was given for 5 days.

2.5 Sample Harvesting and Processing

Animals were sacrificed 6 weeks after augmentation surgery by electrocution (application site between the ear and eye) followed by bleeding in accordance

to Swiss law. The head was separated from the body, sides of mandibles were harvested and augmentation sites were photographed (Nikon D500, Nikon AG, Egg, Switzerland) and macroscopically assessed and findings were classified and scored (see Table 4). Soft tissue in contact with the biodegradable membranes was left intact. The region of interest containing both defect sites was cut from each hemimandible using a bone saw (Bandsäge Kolbe Foodtec K440H, Paul Kolbe GmbH, Elchingen, Germany), radiographed in mediolateral and coronoapical direction (HP Cabinet X-ray System - Faxitron series Model 43855A, Hewlett Packard, Palo Alto, CA, USA) and then fixed in 4% formaldehyde. Radiographs were immediately assessed and abnormal findings were documented (see Table 5).

Samples were later prepared for routine histology of undecalcified bone samples, resulting in embedding of the samples in a methyl metacrylate-based acrylic resin, as described before [75,76]. After polymerisation, thick sections of 700 – 1700 μm were cut in the frontal plane using a diamond bone saw (EXAKT 300, EXAKT Advanced Technologies GmbH, Norderstedt, Germany) and all sections were radiographed (Cabinet X-Ray System LX-60, Faxitron X-Ray Corporation, Tucson, AZ, USA). Microradiographs were then immediately assessed and abnormal findings were documented (see Table 5).

Radiographs of sections were then evaluated by a senior scientist (SST) and sections representing the margin and the center (4000 μm from the margin) of the defects were chosen. Selected sections were glued on opal acrylic slides, grounded to reduce cutting marks and surface-stained with toluidine blue.

2.6 Radiography

Post mortem radiographs from hemimandibles were evaluated for signs of sclerosis or osteolysis. Radiodensity of defects was compared to the density of the adjacent bone and radiographs were described per group.

2.7 Histology

Sections were photographed using a macroscope (Leica Z6 APO A, Leica DFC 450 Digital Camera, Leica Macroscope SmartTouch control unit; Leica Microsystems [Schweiz] AG, Heerbrugg, Switzerland; ImageAccess 12 Standard, Imagic Bildverarbeitung AG, Glattbrugg, Switzerland) and photographs were used for further evaluation.

2.7.1 Qualitative Histology

Center sections of defect sites were scored semi-quantitatively using a scoring system for ingrowth (bridging, autologous ingrowth, overall ingrowth, bone quality), state of biomaterial residues and periosteal outgrowth reaction (see Table 6).

2.7.2 Histomorphometry

Using the 10.0x magnification photograph, matrix, new bone, old bone and biomaterial residues of defects were recolored in the defect area using photo editing software (Adobe Photoshop Elements 10, Adobe Systems Inc., Mountain View, CA, USA). Biomaterial residues within the defect margins were then selected and, based on calibration data from ImageAccess 12 Standard (0.000013566 m/px; 1 mm = 74 px), the selected area was expanded and reduced to represent the 0.1 mm (7 px), 0.2 mm (15 px) and 0.5 mm (37 px) perimeter around residues (see Figure 6). Each photograph was individually evaluated with ImageJ image analysis software (U. S. National Institutes of Health, USA) and relative percentages of tissues in the respective perimeter (excluding biomaterial residues) were calculated.

2.8 Statistics

Data from macroscopic assessments of implant sites and histology of center sections were described. Histomorphometric measurements were further analyzed using a one-way factorial analysis of variance (ANOVA) with Bonferroni post-hoc tests for inter-group comparisons. Significance was set at

$p < 0.05$. Statistical analysis was carried out with the commercial software IBM SPSS Statistics 22 (released 2013, IBM Corp., Armonk, NY, USA).

3 Results

3.1 Animal Model

Two animals had to be replaced by reserve animals included in the animal permission license due to postoperative complications after first stage surgery.

In one animal (23.05), a surplus fourth premolar was left in situ, as it did not influence the augmentation procedure. The bony bridge between the defects of the left hemimandible of animal 23.14 was partially fractured during surgery. Its connection to the mandible was regarded as being stable and therefore, it was left untreated.

All animals recovered well, started eating within an hour of extubation and showed no major signs of discomfort the days following the surgery. There was no reported major clinical abnormality in any animal until sacrifice. Body weight increased 0.9 ± 1.3 (-1 - 4.4) kg between first and second stage surgery.

3.2 Macroscopical Evaluation of Hemimandibles

As the overlying mucosa was not removed from the defect sites, it was not possible to define a clear and sharp demarcation between the mesial or distal defect. Consequently, the hemimandible was macroscopically assessed as a whole. Each hemimandible was grouped as M = Montelukast (two Montelukast defects), S = Simvastatin (two Simvastatin defects), T = Teriparatide (two Teriparatide defects), L = Empty (two Empty defects) or C = control (one defect from either the Autologous or Unmodified group, either distal or mesial, depending the distribution). Every animal had a control side (n=12) and there were n=3 each for the test item groups and the Empty group (see 7.1 Group Distribution, Table 7 and Figure 7 - 12).

Abnormal findings (inflammation, dehiscence, biomaterial remnants, bone sequester, granulation tissue) were found in all groups. Only four hemimandibles (2 controls, 1 Montelukast and 1 Teriparatide) were assessed as being healed without remaining signs of inflammation or other findings. A slight soft tissue inflammatory reaction could be mainly be observed in the

Control group and least in the Teriparatide group. The mucosa around the defect area disclosed a decent reddening with a faint piled up soft tissue scar. Dehiscences were seen in the Control and Empty group. Granulomatous wound healing was seen in all but the Teriparatide group. Biomaterial beads were obvious in all groups except the Empty group. Bone sequester were apparent in the Control and Empty group.

3.2.1 Empty group

A soft tissue dehiscence with a concomitant bone sequester were evident in one hemimandible (see Figure 13). The mucosa disclosed a circumscribed reddening without any pus. In two out of three hemimandibles granulomatous wound healing could be detected. There were no biomaterial beads visible in any case.

3.2.2 Autologous and Unmodified groups

Unmodified and Autologous groups showed the most substantial inflammatory reactions with 83% of hemimandibles being affected. Biomaterial beads in the soft tissue were found in four hemimandibles (see Figure 14). Overall, one dehiscence (9%) and two bone sequesters (17%) could be recognized in 12 hemimandibles.

3.2.3 Montelukast group

There were no apparent soft tissue dehiscences. In one out of three hemimandibles granulomatous wound healing and biomaterial beads in soft tissue were traceable (see Figure 15). Abnormal findings were found in two hemimandibles whereas in one there were no abnormalities seen.

3.2.4 Simvastatin group

Abnormalities were seen in all hemimandibles. The mucosa disclosed undisturbed healing without any dehiscence. Granulomatous wound healing was observed in one hemimandible. Signs of inflammation (reddening) were evident in 2 hemimandibles (see Figure 16).

3.2.5 Teriparatide group

The Teriparatide group showed the least signs of inflammatory reactions with 33%. Dehiscence or granulomatous wound healing was not seen in any hemimandible. In one hemimandible no abnormalities were seen (see Figure 17).

3.3 Radiography

Bone density of defects was lower than surrounding bone structures in all defects. All defect areas showed different degrees of resorption of bone and biomaterial. There was no sign of any sclerosis. Only one out of 23 titanium pins in the bony bridge between both defects could be seen in the radiographs (see Figure 18 and Figure 19). Defect margins and the bony bridge separating defects were observable only in some defects. The defect cortex was not clearly defined in all cases and compared to the trans-cortex, it did present itself as a less clearly defined and less radiodense structure. Isolated, radiopaque structures could be identified in the soft tissue of some defects. There were no signs of abnormal remodeling or fracture. There were no visible remnants of extracted teeth (P1) P2 - P4 from first stage surgery.

3.3.1 Empty group

Radiodensity of defects was clearly reduced in comparison to the surrounding bone. In one radiograph the former osteotomy lines were clearly visible (see Figure 20), whereupon in all other radiographs osteotomy lines could not be identified anymore. In two cases, the root of the canine tooth was partly visible.

3.3.2 Autologous group

Bony structures were seen in defects of the Autologous group with signs of resorption. Beads of the adjacent defect could be seen in the soft tissue surrounding defects in four cases. In one radiograph the autologous bone graft was clearly definable and could be distinguished from its neighboring defect especially in the coronoapical projection (see Figure 19).

In the specimen of the right hemimandible of animal 23.04, the implanted titanium pin in the bony bridge between the defects was visible (see Figure 18 and Figure 19). The height of the defect cortex in this case was also only slightly reduced in contrast to all other cases, where bone loss was much more remarkable, although to varying degrees.

3.3.3 Unmodified group

Some defects could be clearly differentiated from surrounding hard tissue structures. Remodeling of defect walls was less distinctive. Defect fillings showed bead-like structures, traceable to varying degrees. Only in the specimen of the right hemimandible of animal 23.04, the implanted titanium pin was visible (see Figure 18). Isolated, radiopaque structures were seen in the soft tissue right next to five defects (see Figure 21).

3.3.4 Montelukast group

Resorption of defect walls was indicated by blurred defect margins. Bead-like structures could be detected in defects and, in one case, also in the soft tissue covering the defects (see Figure 22). The bony bridge separating the defects was not detectable in any specimen. Isolated, radiopaque structures were seen in the soft tissue right next to defects of one hemimandible. The root of the canine tooth was visible in two cases but was deemed to not be in contact with any defect.

3.3.5 Simvastatin group

The bony bridge separating the defects was missing in one hemimandible as no radiopaque structure was visible (see Figure 23). Yet in one case it could be identified. Bead-like structures could be clearly seen as defect fillings. The height of the defect cortex was reduced in all defects, although to varying degrees. In two out of three cases, the root of the canine tooth was in close contact to the mesial defect.

3.3.6 Teriparatide group

Radiodensity of defects was slightly reduced compared to the surrounding bone. In one hemimandible, bead-like structures were seen in the soft tissue surrounding the defects. Osteotomy lines were clearly distinctive in some defects indicating signs of less remodeling of defect margins (see Figure 24). The defect cortices were not clearly definable, especially when compared to the respective trans-cortices. The root of the canine tooth was visible but did not seem in contact with any defect and no signs of inflammation or resorption could be seen.

3.4 Microradiography of thick Sections

Bone density of defects was lower than surrounding bone in all defects. All defect areas showed signs of resorption of bone and material. There was no sclerosis. There were no striking or significant differences between groups.

3.5 Qualitative Histology

Toluidine blue stained polymerized methyl metacrylate (PMMA) thick sections were semiquantitatively scored and described (see Table 8, Figure 25 - 56).

Absolute bridging of the defect from the buccal periost was quite evident in the Teriparatide group, followed by the Autologous control group. New bone formation was more pronounced at the apical periosteal part of the defect than the coronal part. Absolute endosteal bridging, with an almost complete fusion and aggregation of the defect base with new bone, could be seen in all Teriparatide samples. The Autologous group showed similar findings with 50% of all defects being completely or partly bridged. Increased new bone formation could also be seen in the medullar part of the mandibular bone near the defect. Autologous ingrowth coming from defect walls but excluding ingrowth supported by biomaterial residues showed Autologous and Teriparatide groups being represented in higher scores. Unmodified, Montelukast and Simvastatin groups were scored with lower percentages.

Quality of new bone formation was scored as either being of immature/low quality ("woven bone – low density") or mature quality ("woven bone – high density and lamellar bone"). Immature bone was more often seen in the Autologous, Montelukast, Unmodified and Empty groups, whereas bone with higher density could be seen more often in the Autologous and Teriparatide groups. Fully or partly engulfed biomaterial residues were classified as being with bone ingrowth and could be seen in all test item groups but were more often seen in the Teriparatide and Simvastatin groups compared to others. Residues without bone ingrowth were embedded in matrix and more often seen in the Unmodified and Montelukast groups and less often seen in the Teriparatide group. Simvastatin and Empty groups disclosed more often a higher score of matrix whereas Autologous and Teriparatide groups had samples scoring in the 0 % category.

The resorbable poly-D, L-lactide and poly-L-lactide, and acetyl-tributylcitrate membrane, used to cover the defects, was seen in 22 out of 48 cases independent of group as a translucent, rope-ladder shaped structure. Visible parts of the membrane seem to be structurally intact but over- and partly ingrown by bone (see Figure 47, 50, 54 , 55 and 56). In no sample the membrane was seen completely in situ and fully covering the defect.

In samples where an Inion GTR™ tack could be traced, it was integrated and overgrown with woven bone from the reactive periost (see Figure 49).

3.5.1 Empty group

Defect filling was seen as originating from the defect walls and growing inwards toward the center of the defect. None of the defects were fully bridged including the periosteal, outer side of the defects. One sample showed an almost complete filling of the defect while other defects scored in lower categories regarding defect closure. The Empty group was scored with a higher amount of matrix compared to bone as predominant tissue within the defect. There were no biomaterial residues detectable in any sample. A very prominent

periosteal reaction could be seen in 5/6 samples scoring a periosteal thickness of over 100% compared to the cortex at the apical osteotomy line. Parts of the membrane were only visible in two samples where bone seemed to grow around the membrane remnants. In one case the defect had contact to the root of the canine tooth where no growth was seen. In two cases the root was also seen but was not in contact with the defect.

3.5.2 Autologous group

Absolute bridging of the defect from the buccal periost was seen in 5/12 samples. Absolute endosteal bridging, with an almost complete fusion and aggregation of the defect base with new bone, could be seen in 50 % of cases. Remnants of donor site bone grafts could only been identified as such in three out of twelve samples (see Figure 48). Although filling of defects was heterogeneous, sections scored only in higher scores (26 % filling and above) with half of all sections being almost completely filled (76 - 100 % category). Only in one case was the root of the canine tooth not seen. In two cases it was osteotomized, with no new bone formation in one case and completed bridging with new bone, although of low density, in the other case.

3.5.3 Unmodified group

New bone formation originated from host bone and grew towards the defect center where new bone was still of lower density and organization. Biomaterial residues were visible in all samples to a different degree. Defect volume in one defect was completely preserved (see Figure 49) whereas in one defect with visible membrane remnants and new bone formation over the defect, it could not be clearly determined (see Figure 50). In all other defects of the Unmodified group, beads were clearly lost. Although residues with bone ingrowth could be scarcely seen, residues without bone ingrowth and surrounded by matrix were more prevalent. In two sections the location of the Inion GTR™ tack within the buccal cortex could be seen where it seemed in situ as a translucent structure in

one case (see Figure 49) and either remodeled with new bone or lost in the other case.

3.5.4 Montelukast group

New bone formation was seen as originating from periost, endost and defect walls and grown inwards to the defect center. Biomaterial residues were visible in all but one sample, with all defects being incompletely filled with residues. Only small parts of the membrane were visible in some defects and defect coverage was lost in all defects. There were biomaterial residues in the soft tissue surrounding the defect in two sections. In 4/6 samples, isolated bony structures located in the soft tissue over the defect could be seen (see Figure 52). Residues disclosed less bone ingrowth and were embedded more often in matrix than being engulfed by new bone. In one section, the Inion GTR™ tack was seen dislocated from the buccal cortex in the defect matrix (see Figure 51).

3.5.5 Simvastatin group

Defect bridging by new bone formation could be seen more often at the endosteal (defect base) than at the periosteal part. Defect filling was almost equally spread between scores with one defect being completely filled and other defects only partially filled (see Figure 30). Partly and fully engulfed biomaterial residues were seen in 3/6 defects with two defects not containing any residues at all. The root of the canine tooth was visible in 4/6 samples, being in contact with the defect in two cases and in one case, the root was osteotomized and no bone growth could be seen at that location (see Figure 53). Overall, defects of the Simvastatin group were very heterogenous in morphology, defect filling, amount of biomaterial residues and periosteal reaction.

3.5.6 Teriparatide group

Absolute bridging of the defects from the buccal periost could be observed in 3 out of 6 cases. Endosteal bridging, with a complete fusion and aggregation of

the defect base with new bone was seen in all samples. Biomaterial residues were visible in 3/6 samples. While there was one sample with only a few residues, in two samples the augmentation sites demonstrated a complete filling of the initial defect. In both those samples, parts of the membrane were visible although a complete defect coverage was not obvious. Biomaterial residues were fully or partly engulfed showing thorough bone growth between residues (see Figure 55). Some residues revealed a clear dark blue staining with toluidine blue. Residues embedded in matrix were only scarcely seen. All except one sample scored less than 25% matrix as defect filling, the rest comprised of residues or newly grown bone. The root of the canine tooth was visible in two cases but was never in contact with defect sites.

3.6 Histomorphometry

In 26 out of 30 defects, where unmodified (n=12) or modified PLGA coated β-TCP (n=6 per group) were implanted, biomaterial residues could be seen that were histomorphometrically evaluated (12 Unmodified, 5 Montelukast, 4 Simvastatin, 5 Teriparatide; n = 26). Relative amount of new bone formation was compared between groups within the 0.0 - 0.1 mm, 0.1 - 0.2 mm or 0.2 - 0.5 mm perimeter, respectively (see Table 11 and Figure 57 - 59).

New bone formation was most evident in the Teriparatide group in all three perimeters with 4.86 ± 4.64 %, 16.39 ± 9.25 % and 27.71 ± 12.78 % in the 0.0 - 0.1 mm, 0.1 - 0.2 mm or 0.2 - 0.5 mm perimeter, respectively. Unmodified and Montelukast groups showed less but similar amount of new bone formation, whereupon Montelukast had double as much bone formation in the 0.2 - 0.5 mm perimeter with 17.75 ± 14.50 % versus 9.53 ± 11.36 %. Simvastatin demonstrated the least amount of new bone formation in the 0.0 - 0.1 and 0.1 - 0.2 perimeter with 0.15 ± 0.16 % and 3.09 ± 2.63 %, respectively. Yet overall it was comparable to Montelukast in the 0.2 - 0.5 % perimeter with 14.61 ± 10.10 %.

Statistically, there were no significant differences at a level of $p < 0.05$ comparing new bone formation between groups.

4 Discussion

In the present study, lateral pre-defined crest defects in the atrophic alveolar ridge of 12 minipigs were augmented using a poly(lactic-co-glycolide) (PLGA) coated β-tricalcium phosphate (β-TCP) composite modified with one of three bioactive molecules (Montelukast, Simvastatin or Teriparatide). Results from qualitative and quantitative histologic evaluations revealed, that the modification with Teriparatide showed a clear, but statistically not significant rate of new bone formation with absolute bridging of the bone defect, which was more evident than in other groups.

4.1 Experimental model

Various studies in the cranium, pelvis or long bones as well as extraoral approaches to the mandible have been described to test biocompatibility and in vivo performance of biomaterials[23,24,46,76]. One advantage of these models is the number of defects that might be investigated per animal. In the sheep up to 12 defects might be assessed and although smaller defect numbers are usually analyzed in rodents or rabbits (limited to 6 by International Standard ISO 10993-6, 2007), higher animal numbers can be ethically justified allowing to increase defect number by increase of used animals[77]. Although these extraoral models are practical, reproducible and provide good results to compare biomaterials[24,78], they only allow conclusions of the bone interface but not of interactions with the oral milieu. On the other hand, intraoral models are closer to the clinical situation in the human patient but provide less space for defects and the defect environment is also more complex due to presence of oral microbiotic flora and saliva. While rodents are too small for intraoral studies, sheep and goats are not suited due to different anatomy and physiology of the jaw and gastrointestinal tract in general[78]. Intraoral models in the rabbit are described but space is very limited and access is difficult, leading to a preference of extraoral models for biomaterial testing in this species[78,79]. Consequently, rodent and rabbit models as well as extraoral models in large

animals are used primarily for screening of biomaterials prior to testing in clinically more relevant large animal models such as intraoral models of the dog[80-82] or the minipig[80,83,84]. Dogs have a similar bone structure and remodeling rate to that of human beings but there is a trend to limit their use due to ethical considerations[77,78,85]. The minipig mandible is also similar in morphology, healing and remodeling compared to human bone and has been proven appropriate for defect models[50,77,84,86]. For these reasons, an intraoral lateral alveolar ridge augmentation minipig model was chosen for this pilot study with n=2 defects each per hemimandible and one time point to reduce animal numbers and satisfy ethical claims regarding the 3R (reduce, replace, refine) principle.

Defect sizes and shapes may vary between model from being critical-sized and only supported by two bony walls[48,86,87], to defects being sized considerably smaller with four or five walls or being cylindrically shaped with low diameter and therefore supported by more bone growth stimulated by local tissue[24,46,54,88,89]. Patients presenting with chronic, large bone defects and atrophic alveolar ridges are laterally augmented to increase bone width and height. The analogous animal model for these procedures would be a 1-wall defect model which is clinically very relevant but difficult to cope with especially in animals[83]. In this study, defects with size of 1.0 x 1.0 x 0.7 cm and four defect walls were created in the experimentally induced atrophied alveolar crest. In comparison to the clinical situation, these defects were "freshly" created, acute, contained, supported by defect walls and limited in size. Although these defect characteristics allow better defect healing than chronic situations, this defect morphology can be considered a good compromise between standardization efforts and clinical relevance to assess the in vivo performance of biomaterials.

Intraoperatively, defect width and height were controlled using a sterile positioning device. Defect depth was controlled by using the tip of the piezosurgery device as a guide. Surgical sites were standardized 8 weeks before

augmentation surgery by removal of the premolars and smoothening of remaining bone of the alveolar crest. Depending on the healing capacity of the respective animal, resulting crestal shape and bone quality might have differed between animals and although great efforts were taken, defect morphology might have differed slightly between animals (< 1 mm). Although no intraoperative findings in regard to defect creation were seen, post mortem radiographs and histology of thick sections revealed partial osteotomy lines in the root of the canine tooth in four cases. Similar studies combining a first stage procedure with teeth extractions and later procedures for defect creation also extracted the first molar for additional space[83,90]. In the present breed of minipigs the first molars were not easily accessible but created space for defect creation was deemed enough. In future studies, it might be advisable to relocate defects more distal by additional removal of the first molar to prevent injuries of the root of the canine tooth.

Although of varying age and gender, animals used in this experimental study were considered to be appropriate since procedures were highly standardized and the specific aim of the study was to make an initial screening for further studies. Groups were distributed (left or right; in controls also mesial or distal) to spread and minimize possible physiological or specific inter-individual influences of the specific locations. To save animals, two defects in the same hemimandible were augmented with the same graft and the other side of the mandible was used for autologous bone and unmodified PLGA coated β-TCP as controls. Modified PLGA coated β-TCP substrates containing bioactive molecules could have had cumulative effects or have influenced the controls in the same animal but sample sizes were too low to analyze such effects. The results should therefore be interpreted within the limits of the study design.

4.2 Results

Although no major clinical changes in eating behavior could be seen in the 6 weeks following augmentation surgery, macroscopical, histological and

radiological assessment revealed that parts of the membranes, titanium pins marking the defects and grafting substrates were lost until sacrifice. These findings were not related to any graft substrate as it was seen in all grafting groups as well as in the Empty group. Similar results were seen in another lateral augmentation model in minipigs with varying degrees of soft tissue dehiscences commencing after 2 - 4 weeks postoperatively[83]. In the current study, defects were covered with bioresorbable membranes which were apically fixed with resorbable tacks and closure was achieved by tension-free single sutures. In a study in monkeys, the same membranes were integrated after 6 weeks, and only then started to degrade with resorption being completed after 6 - 12 months[91]. Only parts of membranes were visible in 22 of 48 histologic thick sections after 6 weeks. We concluded that membranes were exposed after surgery leading to a loss of substrates, titanium pins and parts of the membranes themselves. Although animals were only fed with soft feed, bedding included straw, which was chewed on. Removing straw as bedding might have had a positive effect on wound healing but would also lead to a significant reduction of animal welfare and can therefore not be considered. Closing the wound more lateral, deep in the vestibulum, away from crestal chewing forces and less accessible by the tongue, could have led to a more sustainable outcome in regard to wound healing. A minimal-invasive approach with mesial and distal incisions away from defects and leaving the soft tissue covering the defects intact might be another alternative. To the author's best knowledge, minimal-invasive approaches for lateral ridge augmentation in minipigs or dogs have not been described in literature. Additional studies are needed to find a reliable and safe access for lateral ridge augmentation in the minipig large animal model.

In radiographic evaluations, grafts of all groups showed signs of resorption, defect walls were remodeled and radiodensity of defects was still reduced in comparison to adjacent bone. With the chosen scoring system no differences

between groups could be observed. Although radiography might indicate differences with regard to ossification and mineralization of defects, tested bone grafting substrates were all of similar radiodensity and defects were fully augmented with said substrates. Radiodensity was therefore similar in all groups except the empty group, where it was slightly lower. Radiographic analysis in a study comparing β-TCP substrates concluded that conventional radiography was not able to distinguish between local bone formation and radiopaque β-TCP substrates[73]. This was also seen in this study, as new bone formation could not be assessed with radiography but could be nicely seen in toluidine blue stained histologic thick sections. The prominent periost reaction of the minipig mandible made it impossible to perform an objective radiographic assessment of height or width of healed defect sites. Micro-computed tomography (μCT) has been shown to be able to assess bone volume and graft surface or porosity changes, as well as produce 3D reconstructed figures of defects[83,88,92]. A newer study combining confocal scanning with μCT also proved the feasibility of in vivo analysis of bone, soft tissue and graft volume over time in a minipig defect model[90]. If radiographic analysis of defect healing is needed, more specific radiographic methods such as μCT should be preferred to standard post mortem faxitron radiography.

Evaluation of toluidine blue stained histologic thick sections to qualitatively and semiquantitatively assess new bone formation and bone remodeling has been proven to be effective in various studies of our group[54,93-95]. This was confirmed in this study where photographs of macroscopic toluidine blue stained thick sections were suitable to assess overall bone growth within defects as well as beginning degradation and engulfment of biomaterial residues with newly formed bone. Under favorable conditions it was seen that membrane and β-TCP beads withhold soft tissue pressure and conserved defect volume even in the center of the defect. This is a good result especially when compared to an early study using a polymeric hydrogel where collagen membrane-covered

12 x 10 x 12 mm defects in the mandibular angle of 12 minipigs showed signs of collapse leading to a reduction of secluded space[24]. Overall ingrowth of new bone into the defect showed Teriparatide and Autologous groups outperforming all other groups. Interpretation of these results proves difficult as only one time point was chosen in this study and longer term remodeling and final outcome could not be assessed. Similar results were seen with regard to defect bridging, where the modification with teriparatide outperformed autologous grafts. Although the performance of Montelukast and Simvastatin groups was lower than in said groups, they performed both distinctively better than the Empty group. Despite the fact that the defect morphology used in this study was not considered critically sized, defects without treatment were still expected to underperform autologous and β-TCP - based grafts based on results of prior studies comparing no treatment with tricalcium phosphates as defect fillings[24,56]. This was also seen in this study, where the Empty group showed the less favorable results with regard to defect bridging and filling when compared to groups with implanted β-TCP composites.

Teriparatide-modified PLGA coated β-TCP residues, in comparison to unmodified and other modified PLGA coated β-TCP groups, were more prominently engulfed by new bone with signs of early remodeling. This was confirmed with quantitative histology where new bone formation was most evident in the Teriparatide group in all three perimeters with 4.86 ± 4.64 %, 16.39 ± 9.25 % and 27.71 ± 12.78 % in the 0.0 - 0.1 mm, 0.1 - 0.2 mm or 0.2 - 0.5 mm perimeter around residues, respectively. As the assessment of new bone formation in perimeters around biomaterial residues is a novel method, no data for direct comparison could be found in literature. Teriparatide based composites were coated using a layering technique alternating pure PLGA and an aqueous polyvinylpyrrolidone solution mixed with teriparatide as coating layers. The alternating teriparatide and teriparatide-free layer technique was intended to allow intermittent release of embedded teriparatide, depending the

state of degradation of the coating. Studies have shown that pulsatile, intermittent exposure of parathyroid hormones has anabolic effects on bone remodeling whereas continuous exposure has catabolic effects[66]. Choosing a multi-layer technique to achieve intermittent release may have had a positive effect on new bone formation although it remains unknown if the different layering technique itself may have contributed to those effects. A study in a mouse femoral defect model showed that combining a β-TCP scaffold with systemic intermittent teriparatide treatment increases defect filling compared to controls[57]. Similar results were seen in another study in rats, combining systemic intermittent teriparatide treatment with local treatment, which resulted in better defect regeneration compared to empty defects or either treatment alone[96]. Further studies are needed to investigate if the combination of local intermittent release with systemic treatment may even further enhance new bone formation in teriparatide-modified β-TCP composites.

4.3 Conclusion

Qualitative and quantitative histologic evaluations after 6 weeks revealed that coatings with teriparatide led to a pronounced new bone formation. Even though coatings with montelukast and simvastatin demonstrated similar results like teriparatide, the findings were less evident. However, studies with larger case numbers and multiple timepoints are necessary to validate these results. Furthermore, refinements of the minipig model and surgical approach, are needed to avoid exposure to the oral cavity and subsequent loss of substrate.

5 Bibliography

1. Schropp L, Wenzel A, Kostopoulos L, et al: Bone healing and soft tissue contour changes following single-tooth extraction: a clinical and radiographic 12-month prospective study. Int J Periodontics Restorative Dent 23:313-323, 2003.
2. Wennerberg A, Albrektsson T: Current challenges in successful rehabilitation with oral implants. J Oral Rehabil 38:286-294, 2011.
3. Schwartz Z, Goultschin J, Dean DD, et al: Mechanisms of alveolar bone destruction in periodontitis. Periodontol 2000 14:158-172, 1997.
4. Zakhary IE, El-Mekkawi HA, Elsalanty ME: Alveolar ridge augmentation for implant fixation: status review. Oral Surg Oral Med Oral Pathol Oral Radiol 114:S179-189, 2012.
5. Schenk RK, Buser D, Hardwick WR, et al: Healing pattern of bone regeneration in membrane-protected defects: a histologic study in the canine mandible. Int J Oral Maxillofac Implants 9:13-29, 1994.
6. Lekholm U, Adell R, Lindhe J, et al: Marginal tissue reactions at osseointegrated titanium fixtures: (II) A cross-sectional retrospective study. International journal of oral and maxillofacial surgery 15:53-61, 1986.
7. Dietrich U, Lippold R, Dirmeier T, et al: Statistische Ergebnisse zur Implantatprognose am Beispiel von 2017 IMZ-Implantaten unterschiedlicher Indikation der letzten 13 Jahre. Z Zahnärztl Implantol 9:9-18, 1993.
8. Myeroff C, Archdeacon M: Autogenous bone graft: donor sites and techniques. J Bone Joint Surg Am 93:2227-2236, 2011.
9. Stubinger S, Nuss K, Landes C, et al: Harvesting of intraoral autogenous block grafts from the chin and ramus region: preliminary results with a variable square pulse Er:YAG laser. Lasers Surg Med 40:312-318, 2008.
10. Chiapasco M, Abati S, Romeo E, et al: Clinical outcome of autogenous bone blocks or guided bone regeneration with e-PTFE membranes for the reconstruction of narrow edentulous ridges. Clin Oral Implants Res 10:278-288, 1999.
11. Scipioni A, Bruschi GB, Calesini G, et al: Bone regeneration in the edentulous ridge expansion technique: histologic and ultrastructural study of 20 clinical cases. Int J Periodontics Restorative Dent 19:269-277, 1999.
12. Garcez-Filho J, Tolentino L, Sukekava F, et al: Long-term outcomes from implants installed by using split-crest technique in posterior maxillae: 10 years of follow-up. Clin Oral Implants Res:n/a-n/a, 2014.
13. Saulacic N, Iizuka T, Martin MS, et al: Alveolar distraction osteogenesis: a systematic review. Int J Oral Maxillofac Surg 37:1-7, 2008.

14. Cheung LK, Chua HD, Hariri F, et al: Alveolar distraction osteogenesis for dental implant rehabilitation following fibular reconstruction: a case series. J Oral Maxillofac Surg 71:255-271, 2013.
15. Blokhuis TJ, Arts JJ: Bioactive and osteoinductive bone graft substitutes: definitions, facts and myths. Injury 42 Suppl 2:S26-29, 2011.
16. Giannoudis PV, Dinopoulos H, Tsiridis E: Bone substitutes: an update. Injury 36 Suppl 3:S20-27, 2005.
17. Tiwana PS, Kushner GM, Haug RH: Maxillary sinus augmentation. Dent Clin North Am 50:409-424, vii, 2006.
18. Chiapasco M, Zaniboni M: Clinical outcomes of GBR procedures to correct peri-implant dehiscences and fenestrations: a systematic review. Clin Oral Implants Res 20 Suppl 4:113-123, 2009.
19. Grover V, Kapoor A, Malhotra R, et al: Bone allografts: a review of safety and efficacy. Indian J Dent Res 22:496, 2011.
20. Tomford WW: Transmission of disease through transplantation of musculoskeletal allografts. J Bone Joint Surg Am 77:1742-1754, 1995.
21. LeGeros RZ, Lin S, Rohanizadeh R, et al: Biphasic calcium phosphate bioceramics: preparation, properties and applications. J Mater Sci Mater Med 14:201-209, 2003.
22. von Doernberg MC, von Rechenberg B, Bohner M, et al: In vivo behavior of calcium phosphate scaffolds with four different pore sizes. Biomaterials 27:5186-5198, 2006.
23. Jensen SS, Yeo A, Dard M, et al: Evaluation of a novel biphasic calcium phosphate in standardized bone defects: a histologic and histomorphometric study in the mandibles of minipigs. Clin Oral Implants Res 18:752-760, 2007.
24. Buser D, Hoffmann B, Bernard JP, et al: Evaluation of filling materials in membrane--protected bone defects. A comparative histomorphometric study in the mandible of miniature pigs. Clin Oral Implants Res 9:137-150, 1998.
25. Gentile P, Chiono V, Carmagnola I, et al: An overview of poly(lactic-co-glycolic) acid (PLGA)-based biomaterials for bone tissue engineering. Int J Mol Sci 15:3640-3659, 2014.
26. McAllister BS, Haghighat K: Bone augmentation techniques. J Periodontol 78:377-396, 2007.
27. Chiapasco M, Zaniboni M, Boisco M: Augmentation procedures for the rehabilitation of deficient edentulous ridges with oral implants. Clin Oral Implants Res 17 Suppl 2:136-159, 2006.
28. Dimitriou R, Mataliotakis GI, Calori GM, et al: The role of barrier membranes for guided bone regeneration and restoration of large bone defects: current experimental and clinical evidence. BMC Med 10:81, 2012.

29. Lekovic V, Camargo PM, Klokkevold PR, et al: Preservation of alveolar bone in extraction sockets using bioabsorbable membranes. Journal of Periodontology 69:1044-1049, 1998.
30. Tomlin EM, Nelson SJ, Rossmann JA: Ridge preservation for implant therapy: a review of the literature. Open Dent J 8:66-76, 2014.
31. Morjaria KR, Wilson R, Palmer RM: Bone healing after tooth extraction with or without an intervention: a systematic review of randomized controlled trials. Clin Implant Dent Relat Res 16:1-20, 2014.
32. Vignoletti F, Matesanz P, Rodrigo D, et al: Surgical protocols for ridge preservation after tooth extraction. A systematic review. Clin Oral Implants Res 23 Suppl 5:22-38, 2012.
33. Langer R, Vacanti JP: Tissue engineering. Science 260:920-926, 1993.
34. Egusa H, Sonoyama W, Nishimura M, et al: Stem cells in dentistry--Part II: Clinical applications. J Prosthodont Res 56:229-248, 2012.
35. Stadlinger B, Pilling E, Mai R, et al: Effect of biological implant surface coatings on bone formation, applying collagen, proteoglycans, glycosaminoglycans and growth factors. J Mater Sci Mater Med 19:1043-1049, 2008.
36. Liu Y, Huse RO, de Groot K, et al: Delivery mode and efficacy of BMP-2 in association with implants. J Dent Res 86:84-89, 2007.
37. Fu R, Selph S, McDonagh M, et al: Effectiveness and harms of recombinant human bone morphogenetic protein-2 in spine fusion: a systematic review and meta-analysis. Ann Intern Med 158:890-902, 2013.
38. Dimitriou R, Tsiridis E, Giannoudis PV: Current concepts of molecular aspects of bone healing. Injury 36:1392-1404, 2005.
39. Szabo G, Huys L, Coulthard P, et al: A prospective multicenter randomized clinical trial of autogenous bone versus beta-tricalcium phosphate graft alone for bilateral sinus elevation: histologic and histomorphometric evaluation. Int J Oral Maxillofac Implants 20:371-381, 2005.
40. Stiller M, Kluk E, Bohner M, et al: Performance of beta-tricalcium phosphate granules and putty, bone grafting materials after bilateral sinus floor augmentation in humans. Biomaterials 35:3154-3163, 2014.
41. Knabe C, Koch C, Rack A, et al: Effect of beta-tricalcium phosphate particles with varying porosity on osteogenesis after sinus floor augmentation in humans. Biomaterials 29:2249-2258, 2008.
42. Dorozhkin SV: Biphasic, triphasic and multiphasic calcium orthophosphates. Acta Biomater 8:963-977, 2012.
43. Habibovic P, Yuan H, van der Valk CM, et al: 3D microenvironment as essential element for osteoinduction by biomaterials. Biomaterials 26:3565-3575, 2005.
44. Fellah BH, Gauthier O, Weiss P, et al: Osteogenicity of biphasic calcium phosphate ceramics and bone autograft in a goat model. Biomaterials 29:1177-1188, 2008.

45. Walsh WR, Vizesi F, Michael D, et al: Beta-TCP bone graft substitutes in a bilateral rabbit tibial defect model. Biomaterials 29:266-271, 2008.
46. Schmidlin PR, Nicholls F, Kruse A, et al: Evaluation of moldable, in situ hardening calcium phosphate bone graft substitutes. Clin Oral Implants Res 24:149-157, 2013.
47. Karageorgiou V, Kaplan D: Porosity of 3D biomaterial scaffolds and osteogenesis. Biomaterials 26:5474-5491, 2005.
48. Alfotawei R, Naudi KB, Lappin D, et al: The use of TriCalcium Phosphate (TCP) and stem cells for the regeneration of osteoperiosteal critical-size mandibular bony defects, an in vitro and preclinical study. J Craniomaxillofac Surg 42:863-869, 2014.
49. Yuan J, Cui L, Zhang WJ, et al: Repair of canine mandibular bone defects with bone marrow stromal cells and porous beta-tricalcium phosphate. Biomaterials 28:1005-1013, 2007.
50. Gruber RM, Ludwig A, Merten HA, et al: Sinus floor augmentation with recombinant human growth and differentiation factor-5 (rhGDF-5): a pilot study in the Goettingen miniature pig comparing autogenous bone and rhGDF-5. Clin Oral Implants Res 20:175-182, 2009.
51. Ginebra MP, Traykova T, Planell JA: Calcium phosphate cements as bone drug delivery systems: a review. J Control Release 113:102-110, 2006.
52. Thoma K, Pajarola GF, Gratz KW, et al: Bioabsorbable root analogue for closure of oroantral communications after tooth extraction: a prospective case-cohort study. Oral Surg Oral Med Oral Pathol Oral Radiol Endod 101:558-564, 2006.
53. Nair PN, Luder HU, Maspero FA, et al: Biocompatibility of Beta-tricalcium phosphate root replicas in porcine tooth extraction sockets - a correlative histological, ultrastructural, and x-ray microanalytical pilot study. J Biomater Appl 20:307-324, 2006.
54. Luginbuehl V, Ruffieux K, Hess C, et al: Controlled release of tetracycline from biodegradable beta-tricalcium phosphate composites. J Biomed Mater Res B Appl Biomater 92:341-352, 2010.
55. Cakici H, Hapa O, Gideroglu K, et al: The effects of leukotriene receptor antagonist montelukast on histological, radiological and densitometric parameters of fracture healing. Eklem Hastalik Cerrahisi 22:43-47, 2011.
56. Rojbani H, Nyan M, Ohya K, et al: Evaluation of the osteoconductivity of alpha-tricalcium phosphate, beta-tricalcium phosphate, and hydroxyapatite combined with or without simvastatin in rat calvarial defect. J Biomed Mater Res A 98:488-498, 2011.
57. Jacobson JA, Yanoso-Scholl L, Reynolds DG, et al: Teriparatide therapy and beta-tricalcium phosphate enhance scaffold reconstruction of mouse femoral defects. Tissue Eng Part A 17:389-398, 2011.

58. Leff JA, Busse WW, Pearlman D, et al: Montelukast, a leukotriene-receptor antagonist, for the treatment of mild asthma and exercise-induced bronchoconstriction. N Engl J Med 339:147-152, 1998.
59. Altman LC, Munk Z, Seltzer J, et al: A placebo-controlled, dose-ranging study of montelukast, a cysteinyl leukotriene-receptor antagonist. Montelukast Asthma Study Group. J Allergy Clin Immunol 102:50-56, 1998.
60. Manigrasso MB, O'Connor JP: Accelerated fracture healing in mice lacking the 5-lipoxygenase gene. Acta Orthop 81:748-755, 2010.
61. Cottrell JA, O'Connor JP: Pharmacological inhibition of 5-lipoxygenase accelerates and enhances fracture-healing. J Bone Joint Surg Am 91:2653-2665, 2009.
62. Zhang Y, Bradley AD, Wang D, et al: Statins, bone metabolism and treatment of bone catabolic diseases. Pharmacol Res 88C:53-61, 2014.
63. Mundy G, Garrett R, Harris S, et al: Stimulation of bone formation in vitro and in rodents by statins. Science 286:1946-1949, 1999.
64. Hughes A, Rogers MJ, Idris AI, et al: A comparison between the effects of hydrophobic and hydrophilic statins on osteoclast function in vitro and ovariectomy-induced bone loss in vivo. Calcif Tissue Int 81:403-413, 2007.
65. Chen S, Yang JY, Zhang SY, et al: Effects of simvastatin gel on bone regeneration in alveolar defects in miniature pigs. Chin Med J (Engl) 124:3953-3958, 2011.
66. Jilka RL: Molecular and cellular mechanisms of the anabolic effect of intermittent PTH. Bone 40:1434-1446, 2007.
67. Jiang Y, Zhao JJ, Mitlak BH, et al: Recombinant human parathyroid hormone (1-34) [teriparatide] improves both cortical and cancellous bone structure. J Bone Miner Res 18:1932-1941, 2003.
68. Macdonald HM, Nishiyama KK, Hanley DA, et al: Changes in trabecular and cortical bone microarchitecture at peripheral sites associated with 18 months of teriparatide therapy in postmenopausal women with osteoporosis. Osteoporos Int 22:357-362, 2011.
69. Kurland ES, Cosman F, McMahon DJ, et al: Parathyroid hormone as a therapy for idiopathic osteoporosis in men: effects on bone mineral density and bone markers. J Clin Endocrinol Metab 85:3069-3076, 2000.
70. Hodsman AB, Bauer DC, Dempster DW, et al: Parathyroid hormone and teriparatide for the treatment of osteoporosis: a review of the evidence and suggested guidelines for its use. Endocr Rev 26:688-703, 2005.
71. Bashutski JD, Eber RM, Kinney JS, et al: Teriparatide and osseous regeneration in the oral cavity. N Engl J Med 363:2396-2405, 2010.
72. Kawane T, Takahashi S, Saitoh H, et al: Anabolic effects of recombinant human parathyroid hormone (1 - 84) and synthetic human parathyroid hormone (1 - 34) on the mandibles of osteopenic ovariectomized rats with maxillary molar extraction. Horm Metab Res 34:293-302, 2002.

73. Yun JI, Wikesjo UM, Borke JL, et al: Effect of systemic parathyroid hormone (1-34) and a beta-tricalcium phosphate biomaterial on local bone formation in a critical-size rat calvarial defect model. J Clin Periodontol 37:419-426, 2010.
74. Andreassen TT, Ejersted C, Oxlund H: Intermittent parathyroid hormone (1-34) treatment increases callus formation and mechanical strength of healing rat fractures. J Bone Miner Res 14:960-968, 1999.
75. Theiss F, Apelt D, Brand B, et al: Biocompatibility and resorption of a brushite calcium phosphate cement. Biomaterials 26:4383-4394, 2005.
76. Kuemmerle JM, Oberle A, Oechslin C, et al: Assessment of the suitability of a new brushite calcium phosphate cement for cranioplasty - an experimental study in sheep. J Craniomaxillofac Surg 33:37-44, 2005.
77. Pearce AI, Richards RG, Milz S, et al: Animal models for implant biomaterial research in bone: a review. Eur Cell Mater 13:1-10, 2007.
78. Oortgiesen DW, Meijer G, de Vries RM, et al: Animal Models for the Evaluation of Tissue Engineering Constructs, in Pallua N, Suscheck CV (eds): Tissue Engineering, Vol Springer Berlin Heidelberg, 2011, pp 131-154.
79. Stubinger S, Dard M: The rabbit as experimental model for research in implant dentistry and related tissue regeneration. J Invest Surg 26:266-282, 2013.
80. Ivanovic A, Bosshardt DD, Mihatovic I, et al: Effect of pulverized natural bone mineral on regeneration of three-wall intrabony defects. A preclinical study. Clin Oral Investig 18:1319-1328, 2014.
81. Schwarz F, Ferrari D, Balic E, et al: Lateral ridge augmentation using equine- and bovine-derived cancellous bone blocks: a feasibility study in dogs. Clin Oral Implants Res 21:904-912, 2010.
82. Schliephake H, Drewes M, Mihatovic I, et al: Use of a self-curing resorbable polymer in vertical ridge augmentations - a pilot study in dogs. Clin Oral Implants Res 25:435-440, 2014.
83. Yeo A, Cheok C, Teoh SH, et al: Lateral ridge augmentation using a PCL-TCP scaffold in a clinically relevant but challenging micropig model. Clin Oral Implants Res 23:1322-1332, 2012.
84. Catros S, Wen B, Schleier P, et al: Use of a perforated scaffold-retaining abutment to achieve vertical bone regeneration around dental implants in the minipig. Int J Oral Maxillofac Implants 28:432-443, 2013.
85. Aerssens J, Boonen S, Lowet G, et al: Interspecies differences in bone composition, density, and quality: potential implications for in vivo bone research. Endocrinology 139:663-670, 1998.
86. Mardas N, Dereka X, Donos N, et al: Experimental model for bone regeneration in oral and cranio-maxillo-facial surgery. J Invest Surg 27:32-49, 2014.

87. Huh JY, Choi BH, Kim BY, et al: Critical size defect in the canine mandible. Oral Surg Oral Med Oral Pathol Oral Radiol Endod 100:296-301, 2005.
88. Dahlin C, Obrecht M, Dard M, et al: Bone tissue modelling and remodelling following guided bone regeneration in combination with biphasic calcium phosphate materials presenting different microporosity. Clin Oral Implants Res, 2014.
89. Kim CS, Choi SH, Chai JK, et al: Periodontal repair in surgically created intrabony defects in dogs: influence of the number of bone walls on healing response. J Periodontol 75:229-235, 2004.
90. Clozza E, Obrecht M, Dard M, et al: A novel three-dimensional analysis of standardized bone defects by means of confocal scanner and micro-computed tomography. Clin Oral Investig 18:1245-1250, 2014.
91. Gottlow J, Laurell L, Lundgren D, et al: Periodontal tissue response to a new bioresorbable guided tissue regeneration device: a longitudinal study in monkeys. Int J Periodontics Restorative Dent 14:436-449, 1994.
92. Jensen T, Schou S, Svendsen PA, et al: Volumetric changes of the graft after maxillary sinus floor augmentation with Bio-Oss and autogenous bone in different ratios: a radiographic study in minipigs. Clin Oral Implants Res 23:902-910, 2012.
93. Stubinger S, Nuss K, Pongratz M, et al: Comparison of Er:YAG laser and piezoelectric osteotomy: An animal study in sheep. Lasers Surg Med 42:743-751, 2010.
94. Nuss KM, Auer JA, Boos A, et al: An animal model in sheep for biocompatibility testing of biomaterials in cancellous bones. BMC Musculoskelet Disord 7:67, 2006.
95. Plecko M, Sievert C, Andermatt D, et al: Osseointegration and biocompatibility of different metal implants - a comparative experimental investigation in sheep. BMC Musculoskelet Disord 13:32, 2012.
96. Chen H, Frankenburg EP, Goldstein SA, et al: Combination of local and systemic parathyroid hormone enhances bone regeneration. Clin Orthop Relat Res:291-302, 2003.

6 List of Abbreviations

5-LO	5-lipoxygenase
ANOVA	Analysis of variance
BID	Bis in die (twice a day)
BMP(s)	Bone morphogenic protein(s)
BW	Bodyweight
CRI	Constant rate infusion
e-PTFE	Expanded polytetrafluoroethylene
eg	For example
f	Female
GBR	Guided bone regeneration
HA	Hydroxyapatite
im	intramuscularly
iv	intravenously
m	Male
µCT	Micro-computed tomography
no	Number
P1-P4	Premolar (1-4)
PGA	poly(glycolic acid)
PLA	poly(lactic acid)
PLLA	poly(L-lactide)
PLGA	poly(lactic-co-glycolide)
(P)MMA	(Polymerized) Methyl methacrylate
po	per oral
px	Pixel
β-TCP	Beta - tricalcium phosphate
SD	Standard deviation
SID	Semel in die (once a day)
Sig	Significance
SST	PD Dr. med. dent. Stefan Stübinger
TGF- β	Transforming growth factor beta

7 Appendix

7.1 Group Distribution

Each animal was randomly assigned a group at the day of first stage surgery. Of the two hemimandibles, one contained two defects of the assigned group (Empty, Simvastatin, Montelukast or Teriparatide) and the other acted as control, containing 1 defect from the Autologous group and 1 defect form the Unmodified group.

Depending on the reference, the group may refer to the animal group (L, S, M, T), the group of the hemimandible (L, S, M, T, or C) or the group of the individual defect.

Table 3: Group distribution

Animal Study ID	**Location**			**Group**		
	Gender	Side	Mesial / distal	Animal	Defect	Hemimandible
23.01	f	left	distal	L	l	L
			mesial		l	
		right	distal		u	C
			mesial		a	
23.03	f	left	distal	T	t	T
			mesial		t	
		right	distal		u	C
			mesial		a	
23.04	f	left	distal	M	m	M
			mesial		m	
		right	distal		u	C
			mesial		a	
23.05	f	left	distal	T	u	C
			mesial		a	
		right	distal		t	T
			mesial		t	
23.06	f	left	distal	M	u	C
			mesial		a	
		right	distal		m	M
			mesial		m	
23.07	f	left	distal	S	s	S
			mesial		s	
		right	distal		u	C
			mesial		a	
23.09	f	left	distal	S	u	C

			mesial		a	
		right	distal		s	S
			mesial		s	
23.10	f	left	distal	L	u	C
			mesial		a	
		right	distal		l	L
			mesial		l	
23.11	m	left	distal	T	t	T
			mesial		t	
		right	distal		a	C
			mesial		u	
23.12	m	left	distal	S	s	S
			mesial		s	
		right	distal		a	C
			mesial		u	
23.13	f	left	distal	M	m	M
			mesial		m	
		right	distal		a	C
			mesial		u	
23.14	m	left	distal	L	l	L
			mesial		l	
		right	distal		a	C
			mesial		u	

f: female; m: male

M/m: Montelukast group; S/s: Simvastatin group; T/t: Teriparatide group; u: Unmodified group; a: Autologous group; L/l: Empty group; C: control hemimandible (1 Unmodified + 1 Autologous defect; mesial or distal respectively)

7.2 Tables

Table 4: Classification and scoring system of macroscopic assessment findings

Criteria	Score	Description
Abnormalities	0	no abnormal findings, slight reddening allowed
	1	abnormal findings
Inflammation	0	no reddening
	1	reddening
Dehiscence	0	not seen
	1	seen
Granulomatous wound healing	0	not seen/nicely healed
	1	seen
Biomaterial beads in soft tissue	0	no beads
	1	beads are visible in the mucosa
Bone sequester in soft tissue	0	not seen
	1	seen

Table 5: Scoring system of radiographic/microradiographic assessment

Criteria	Score	Description
Bone density	0	Defect bone density lower than surrounding bone
	1	Defect bone density equal or higher than surrounding bone
Signs of bone resorption	0	Defect boundaries clearly definable (no resorption)
	1	Defect boundaries not clearly definable (resorption)
Signs of material resorption	0	Material visible as chip (autologous bone) or granular (biomaterial beads) structured opacity as expected at day of surgery (no resorption)
	1	Unstructured opacity (signs of resorption)
Sclerosis	0	No sclerosis seen
	1	Sclerosis seen

Table 6: Qualitative histology scoring system

Category	Criteria	Description	Score
Defect ingrowth	Absolute Bridging - Periost	Absolute connection of osteotomy sites	0 = no 1 = yes
	Absolute Bridging - Endost		
	Autologous - Periost	Amount of autologous ingrowth from that origin	0 = 0% 1 = 1-25% 2 = 26-50% 3 = 51-75% 4 = 76-100%
	Autologous - Endost		
	Autologous - Overall		
	Overall	Overall ingrowth, including biomaterial residues with bone ingrowth (overall defect filling)	0 = 0% 1 = 1-25% 2 = 26-50% 3 = 51-75% 4 = 76-100%
	Bone Quality - Woven bone/low density	Quality of the tissue filling the defect	0 = 0% 1 = 1-25% 2 = 26-50% 3 = 51-75% 4 = 76-100%
	Woven bone - high density + lamellar bone		
	Biomaterial residues with bone ingrowth		
	Biomaterial residues without bone ingrowth		
	Matrix (soft/fibrous tissue)		
Biomaterial residues	Residues	Existence	0 = no 1 = yes
	Quantity	Defect filling with residues	0 = 0% 1 = 1-25% 2 = 26-50%

			3 = 51-75% 4 = 76-100%
	Quality - Defect center	Evaluation of degradation process at 3 locations and overall rating of residue degradation	0 = Intact, round, free from bone 1 = Intact, round, encapsulated in bone 2 = Not-intact, round-formy, encapsulated in bone 3 = Not-intact, not round, definable mass, encapsulated in bone 9 = No residues visible
	Quality - Defect lingual site		
	Quality - Defect buccal site		
	Quality - Overall		
Periost	Outgrowth Reaction	New bone formation from the periost at the level of the labial/buccal osteotomy site in relation to cortical thickness	0 = less than 10% 1 = 11-50% 2 = 51-100% 3 = 101-150% 4 = more than 150%
Membrane	Existence and Location - Cortex	Existence is supported when colorless areas are visible (rope-ladder shape)	0 = no 1 = yes 9 = not sure
	Existence and Location - Defect		
Other	Isolated Bone Structures - Woven bone	Visible isolated bone structures in matrix/soft tissue surrounding defect	0 = 0 1 = 1 2 = 2 3 = 2+
	Isolated Bone Structures - Lamellar bone		
	Root of Canine Tooth	Visibility and contact of the root of the canine tooth to the defect	0 = no root visible 1 = yes, no contact 2 = yes, contact, no new bone 3 = yes, contact, new bone
	Pin	Visibility of Inion GTR™ tack on slide	0 = no 1 = yes

Table 7: Macroscopic assessment - Results

Animal Study ID	**Group**		**Location**	**Sacrifice**	**Macroscopic Asessment**					
	Animal	Hemimandible		Date	Abn	Infl	Deh	Gran	Beads	Bone seq
23.01	L	L	left	28.02.2013	1	1	1	0	0	1
23.01	L	C	right	28.02.2013	1	1	1	0	1	0
23.03	T	T	left	04.03.2013	0	0	0	0	0	0
23.03	T	C	right	04.03.2013	0	0	0	0	0	0
23.04	M	M	left	04.03.2013	0	0	0	0	0	0
23.04	M	C	right	04.03.2013	1	0	0	0	1	0
23.05	T	C	left	05.03.2013	1	1	0	0	0	0
23.05	T	T	right	05.03.2013	1	0	0	0	0	0
23.06	M	C	left	05.03.2013	1	1	0	0	0	0
23.06	M	M	right	05.03.2013	1	1	0	0	0	0
23.07	S	S	left	28.02.2013	1	0	0	1	0	0
23.07	S	C	right	28.02.2013	0	1	0	0	0	0
23.09	S	C	left	06.03.2013	1	1	0	0	0	0
23.09	S	S	right	06.03.2013	1	1	0	0	0	0
23.10	L	C	left	06.03.2013	1	1	0	0	1	0
23.10	L	L	right	06.03.2013	1	1	0	1	0	0
23.11	T	T	left	07.03.2013	1	1	0	0	1	0
23.11	T	C	right	07.03.2013	1	1	0	0	0	1
23.12	S	S	left	07.03.2013	1	1	0	0	1	0
23.12	S	C	right	07.03.2013	1	1	0	0	0	0
23.13	M	M	left	11.03.2013	1	1	0	1	1	0
23.13	M	C	right	11.03.2013	1	1	0	1	1	1
23.14	L	L	left	11.03.2013	1	0	0	1	0	0
23.14	L	C	right	11.03.2013	1	1	0	1	0	0

Group: see 7.1 Group Distribution; Classification and scoring system see Table 4

Abn: Abnormalities; Infl: Inflammation; Deh: Dehiscence; Gran: Granulomatous wound healing; Beads: Biomaterial beads in soft tissue; Bone seq: Bone sequester in soft tissue

Table 8: Qualitative histology - Results 1/2

Animal ID	Side	Defect location	Defect group	Ingrowth - Absolute Bridging [Periost]	Ingrowth - Absolute Bridging [Endost]	Ingrowth - Autologous [Periost]	Ingrowth - Autologous [Endost]	Ingrowth - Autologous [Overall autologous ingrowth]	Ingrowth - Overall [Defect]	Ingrowth - Bone Quality [Woven bone - low density]	Ingrowth - Bone Quality [Woven bone - high density + lamellar bone]	Ingrowth - Bone Quality [Biomaterial residues with bone ingrowth]	Ingrowth - Bone Quality [Biomaterial residues without bone ingrowth]	Ingrowth - Bone Quality [Soft/fibrous tissue]
23.01	Left	Distal	l	0	0	4	4	3	3	1	2	0	0	2
23.01	Left	Mesial	l	0	0	2	4	2	2	1	2	0	0	3
23.01	Right	Distal	u	0	0	1	1	1	2	1	1	1	1	2
23.01	Right	Mesial	a	0	0	3	4	3	3	1	2	0	0	2
23.03	Left	Distal	t	1	1	4	4	4	4	0	4	0	0	0
23.03	Left	Mesial	t	0	1	3	4	4	4	1	2	1	1	1
23.03	Right	Distal	u	0	0	3	4	4	4	1	3	0	1	1
23.03	Right	Mesial	a	1	1	4	4	4	4	1	3	0	0	1
23.04	Left	Distal	m	0	0	4	1	2	2	1	2	0	2	1
23.04	Left	Mesial	m	1	1	4	4	4	4	1	2	1	0	1
23.04	Right	Distal	u	0	0	1	3	1	1	0	1	0	3	1
23.04	Right	Mesial	a	1	1	4	4	4	4	1	3	0	0	1
23.05	Left	Distal	u	0	0	1	3	2	2	1	1	1	1	2
23.05	Left	Mesial	a	0	0	4	3	3	3	2	1	0	0	2
23.05	Right	Distal	t	0	1	2	4	2	2	1	2	0	0	2
23.05	Right	Mesial	t	1	1	4	4	3	4	1	2	1	0	1
23.06	Left	Distal	u	0	0	3	3	3	3	1	2	0	1	2
23.06	Left	Mesial	a	1	1	4	4	4	4	1	4	0	0	0
23.06	Right	Distal	m	0	0	1	1	1	1	1	1	0	1	3
23.06	Right	Mesial	m	0	0	4	4	2	3	1	1	1	1	1
23.07	Left	Distal	s	0	0	2	4	2	2	1	2	1	1	2
23.07	Left	Mesial	s	0	1	2	4	3	3	1	2	0	0	2
23.07	Right	Distal	u	0	0	3	4	1	2	1	1	1	1	3
23.07	Right	Mesial	a	0	1	4	4	3	3	1	2	0	0	2
23.09	Left	Distal	u	0	1	2	4	4	4	2	2	0	1	1
23.09	Left	Mesial	a	0	0	4	3	3	3	1	3	0	0	1
23.09	Right	Distal	s	1	1	4	4	4	4	1	3	1	1	1
23.09	Right	Mesial	s	0	0	2	2	1	1	1	1	0	0	3
23.10	Left	Distal	u	0	0	3	2	1	1	1	1	1	1	3
23.10	Left	Mesial	a	0	1	3	4	4	4	2	2	0	0	1
23.10	Right	Distal	l	0	0	2	3	2	2	1	2	0	0	3
23.10	Right	Mesial	l	0	0	4	3	3	3	1	2	0	0	2
23.11	Left	Distal	t	0	1	4	4	2	2	0	2	2	1	1
23.11	Left	Mesial	t	1	1	4	4	3	3	1	2	1	1	1
23.11	Right	Distal	a	1	0	4	4	4	4	1	3	0	0	1
23.11	Right	Mesial	u	0	0	4	3	3	3	1	2	1	1	1
23.12	Left	Distal	s	0	0	3	3	3	3	1	2	1	1	2
23.12	Left	Mesial	s	0	0	2	1	1	1	1	1	1	1	3
23.12	Right	Distal	a	0	0	2	4	2	2	1	2	0	0	3
23.12	Right	Mesial	u	0	0	4	3	3	3	2	1	0	0	2
23.13	Left	Distal	m	0	1	1	4	1	3	1	2	1	1	2
23.13	Left	Mesial	m	0	0	2	4	2	3	2	2	0	0	2
23.13	Right	Distal	a	0	0	1	4	2	2	1	1	0	0	3
23.13	Right	Mesial	u	1	0	4	1	2	2	1	2	1	2	1
23.14	Left	Distal	l	0	1	4	4	4	4	1	3	0	0	1
23.14	Left	Mesial	l	0	0	3	4	3	3	2	2	0	0	2
23.14	Right	Distal	a	1	1	4	4	4	4	3	2	0	0	1
23.14	Right	Mesial	u	0	0	3	3	3	3	2	1	0	1	2

Defect group see 7.1 Group Distribution; Scoring see Table 6: Qualitative histology scoring system

Table 9: Qualitative histology - Results 2/2

Animal ID	Side	Defect location	Defect group	Biomaterial - Residues	Biomaterial - Quality [Defect center]	Biomaterial - Quality [Defect lingual site]	Biomaterial - Quality [Defect buccal site]	Biomaterial - Quality [Overall]	Periost - Outgrowth Reaction [Periosteal outgrowth]	Membrane - Existence and Location [Cortex]	Membrane - Existence and Location [Defect]	Other - Isolated Bone Structures [Woven bone]	Other - Isolated Bone Structures [Lamellar bone]	Other - Root of Canine Tooth	Other - Pin
23.01	Left	Distal	l	0	9	9	9	9	3	0	0	0	0	1	0
23.01	Left	Mesial	l	0	9	9	9	9	4	0	0	0	0	1	0
23.01	Right	Distal	u	1	0	1	9	1	3	0	0	2	0	1	0
23.01	Right	Mesial	a	0	9	9	9	9	2	1	1	0	1	2	1
23.03	Left	Distal	t	0	9	9	9	9	1	0	0	0	0	0	0
23.03	Left	Mesial	t	1	1	9	9	1	3	0	0	0	0	1	1
23.03	Right	Distal	u	1	0	9	9	0	2	0	0	3	0	0	0
23.03	Right	Mesial	a	0	9	9	9	9	3	0	0	0	0	1	0
23.04	Left	Distal	m	1	0	9	9	0	2	0	0	1	0	0	0
23.04	Left	Mesial	m	1	1	9	9	1	3	1	0	0	0	1	0
23.04	Right	Distal	u	1	0	0	0	0	1	1	1	1	0	0	1
23.04	Right	Mesial	a	0	9	9	9	9	0	1	1	0	0	1	0
23.05	Left	Distal	u	1	0	9	9	0	2	0	0	1	0	0	0
23.05	Left	Mesial	a	0	9	9	9	9	2	0	0	0	0	1	0
23.05	Right	Distal	t	0	9	9	9	9	2	1	9	1	0	0	0
23.05	Right	Mesial	t	1	1	9	9	1	4	0	1	1	0	0	1
23.06	Left	Distal	u	1	0	9	9	0	2	0	0	1	0	0	0
23.06	Left	Mesial	a	0	9	9	9	9	4	0	0	1	0	1	0
23.06	Right	Distal	m	1	0	9	9	0	2	0	1	0	1	0	1
23.06	Right	Mesial	m	1	0	9	9	0	1	0	1	1	0	1	0
23.07	Left	Distal	s	1	0	1	9	0	1	1	1	1	0	0	0
23.07	Left	Mesial	s	0	9	9	9	9	1	1	1	0	0	3	0
23.07	Right	Distal	u	1	0	0	9	0	2	0	0	1	0	0	1
23.07	Right	Mesial	a	0	9	9	9	9	3	0	0	0	0	1	0
23.09	Left	Distal	u	1	0	9	9	0	2	0	0	1	0	0	0
23.09	Left	Mesial	a	0	9	9	9	9	2	0	0	1	0	2	0
23.09	Right	Distal	s	1	1	9	9	1	2	1	0	0	0	0	0
23.09	Right	Mesial	s	0	9	9	9	9	3	1	1	0	0	2	0
23.10	Left	Distal	u	1	2	1	9	1	2	0	1	2	0	0	0
23.10	Left	Mesial	a	0	9	9	9	9	3	0	0	0	0	3	0
23.10	Right	Distal	l	0	9	9	9	9	3	1	0	0	1	0	0
23.10	Right	Mesial	l	0	9	9	9	9	4	0	0	1	0	2	0
23.11	Left	Distal	t	1	1	1	0	1	1	1	0	0	0	1	0
23.11	Left	Mesial	t	1	0	1	1	1	2	1	1	1	1	1	1
23.11	Right	Distal	a	0	9	9	9	9	3	0	0	0	0	1	0
23.11	Right	Mesial	u	1	1	9	0	0	3	1	0	1	0	1	1
23.12	Left	Distal	s	1	0	9	9	0	2	0	0	3	0	1	0
23.12	Left	Mesial	s	1	0	0	9	0	4	0	1	2	0	1	0
23.12	Right	Distal	a	0	9	9	9	9	3	0	0	1	0	1	0
23.12	Right	Mesial	u	0	9	9	9	9	4	0	0	1	0	1	0
23.13	Left	Distal	m	1	0	1	1	0	3	0	0	0	1	0	0
23.13	Left	Mesial	m	0	9	9	9	9	3	0	0	1	0	1	0
23.13	Right	Distal	a	0	9	9	9	9	2	0	1	0	0	0	0
23.13	Right	Mesial	u	1	0	1	0	0	1	0	1	2	0	0	0
23.14	Left	Distal	l	0	9	9	9	9	1	0	0	0	0	0	0
23.14	Left	Mesial	l	0	9	9	9	9	3	1	1	0	0	0	0
23.14	Right	Distal	a	0	9	9	9	9	2	0	0	0	0	1	0
23.14	Right	Mesial	u	1	0	9	9	0	3	0	1	1	0	1	0

Defect group see 7.1 Group Distribution; Scoring see Table 6: Qualitative histology scoring system

Table 10: Histomorphometry - Results

Animal Study ID	Group	Location		0.0-0.1mm			0.1-0.2mm			0.2-0.5mm		
	Defect	Side	Defect	Old bone in %	New bone in %	Matrix in %	Old bone in %	New bone in %	Matrix in %	Old bone in %	New bone in %	Matrix in %
23.01	a	right	mesial	*	*	*	*	*	*	*	*	*
23.01	u	right	distal	0.00	10.43	89.57	0.00	23.51	76.49	0.00	30.13	69.87
23.01	l	left	distal	*	*	*	*	*	*	*	*	*
23.01	l	left	mesial	*	*	*	*	*	*	*	*	*
23.03	a	right	mesial	*	*	*	*	*	*	*	*	*
23.03	u	right	distal	0.00	0.68	99.32	0.00	5.20	94.80	0.00	9.72	90.28
23.03	t	left	distal	-	-	-	-	-	-	-	-	-
23.03	t	left	mesial	0.00	0.13	99.87	0.00	4.51	95.49	0.00	5.75	94.25
23.04	a	right	mesial	*	*	*	*	*	*	*	*	*
23.04	u	right	distal	0.00	0.02	99.98	0.00	0.68	99.32	0.00	3.76	96.24
23.04	m	left	distal	0.00	0.02	99.98	0.00	1.68	98.32	0.00	5.17	94.83
23.04	m	left	mesial	0.00	9.84	90.16	0.00	22.32	77.68	0.00	33.18	66.82
23.05	a	left	mesial	*	*	*	*	*	*	*	*	*
23.05	u	left	distal	0.00	0.03	99.97	0.00	0.20	99.80	0.00	1.75	98.25
23.05	t	right	distal	0.00	11.52	88.48	0.00	23.91	76.09	0.00	34.37	65.63
23.05	t	right	mesial	0.00	0.94	99.06	0.00	8.26	91.74	0.00	29.83	70.17
23.06	a	left	mesial	*	*	*	*	*	*	*	*	*
23.06	u	left	distal	0.00	0.00	100.00	0.00	0.36	99.64	0.00	2.17	97.83
23.06	m	right	distal	0.00	0.00	100.00	0.00	0.00	100.00	0.00	0.37	99.63
23.06	m	right	mesial	0.00	0.90	99.10	0.00	5.81	94.19	0.00	20.71	79.29
23.07	a [1)]	right	mesial	0.00	0.00	100.00	0.00	0.00	100.00	0.00	0.00	100.00
23.07	u	right	distal	0.00	0.41	99.59	0.00	2.03	97.97	0.00	3.93	96.07
23.07	s	left	distal	0.00	0.37	99.63	0.00	1.82	98.18	0.00	12.51	87.49
23.07	s	left	mesial	-	-	-	-	-	-	-	-	-
23.09	a	left	mesial	*	*	*	*	*	*	*	*	*
23.09	u	left	distal	0.00	0.00	100.00	0.00	0.00	100.00	0.00	0.00	100.00
23.09	s	right	distal	0.00	0.14	99.86	0.00	5.45	94.55	0.00	21.65	78.35
23.09	s	right	mesial	-	-	-	-	-	-	-	-	-
23.10	a	left	mesial	*	*	*	*	*	*	*	*	*
23.10	u	left	distal	0.00	0.49	99.51	0.00	0.78	99.22	0.00	0.83	99.17
23.10	l	right	distal	*	*	*	*	*	*	*	*	*
23.10	l	right	mesial	*	*	*	*	*	*	*	*	*
23.11	a [1)]	right	distal	0.00	0.00	100.00	0.00	0.00	100.00	0.00	0.00	100.00
23.11	u	right	mesial	0.37	2.31	97.32	2.00	9.07	88.93	2.60	16.00	81.39
23.11	t	left	distal	0.00	6.70	93.30	0.00	22.96	77.04	0.00	38.49	61.51
23.11	t	left	mesial	0.00	5.03	94.97	0.00	22.33	77.67	0.00	30.10	69.90
23.12	a	right	distal	*	*	*	*	*	*	*	*	*
23.12	u	right	mesial	0.00	24.93	75.07	8.75	38.48	52.77	11.39	33.05	55.56
23.12	s	left	distal	0.00	0.00	100.00	0.00	0.00	100.00	0.00	1.18	98.82
23.12	s	left	mesial	0.00	0.09	99.91	0.00	5.08	94.92	0.24	23.09	76.67
23.13	a	right	distal	*	*	*	*	*	*	*	*	*
23.13	u	right	mesial	0.00	0.27	99.73	0.00	3.13	96.87	0.00	10.83	89.17
23.13	m	left	distal	0.00	1.92	98.08	0.00	12.87	87.13	0.46	29.33	70.21
23.13	m	left	mesial	-	-	-	-	-	-	-	-	-
23.14	a	right	distal	*	*	*	*	*	*	*	*	*
23.14	u	right	mesial	0.00	0.00	100.00	0.00	0.00	100.00	0.00	2.23	97.77
23.14	l	left	distal	*	*	*	*	*	*	*	*	*
23.14	l	left	mesial	*	*	*	*	*	*	*	*	*

Defect group see 7.1 Group Distribution

[1)] biomaterial residues were found although not implanted at that specific defect location

*: no biomaterial implanted/cell intentionally left blank

-: biomaterial implanted but no residues seen on slide and therefore not evaluated

Table 11: Histomorphometry - Descriptives and Analysis of Variance

Dependent Variable:	**Old bone (0.0-0.1mm)**	**UNIANOVA Sig.:**	**0.783**
Defect	Mean	Std. Deviation	N
unmodified	0.03	0.11	12
montelukast	0.00	0.00	5
simvastatin	0.00	0.00	4
teriparatide	0.00	0.00	5
Total	0.01	0.07	26
Dependent Variable:	**New bone (0.0-0.1mm)**	**UNIANOVA Sig.:**	**0.685**
Defect	Mean	Std. Deviation	N
unmodified	3.30	7.42	12
montelukast	2.53	4.16	5
simvastatin	0.15	0.16	4
teriparatide	4.86	4.62	5
Total	2.97	5.70	26
Dependent Variable:	**Fibrous tissue (0.0-0.1mm)**	**UNIANOVA Sig.:**	**0.684**
Defect	Mean	Std. Deviation	N
unmodified	96.67	7.42	12
montelukast	97.47	4.16	5
simvastatin	99.85	0.16	4
teriparatide	95.14	4.62	5
Total	97.02	5.70	26
Dependent Variable:	**Old bone (0.1-0.2mm)**	**UNIANOVA Sig.:**	**0.662**
Defect	Mean	Std. Deviation	N
unmodified	0.90	2.54	12
montelukast	0.00	0.00	5
simvastatin	0.00	0.00	4
teriparatide	0.00	0.00	5
Total	0.41	1.74	26
Dependent Variable:	**New bone (0.1-0.2mm)**	**UNIANOVA Sig.:**	**0.249**
Defect	Mean	Std. Deviation	N
unmodified	6.95	11.98	12
montelukast	8.54	9.17	5
simvastatin	3.09	2.63	4
teriparatide	16.39	9.25	5
Total	8.48	10.46	26
Dependent Variable:	**Fibrous tissue (0.1-0.2mm)**	**UNIANOVA Sig.:**	**0.376**
Defect	Mean	Std. Deviation	N
unmodified	92.15	14.17	12
montelukast	91.46	9.17	5
simvastatin	96.91	2.63	4
teriparatide	83.61	9.25	5
Total	91.11	11.55	26
Dependent Variable:	**Old bone (0.2-0.5mm)**	**UNIANOVA Sig.:**	**0.692**
Defect	Mean	Std. Deviation	N
unmodified	1.17	3.31	12
montelukast	0.09	0.21	5
simvastatin	0.06	0.12	4
teriparatide	0.00	0.00	5
Total	0.57	2.27	26
Dependent Variable:	**New bone (0.2-0.5mm)**	**UNIANOVA Sig.:**	**0.068**
Defect	Mean	Std. Deviation	N
unmodified	9.53	11.36	12
montelukast	17.75	14.50	5
simvastatin	14.61	10.10	4
teriparatide	27.71	12.78	5
Total	15.39	13.30	26
Dependent Variable:	**Fibrous tissue (0.2-0.5mm)**	**UNIANOVA Sig.:**	**0.150**
Defect	Mean	Std. Deviation	N
unmodified	89.30	13.85	12
montelukast	82.16	14.60	5

simvastatin	85.33	10.17	4
teriparatide	72.29	12.78	5
Total	84.05	14.10	26

UNIANOVA Sig.: p-value from univariate analysis of variance, $p < 0.05$ is considered significant; Std. Deviation: Standard deviation; N: Number of valid cases

7.3 Figures

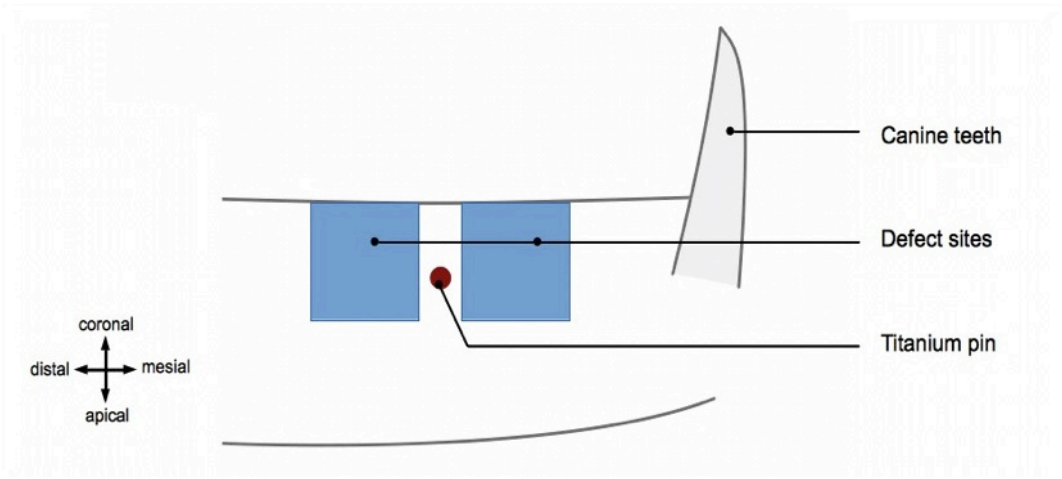

Figure 1: Second stage surgery - location of titanium pin

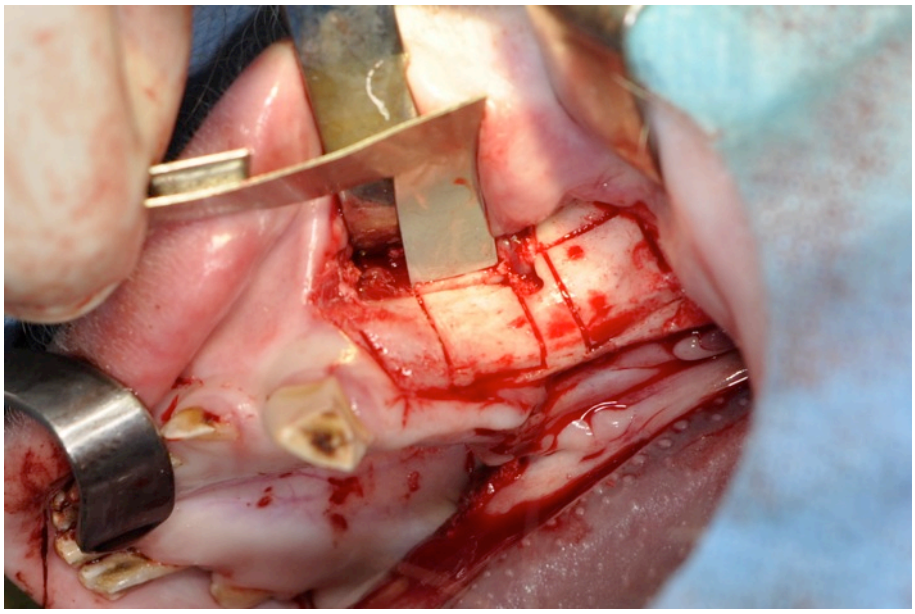

Figure 2: Intraoperative photograph of defect margins (23.01 right hemimandible)

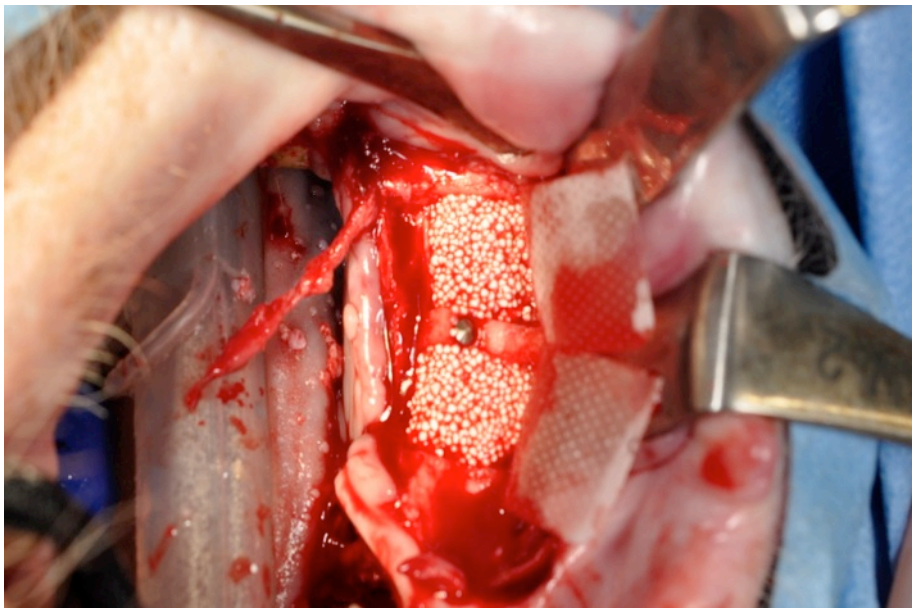

Figure 3: Intraoperative photograph of filled defects with montelukast-modified PLGA coated β-TCP, titanium pin in the bony bridge separating the defects and membranes ready for closure (23.04 left hemimandible)

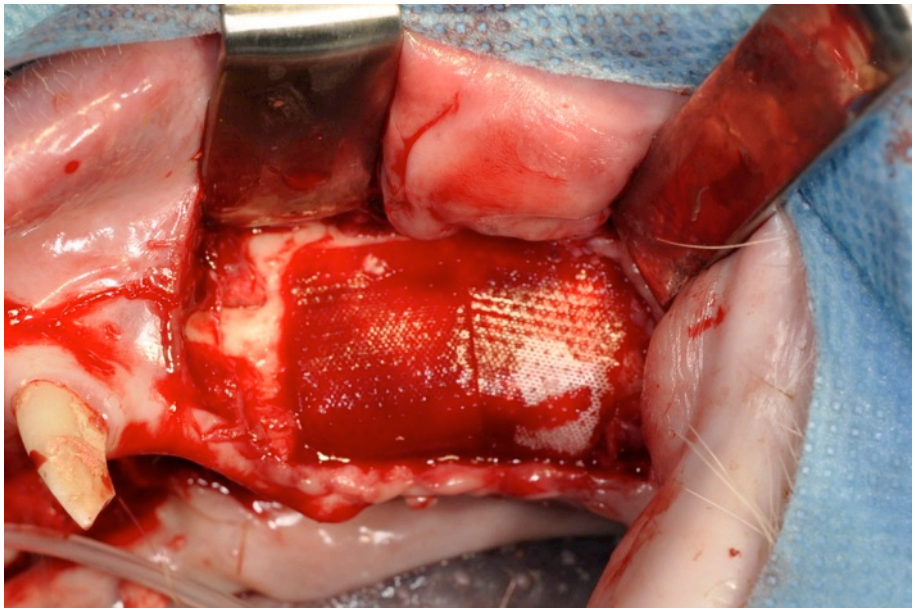

Figure 4: Intraoperative photograph on membranes of closed defects (23.04 right hemimandible)

Figure 5: Intraoperative photograph of closed mucoperiosteal flap with single, interrupted sutures (23.04 left hemimandible)

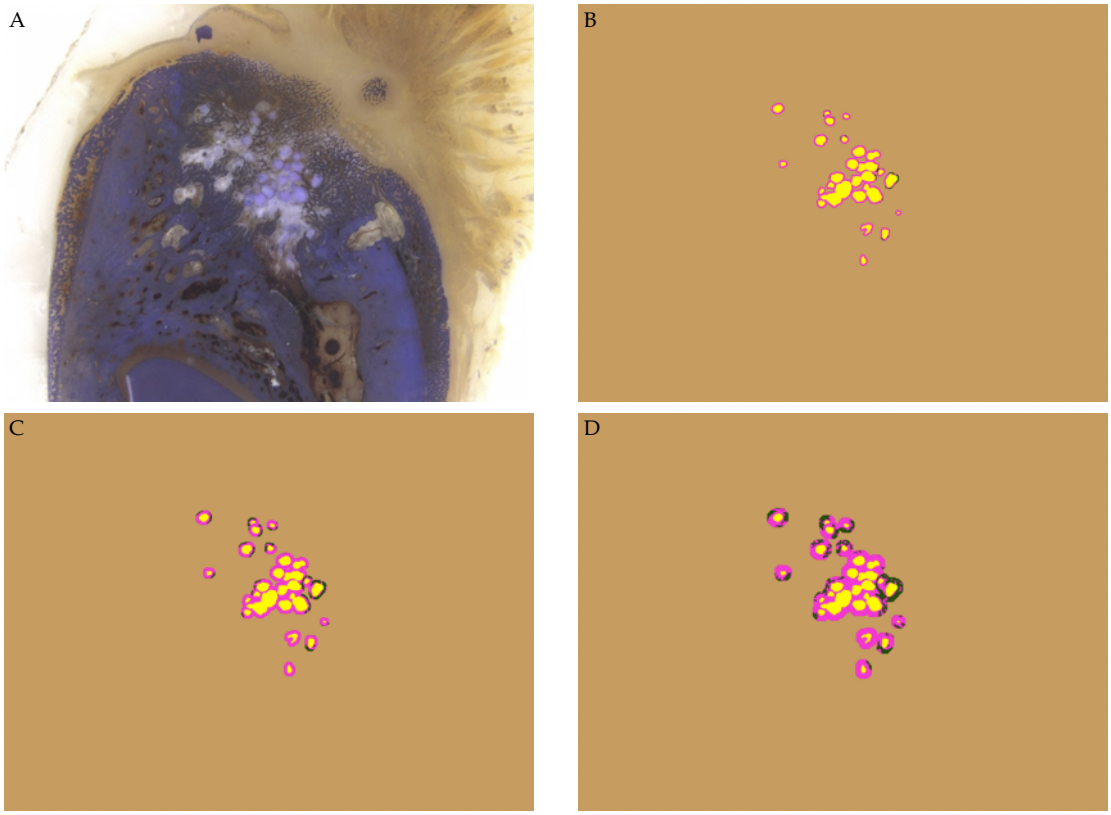

Figure 6: Histomorphometry - original (A) and recolored perimeters (B-D)

A: Histologic PMMA-thick section, toluidine blue surface staining, Montelukast group; center of the defect, perpendicular to the mandible; animal 23.11, left mandible, mesial defect, 10x magnification
B-D: Recolored for histomorphometry (background, soft tissue/matrix, biomaterial residues, new bone)
B: biomaterial residues and 0.0 - 0.1 mm perimeter (7 px), rest background
C: biomaterial residues and 0.0 - 0.2 mm perimeter (15 px), rest background
D: biomaterial residues and 0.0 - 0.5 mm perimeter (37 px), rest background

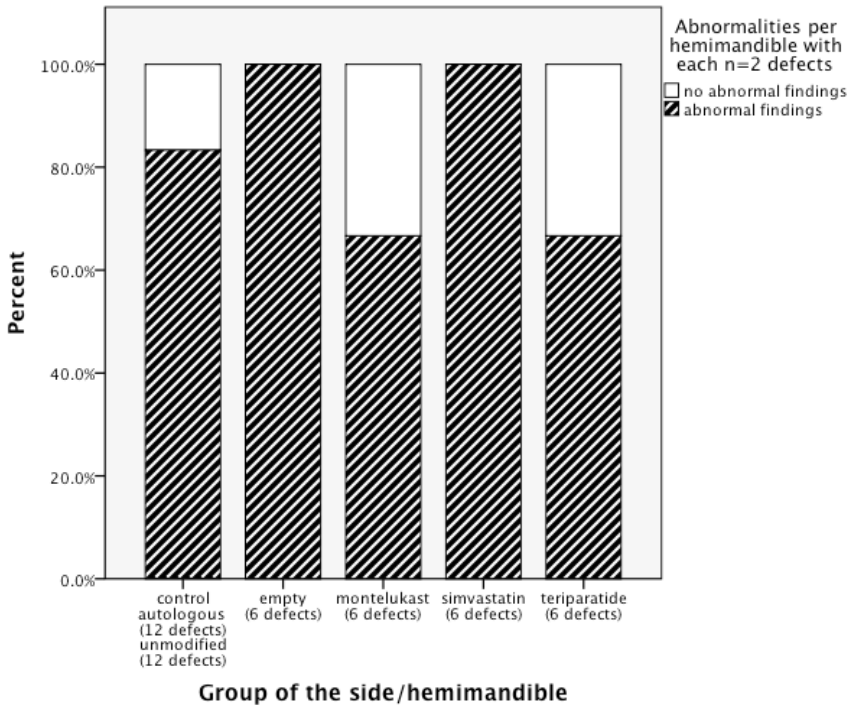

Figure 7: Macroscopic assessment of hemimandibles (n=24) - Abnormalities

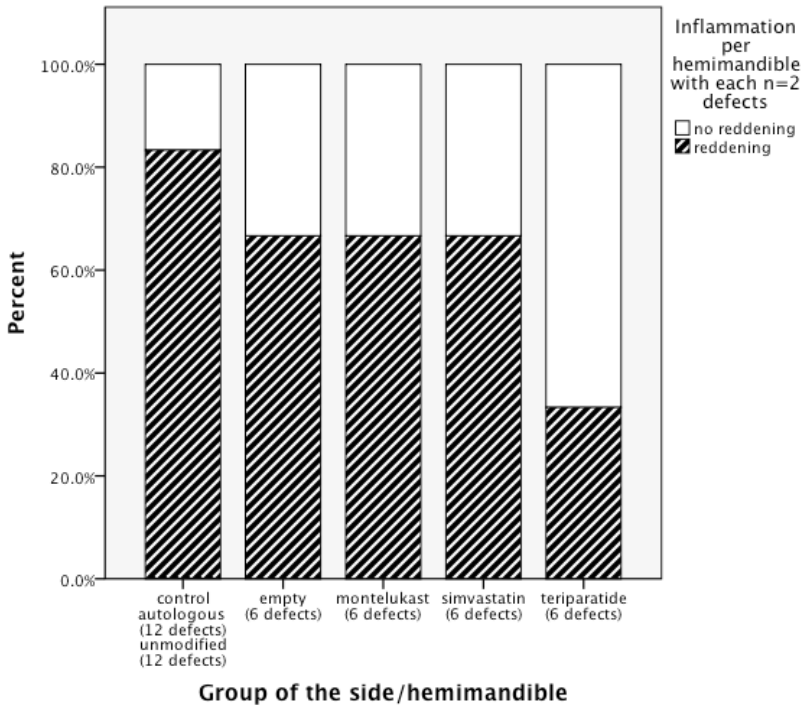

Figure 8: Macroscopic assessment of hemimandibles (n=24) - Inflammation

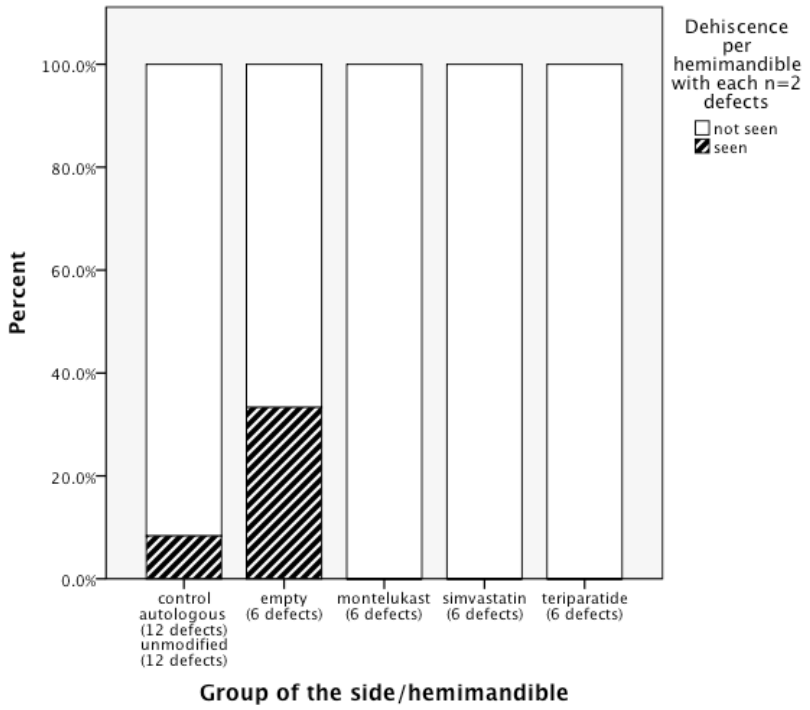

Figure 9: Macroscopic assessment of hemimandibles (n=24) - Dehiscence

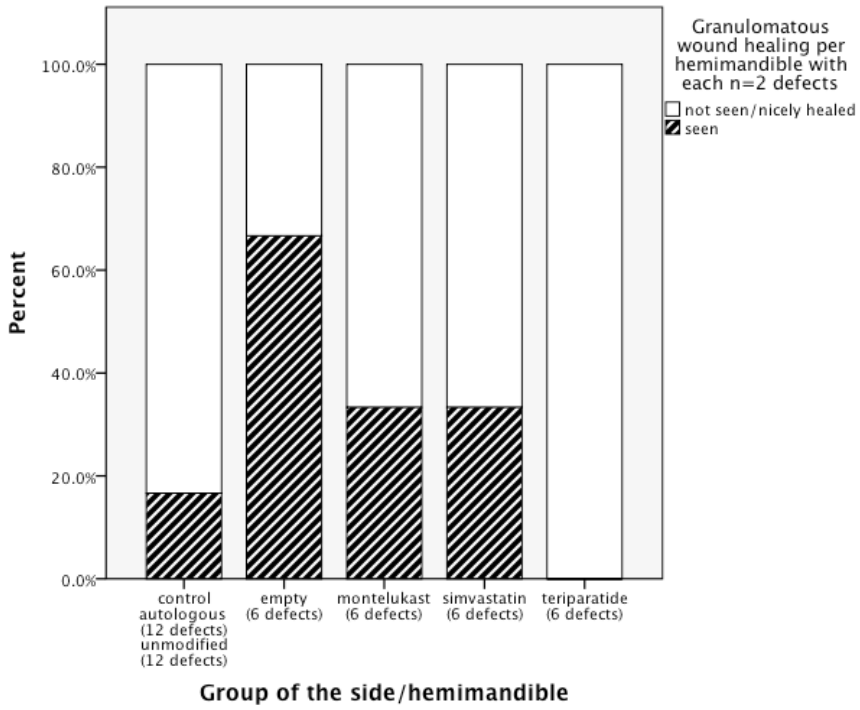

Figure 10: Macroscopic assessment of hemimandibles (n=24) - Granulomatous wound healing

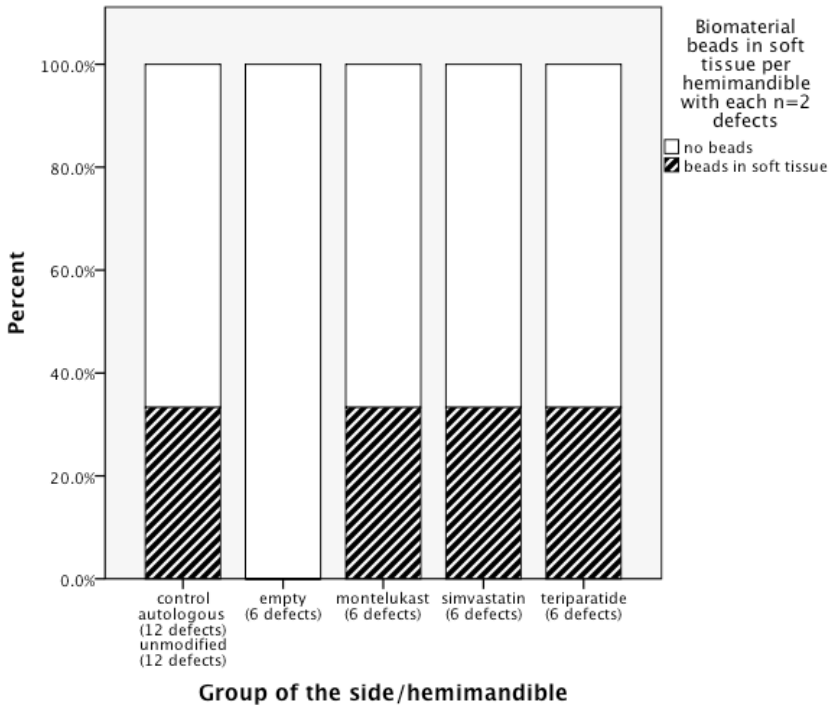

Figure 11: Macroscopic assessment of hemimandibles (n=24) - Biomaterial beads in soft tissue

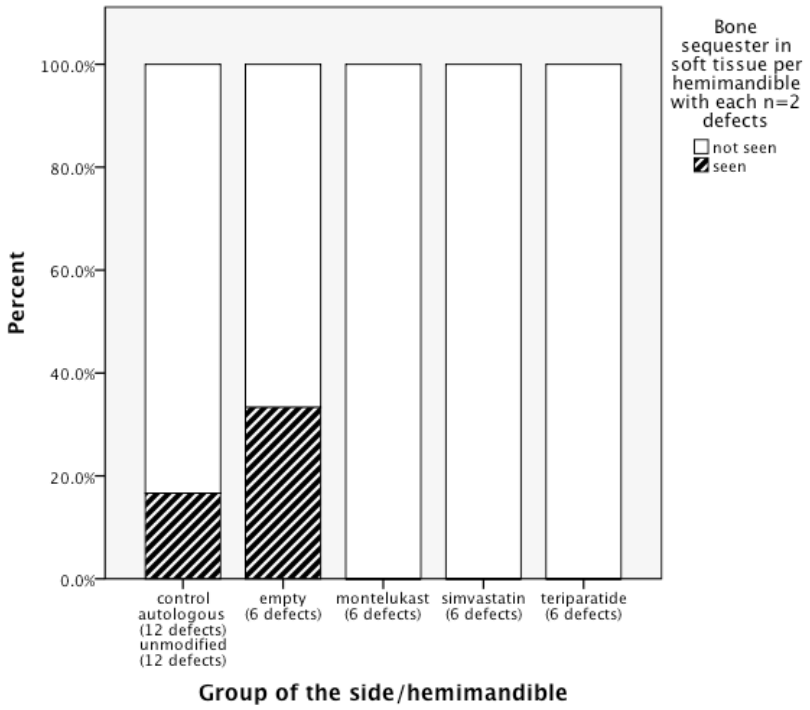

Figure 12: Macroscopic assessment of hemimandibles (n=24) - Bone sequester in soft tissue

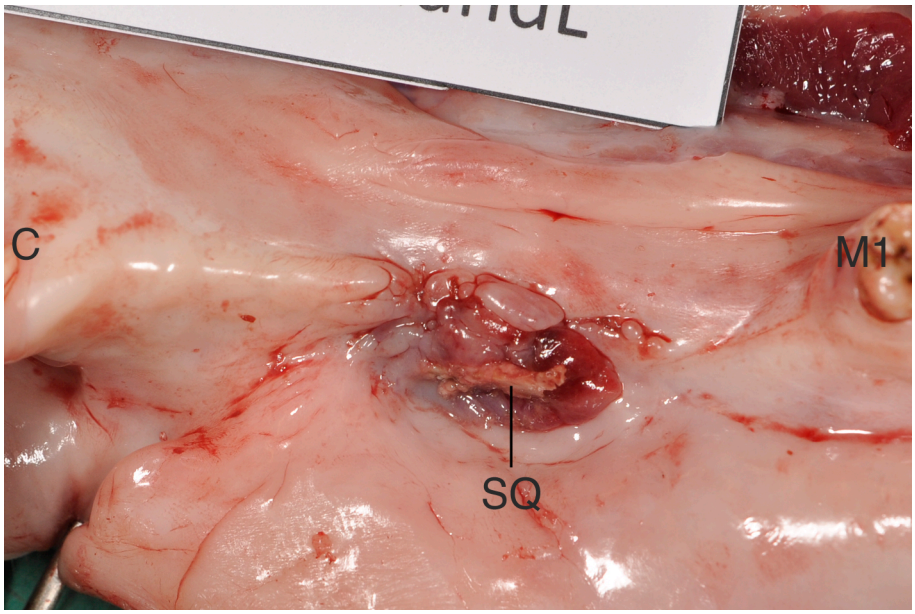

Figure 13: Macroscopic assessment - 23.01 left hemimandible, Empty group

Canine tooth (C); defect wound with dehiscence, reddening and bone sequester (SQ); first molar (M1)

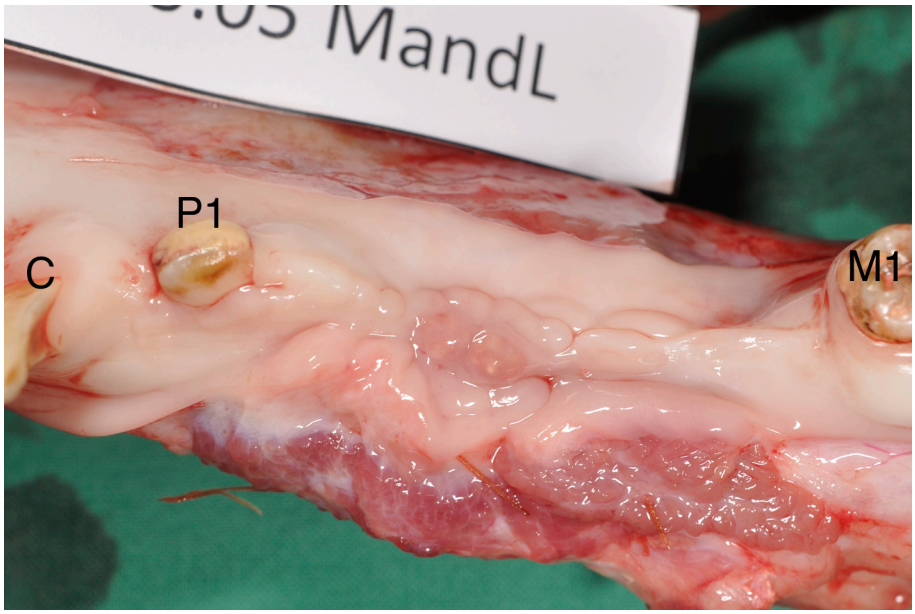

Figure 14: Macroscopic assessment - 23.05 left hemimandible, Control group

Control group (mesial defect Autologous group, distal defect Unmodified group); canine tooth (C); first premolar (P1); defect with reddening, beads and granulomatous wound healing; first molar (M1)

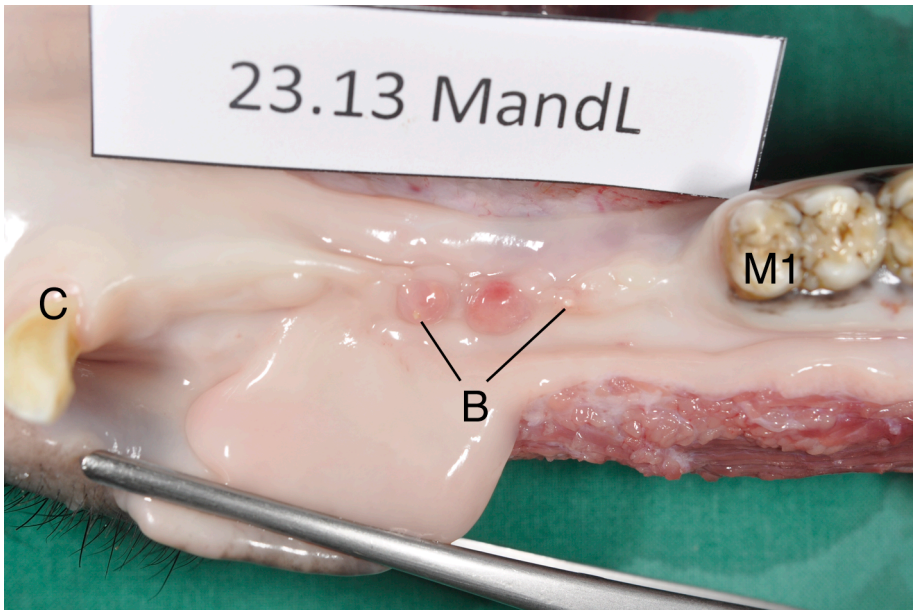

Figure 15: Macroscopic assessment - 23.13 left hemimandible, Montelukast group

Canine tooth (C); defect with granulomatous wound healing and white beads (B) in soft tissue; first molar (M1)

Figure 16: Macroscopic Assessment - 23.09 right hemimandible, Simvastatin group

Canine tooth (C); defect with signs of inflammation (reddening); first molar (M1)

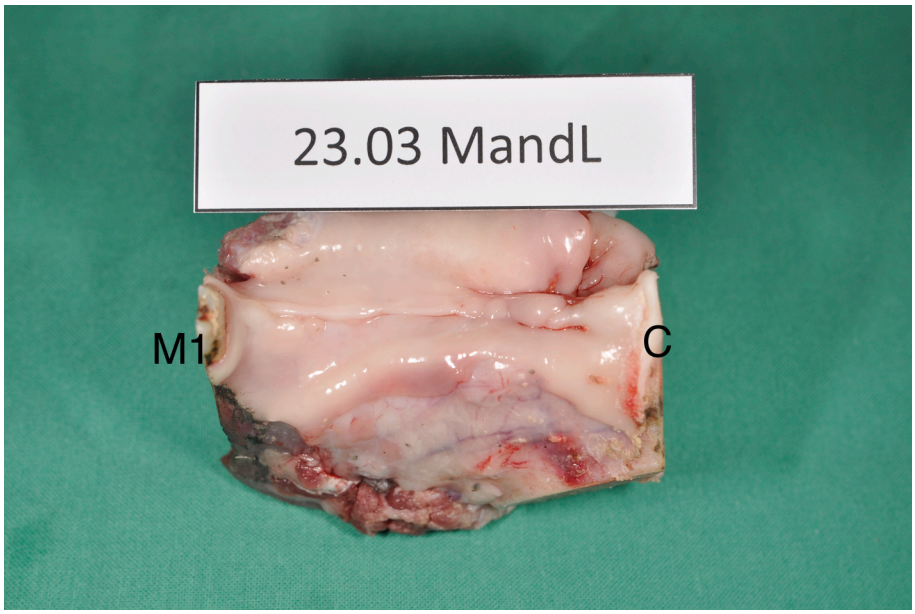

Figure 17: Macroscopic Assessment - specimen of 23.03 left hemimandible, Teriparatide group

Gingiva of canine tooth (C); defect without signs of inflammation or other abnormalities; mesial part of first molar (M1)

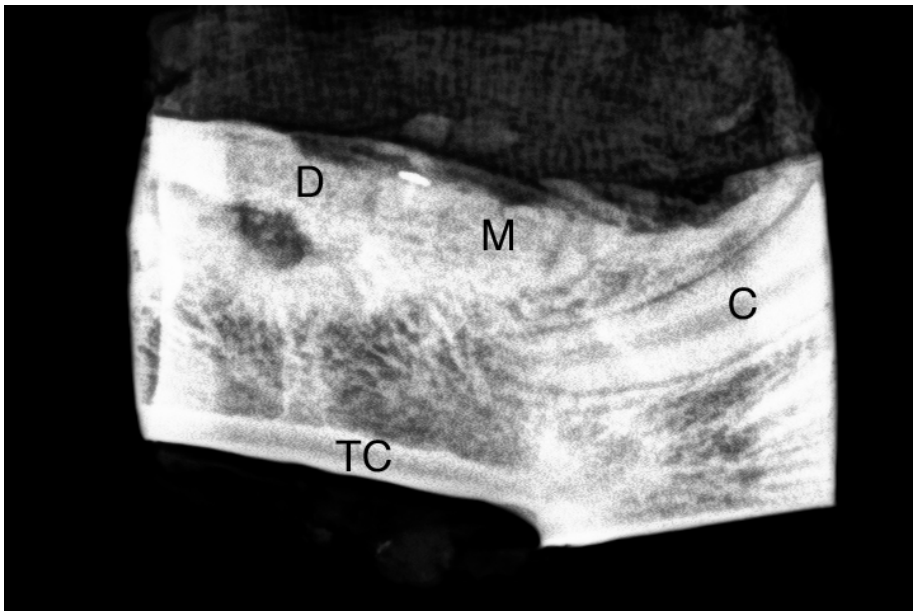

Figure 18: Radiography 23.04 right, coronoapical projection, Control group

Root of canine tooth (C); mesial defect = Autologous group (M), bony structures almost not definable (sign of resorption); defect filling 90 - 100%; distal defect = Unmodified group (D), blurry bead-like structures indicate resorption; membrane and/or periosteal outgrowth reaction; spongiosa; clearly defined trans-cortex (TC); no signs of fracture or abnormal remodeling

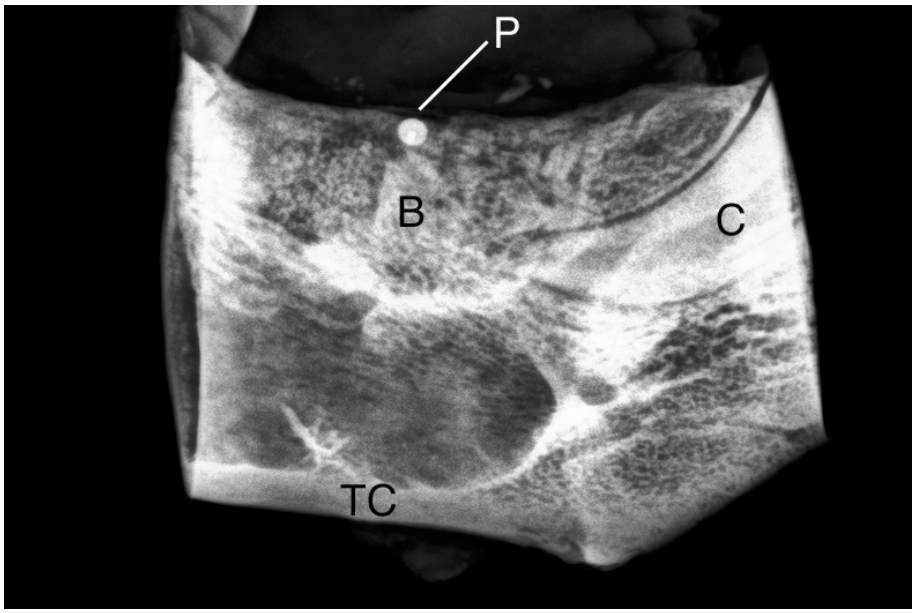

Figure 19: Radiography 23.04 right, mediolateral projection, Control group

Root of canine tooth (C); mesial defect = Autologous group (M), bony structures distinctable; distal defect = Unmodified group, bead-like structures; radiopaque bony bridge (B) separating defects with titanium pin (P); clearly defined trans-cortex (TC); bone marrow; no signs of fracture or abnormal remodeling

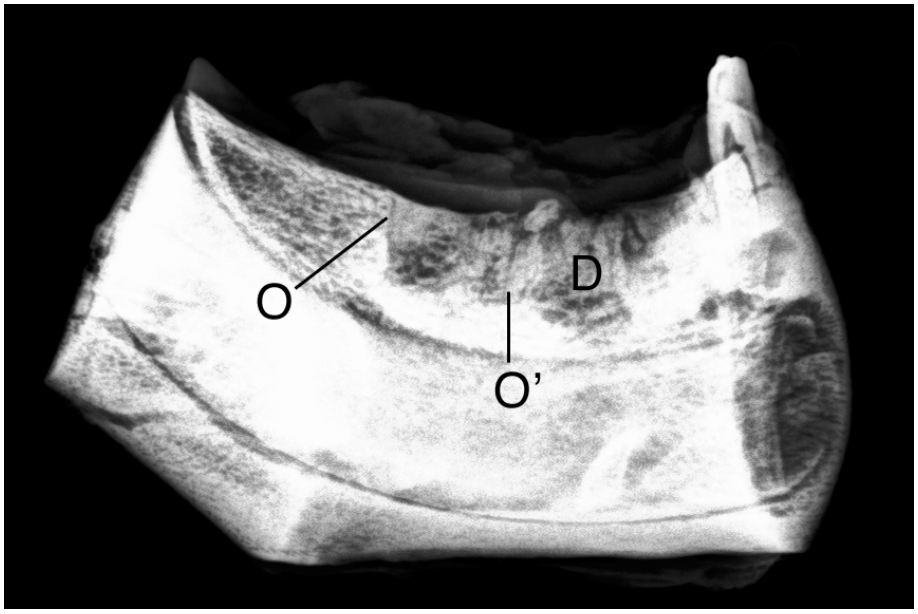

Figure 20: Radiography 23.14 left, mediolateral projection, Empty group

Mesial and distal (D) defect; clearly visible and defined osteotomy lines of mesial defect (O, O'); margins of distal defect not definable; defect cortex only slightly reduced; reduced radiodensity of defect sites; no titanium pin visible; no signs of fracture

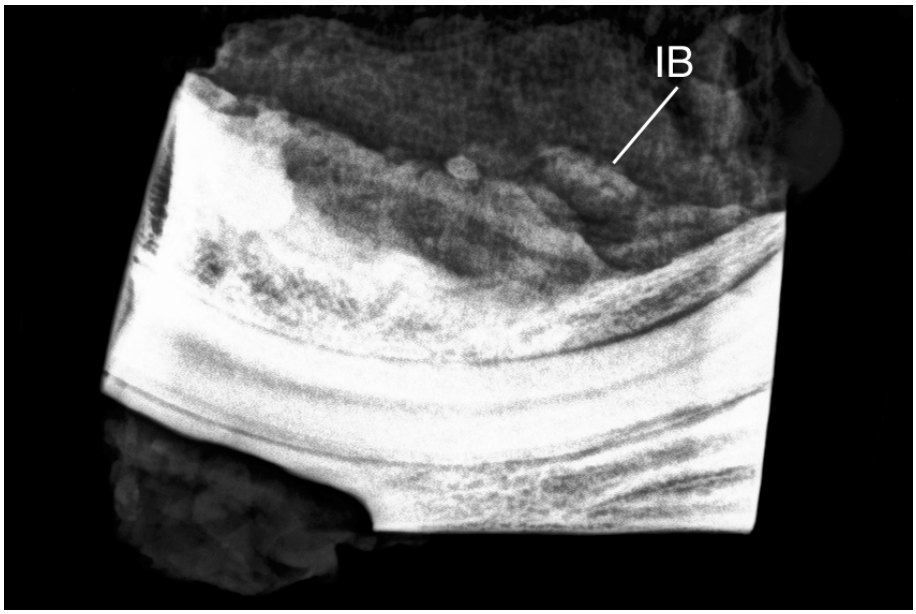

Figure 21: Radiography 23.12 right, coronoapical projection, Control group

Mesial defect = Unmodified group, not distinctable from distal defect = Autologous group; radiopaque isolated structure at mesial defect site (IB); clearly defined trans-cortex; no signs of fracture; no titanium pin

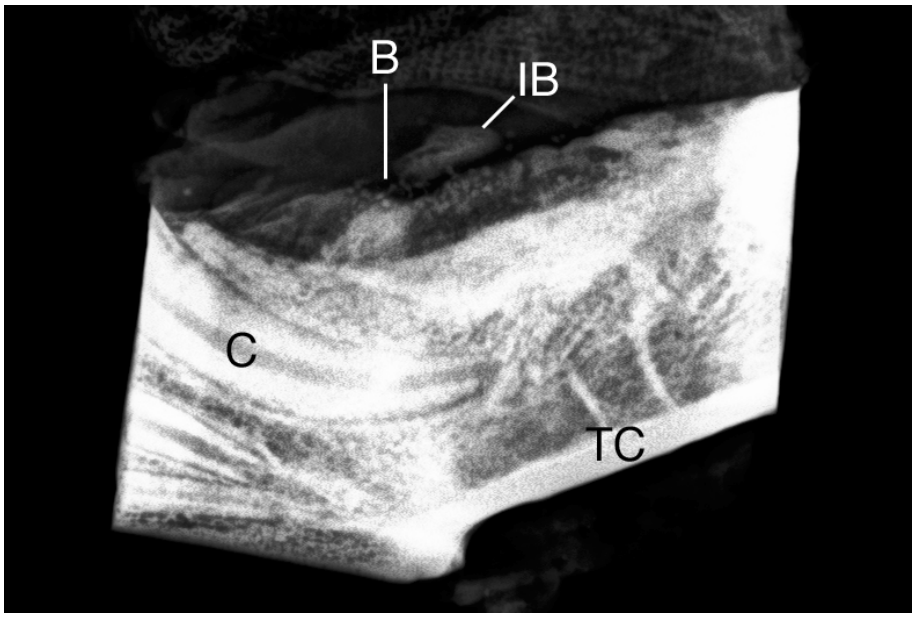

Figure 22: Radiography 23.04 left, coronoapical projection, Montelukast group

Root of canine tooth without defect contact (C); mesial defect separated from distal defect by radiopaque bony bridge (B); defect sites clearly less radiodense than surrounding bone, with bead-like radiopaque structures; isolated radiopaque structure in soft tissue (IB); clearly defined trans-cortex (TC); no signs of fracture; no titanium pin

Figure 23: Radiography 23.12 left, coronoapical projection, Simvastatin group

Missing radiopaque bony bridge separating defects; mesial and distal defect visible as single radiolucent defect area (A, A'); roots of incisivi (I); soft tissue with slight radiopaque structures; trans-cortex clearly definable; no signs of fracture

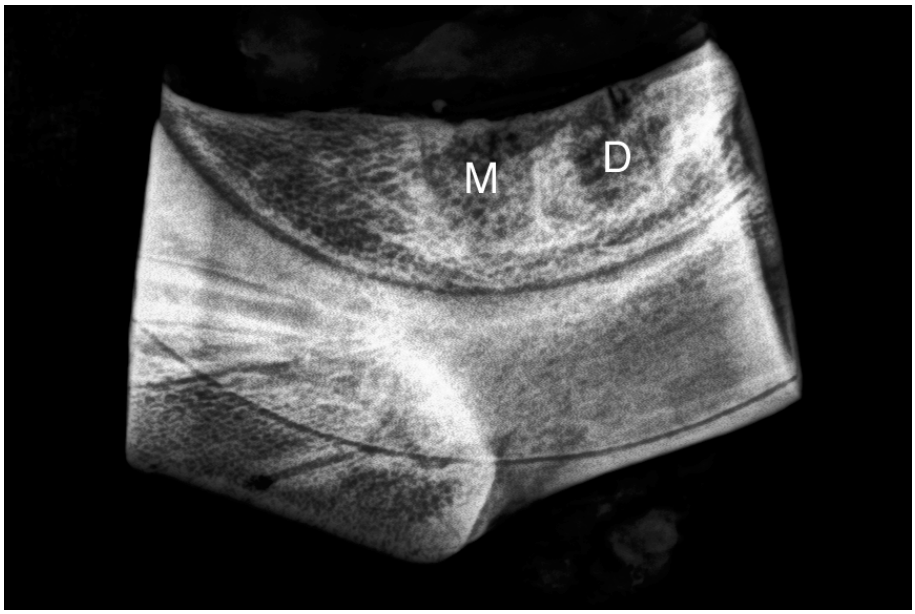

Figure 24: Radiography 23.11 left, mediolateral projection, Teriparatide group

Root of incisivi; mesial (M) and distal (D) defect with clearly visible and defined outer osteotomy; radiopaque appearance of bony bridge separating defects; no titanium pin visible

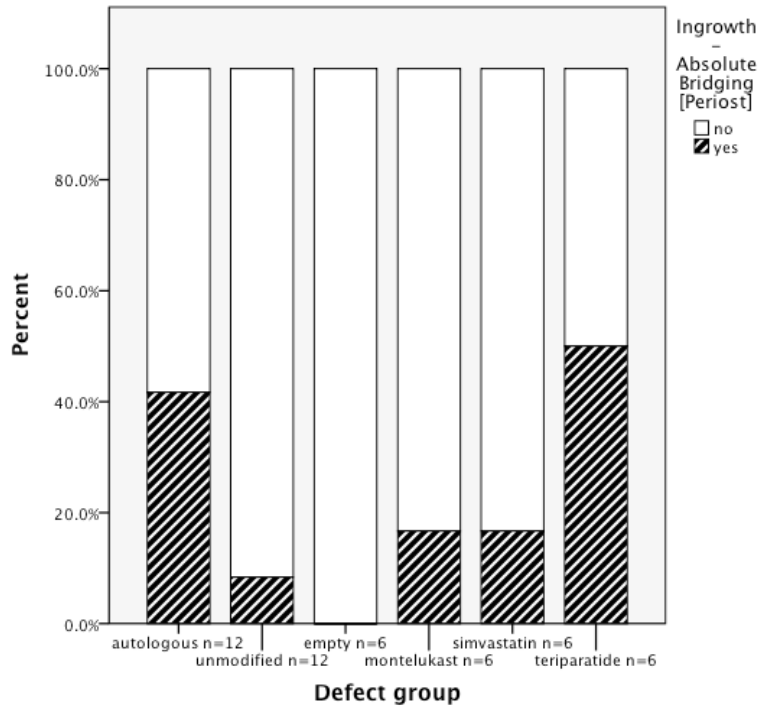

Figure 25: Qualitative histology - Ingrowth - Absolute Bridging [Periost]

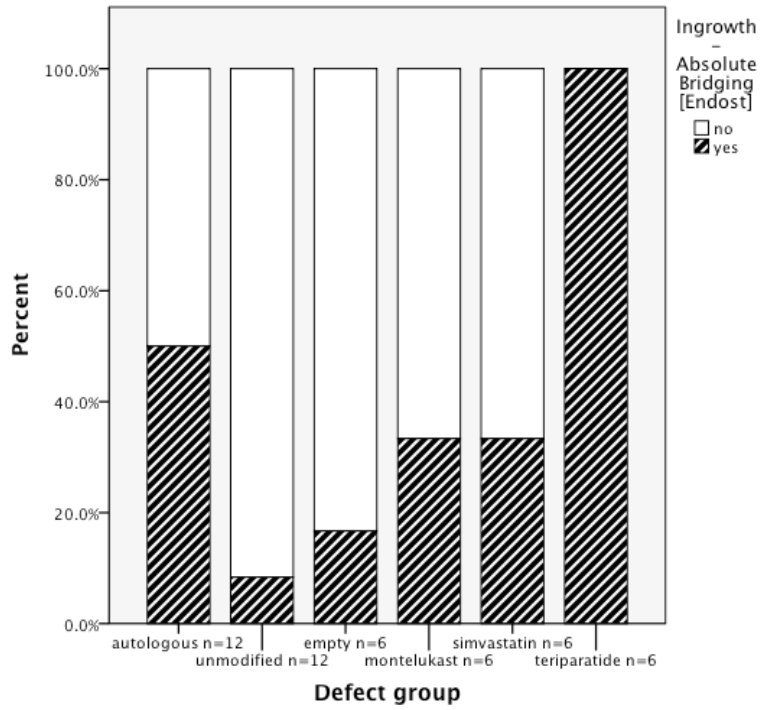

Figure 26: Qualitative histology - Ingrowth - Absolute Bridging [Endost]

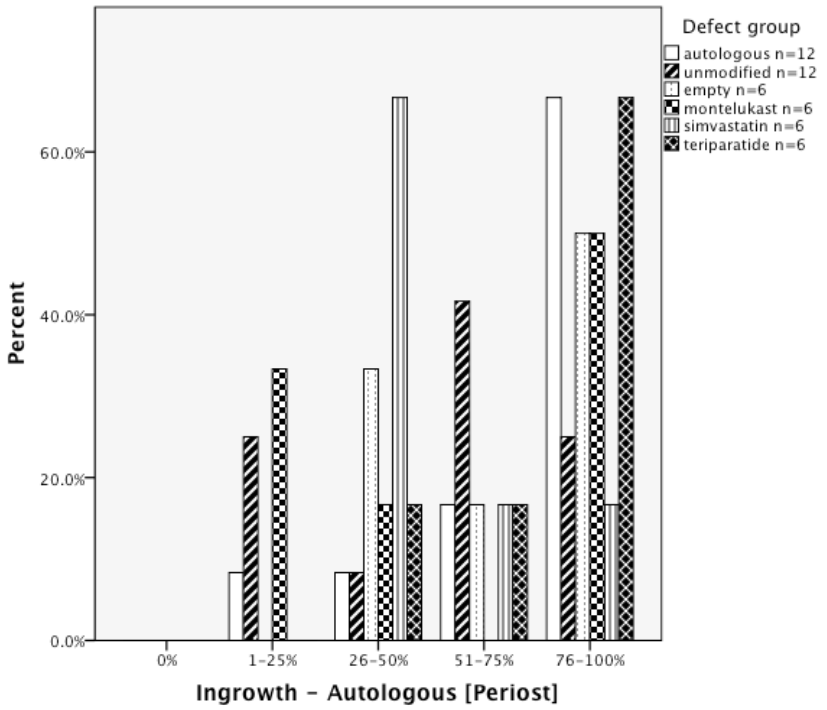

Figure 27: Qualitative histology - Ingrowth - Autologous [Periost]

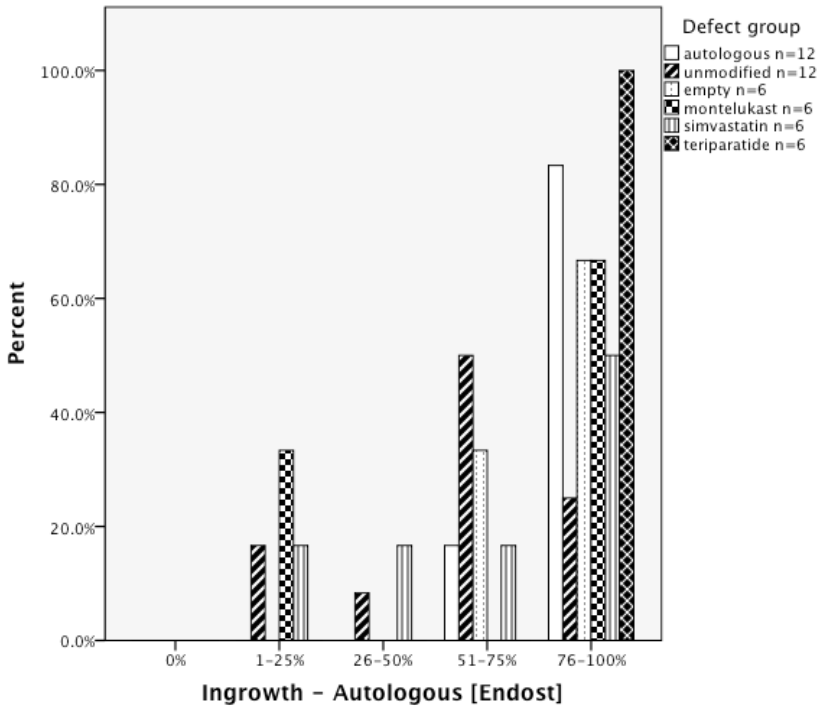

Figure 28: Qualitative histology - Ingrowth - Autologous [Endost]

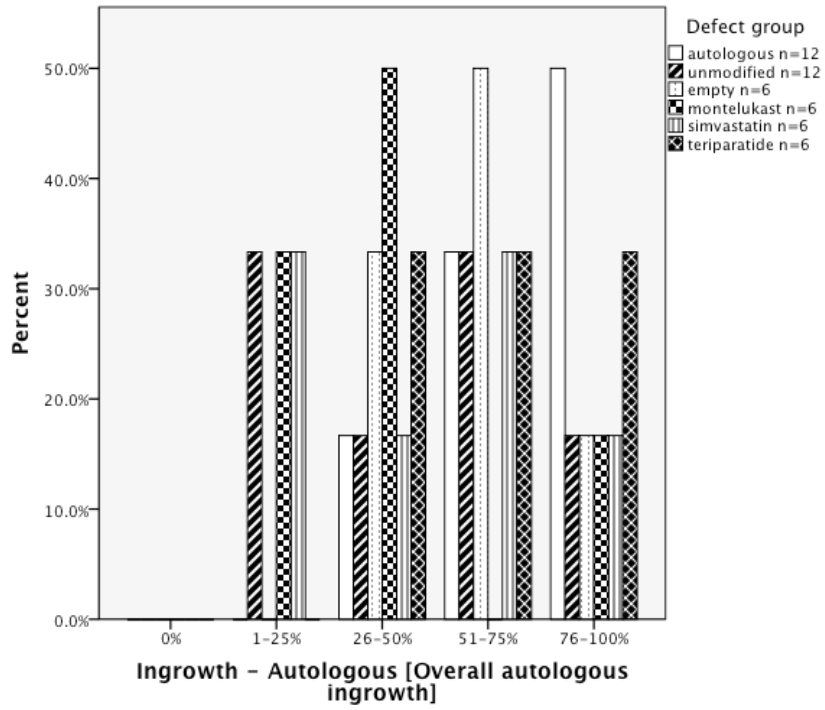

Figure 29: Qualitative histology - Ingrowth - Autologous [Overall autologous ingrowth]

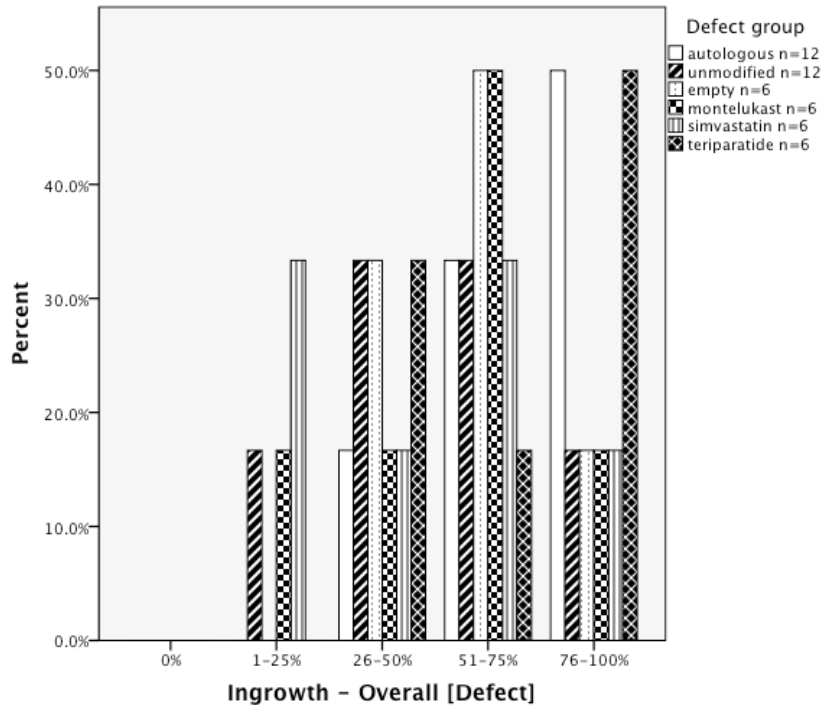

Figure 30: Qualitative histology - Ingrowth - Overall [Defect]

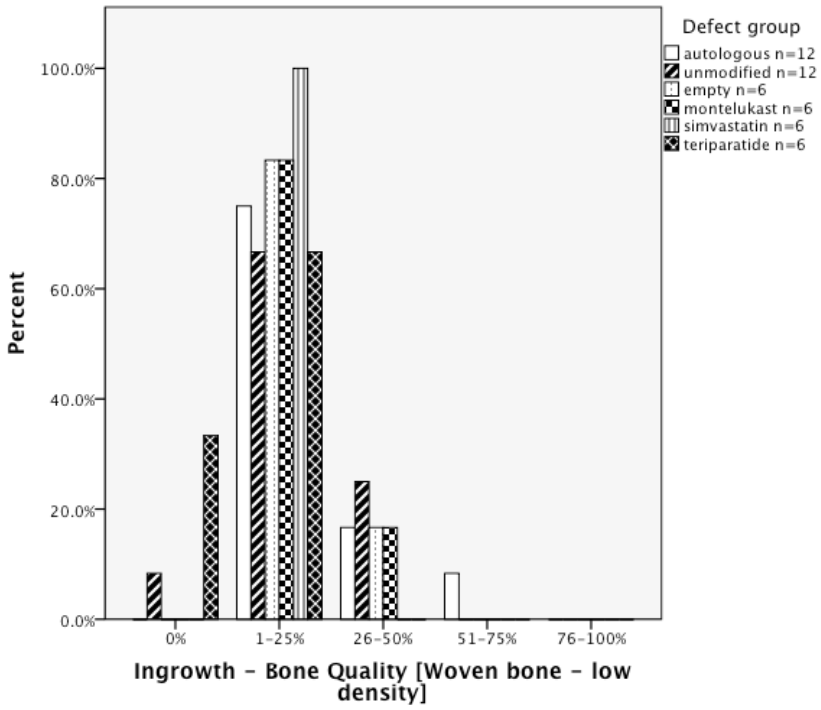

Figure 31: Qualitative histology - Ingrowth - Bone Quality (Woven bone - low density)

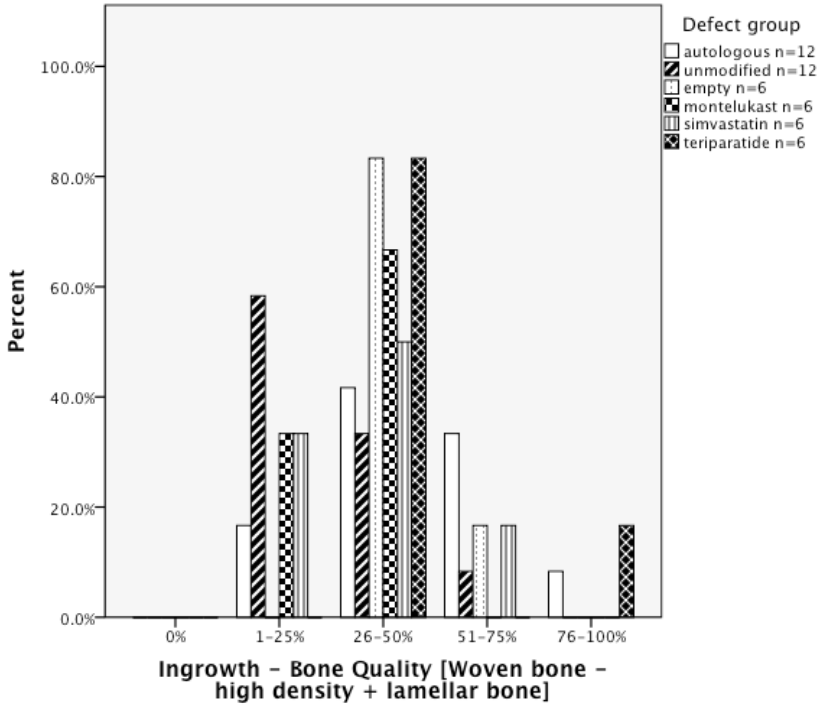

Figure 32: Qualitative histology - Ingrowth - Bone Quality (Woven bone - high density + lamellar bone)

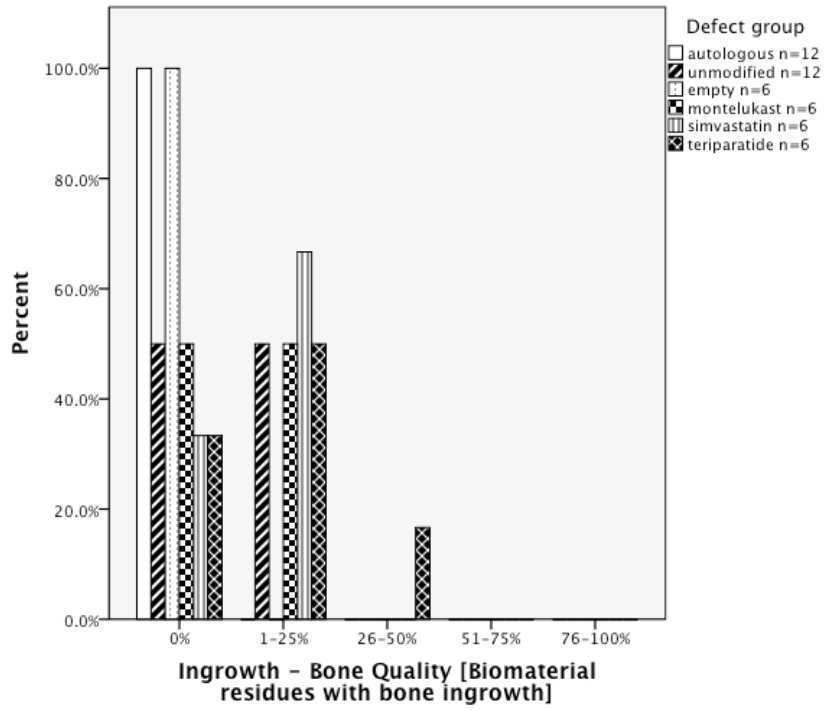

Figure 33: Qualitative histology - Ingrowth - Bone Quality (Biomaterial residues with bone ingrowth)

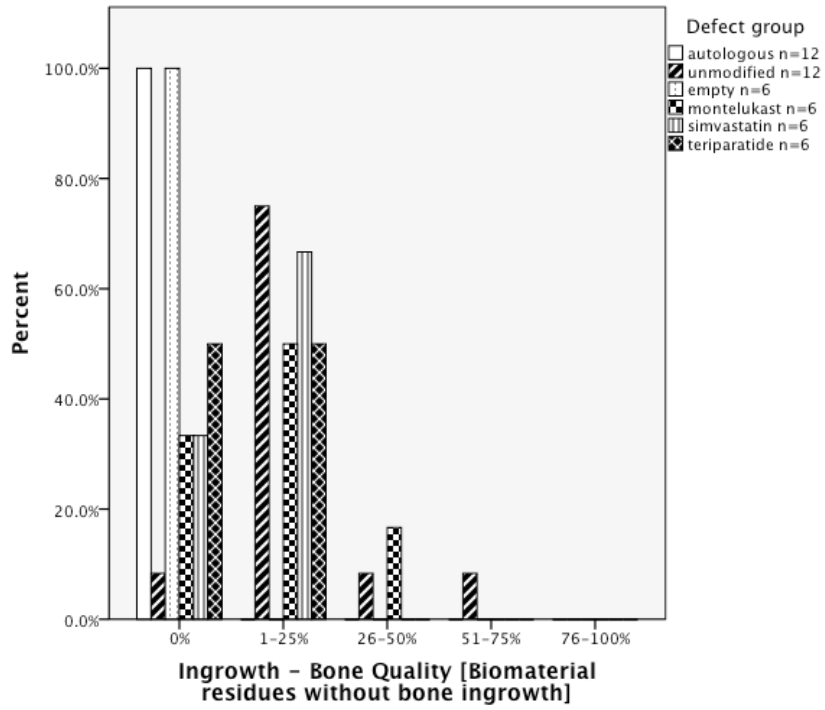

Figure 34: Qualitative histology - Ingrowth - Bone Quality (Biomaterial residues without bone ingrowth)

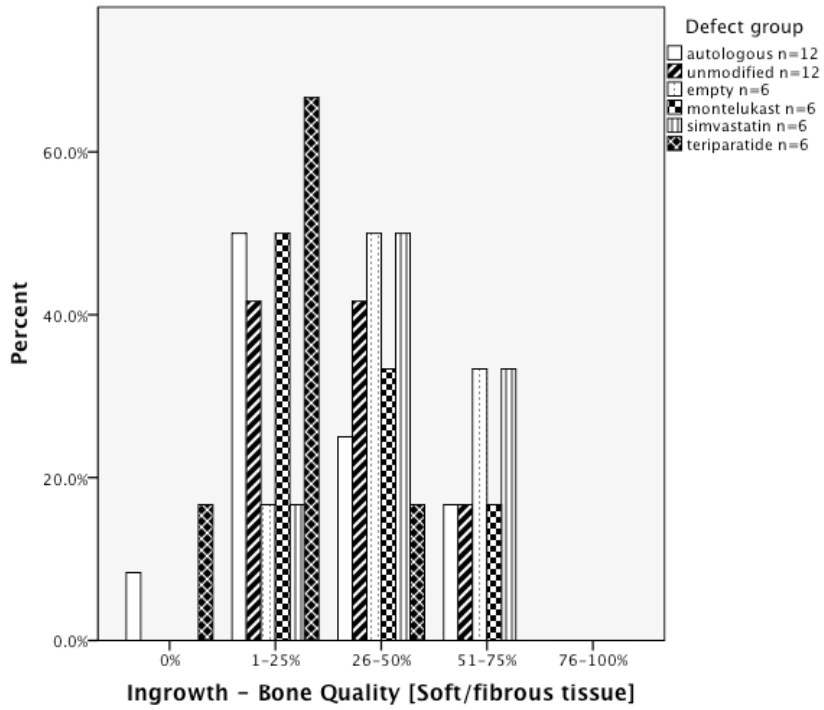

Figure 35: Qualitative histology - Ingrowth - Bone Quality (Soft/fibrous tissue)

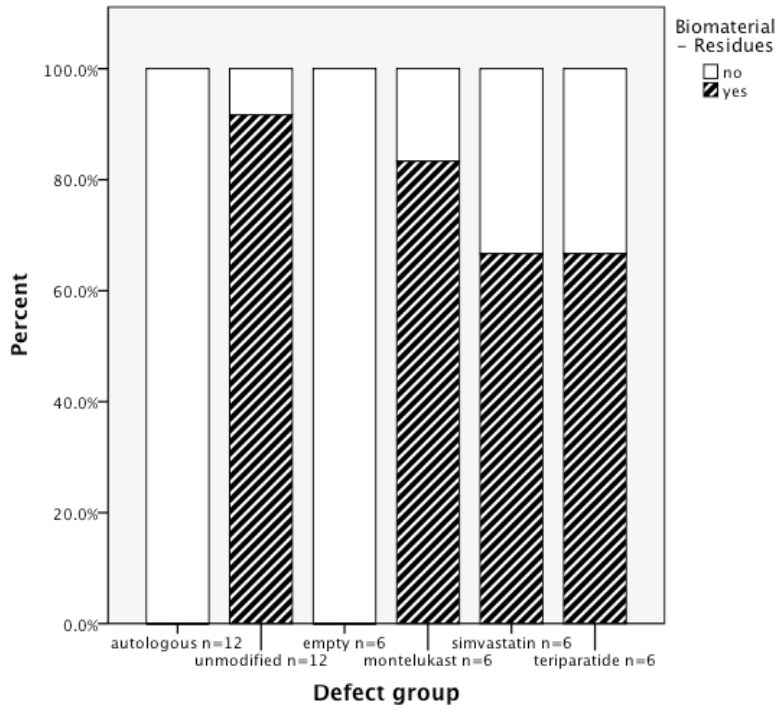

Figure 36: Qualitative histology - Biomaterial - Residues

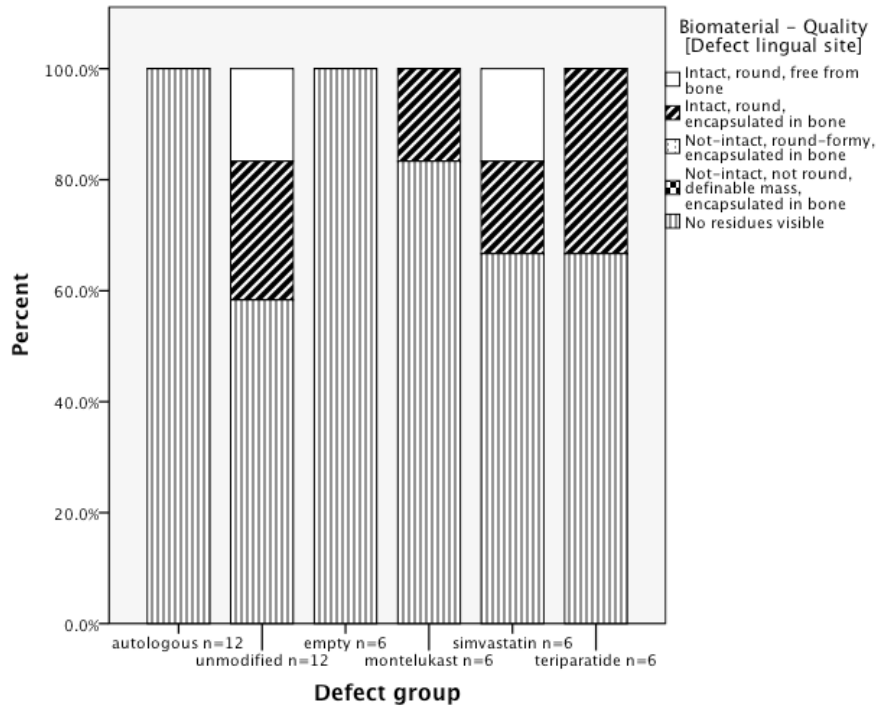

Figure 37: Qualitative histology - Biomaterial - Quality (Defect lingual site)

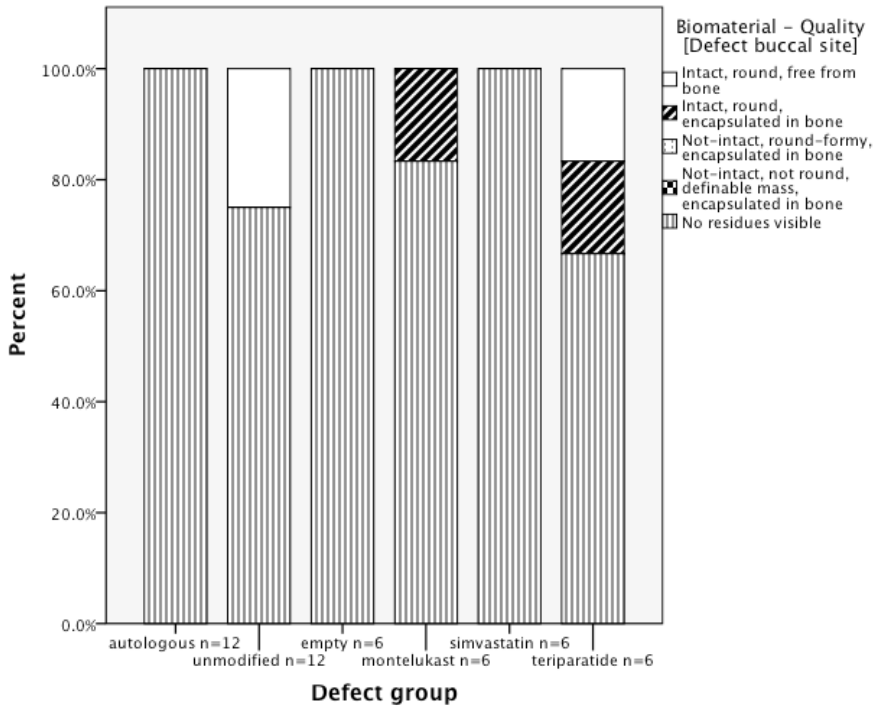

Figure 38: Qualitative histology - Biomaterial - Quality (Defect buccal site)

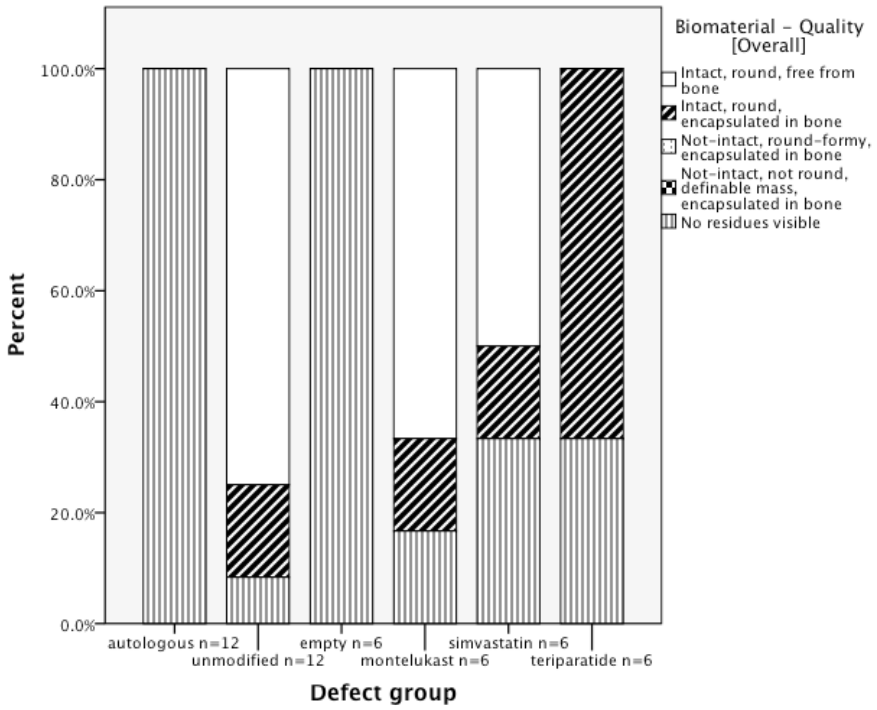

Figure 39: Qualitative histology - Biomaterial - Quality (Overall)

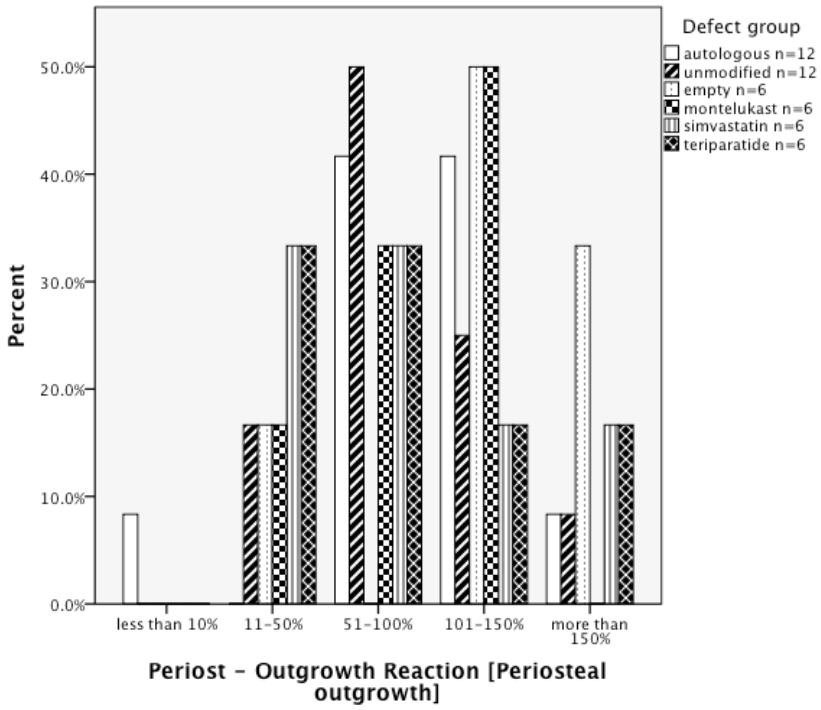

Figure 40: Qualitative histology - Periost - Outgrowth Reaction (Periosteal outgrowth)

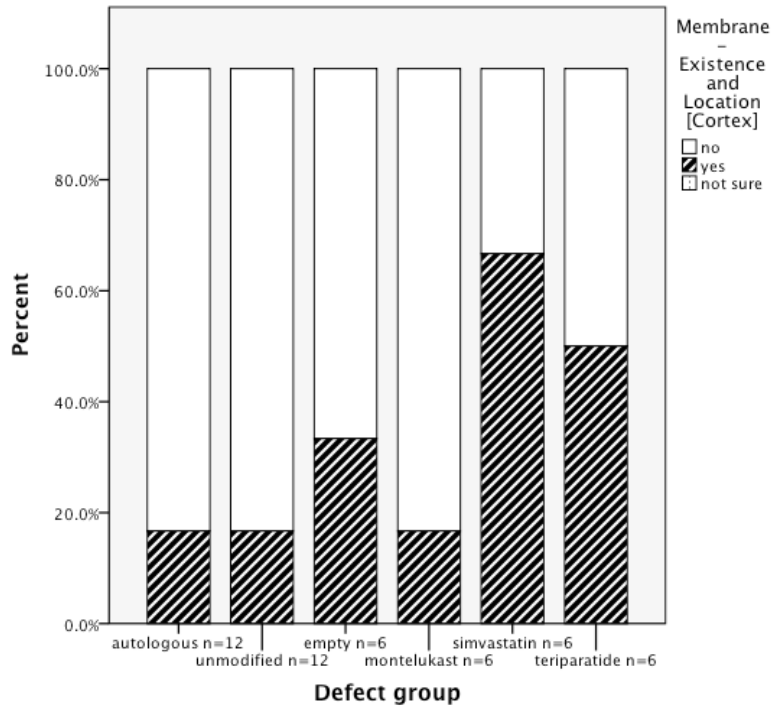

Figure 41: Qualitative histology - Membrane - Existence and Location (Cortex)

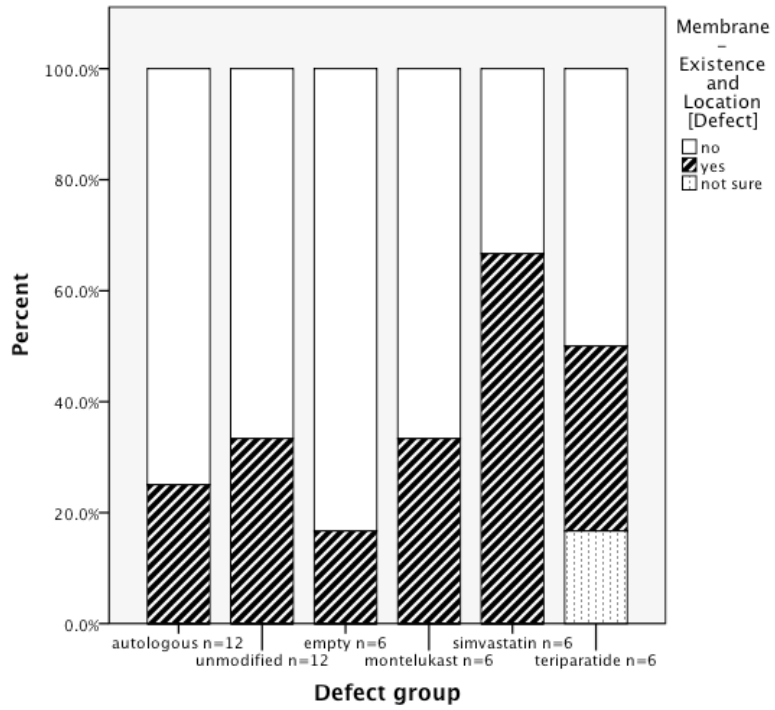

Figure 42: Qualitative histology - Membrane - Existence and Location (Defect)

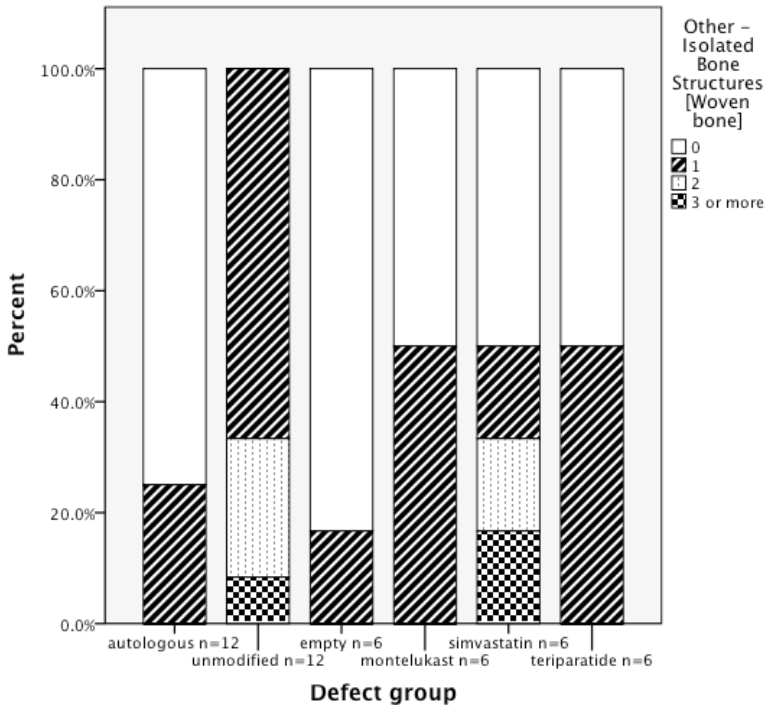

Figure 43: Qualitative histology - Other - Isolated Bone Structures (Woven bone)

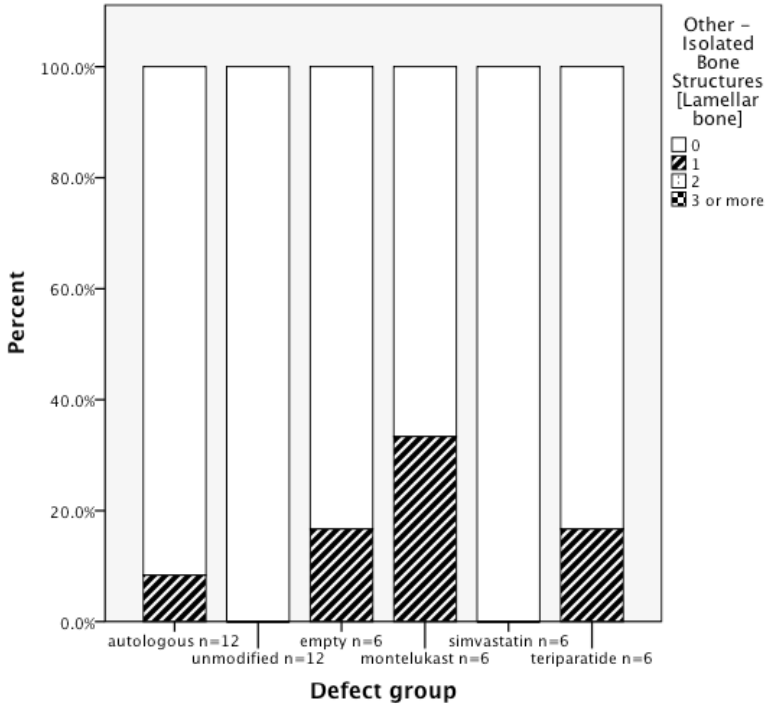

Figure 44: Qualitative histology - Other - Isolated Bone Structures (Lamellar bone)

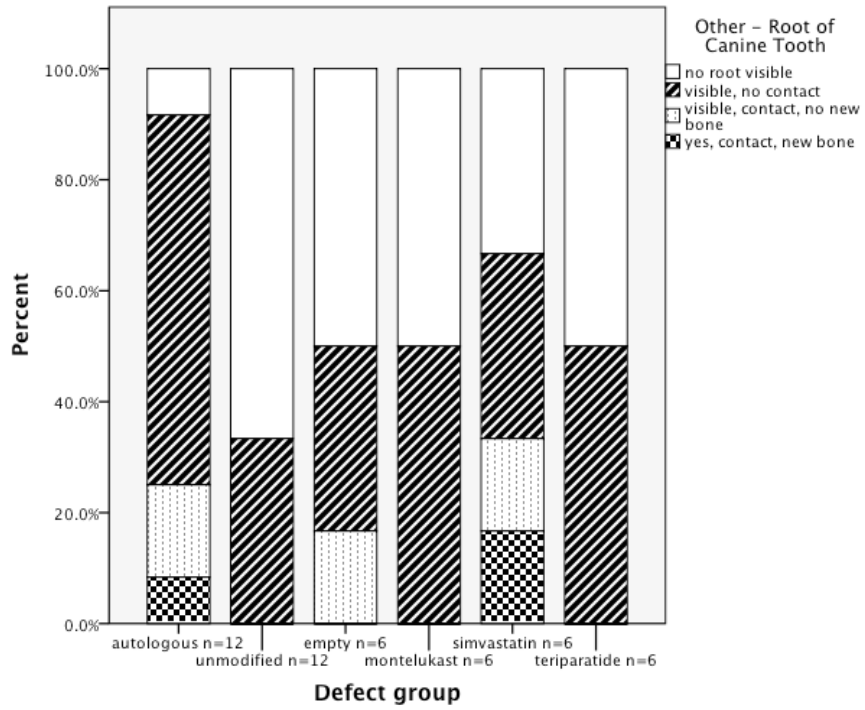

Figure 45: Qualitative histology - Other - Root of Canine Tooth

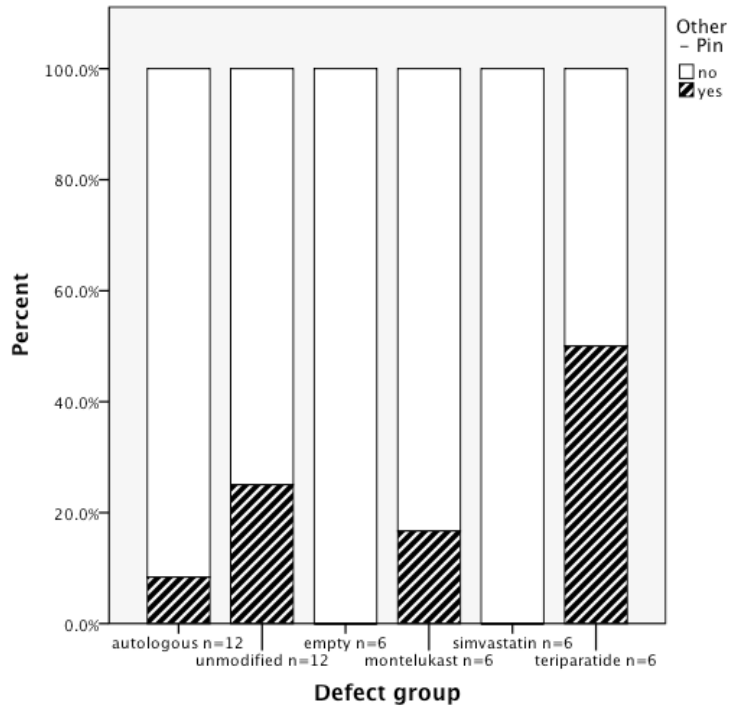

Figure 46: Qualitative histology - Other - Pin

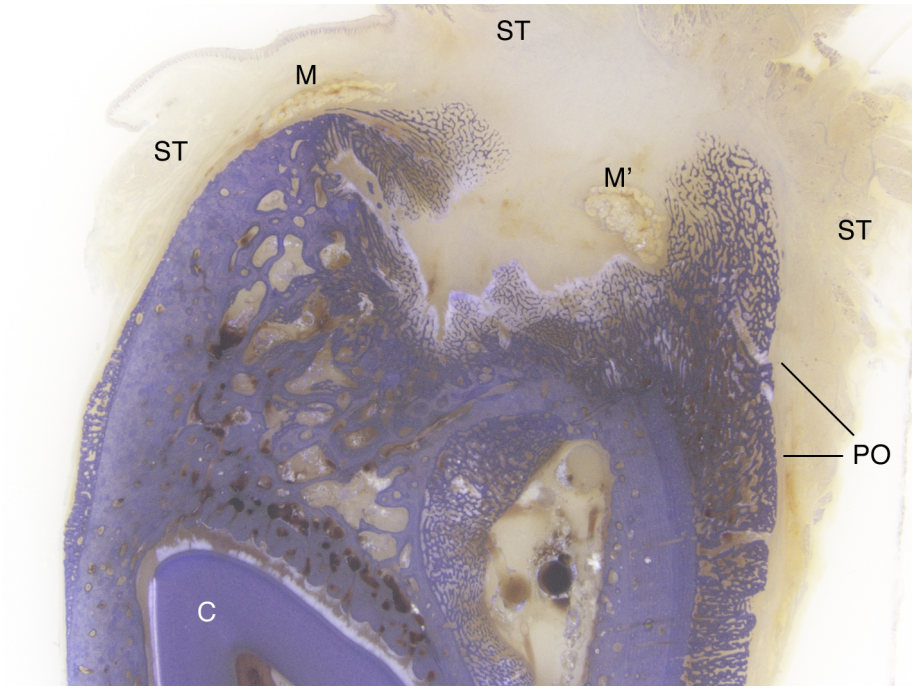

Figure 47: Histologic thick section, toluidine blue surface staining, Empty group

Histologic PMMA-thick section, toluidine blue surface staining, Empty group; center of the defect, perpendicular to the mandible; animal 23.14, left mandible, mesial defect. Defect not closed, autologous ingrowth from all sides of the defect; membrane visible as slope-ladder-shaped translucent structure on lingual cortex (M) and partly in defect center (M'); periosteal outgrowth reaction of buccal cortex (PO); root of canine tooth (C); soft tissue (ST)

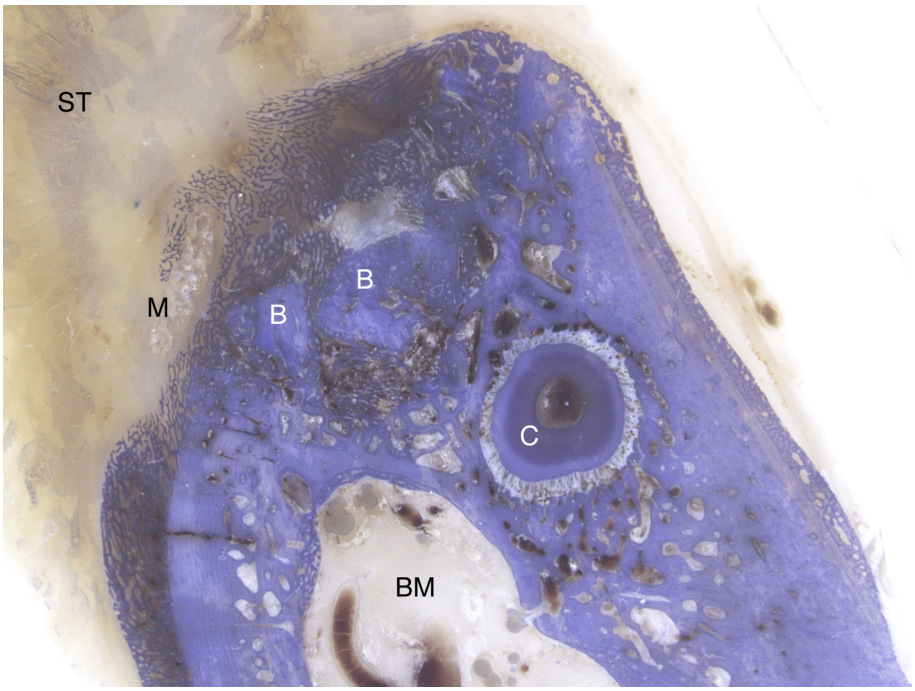

Figure 48: Histologic thick section, toluidine blue surface staining, Autologous group

Histologic PMMA-thick section, toluidine blue surface staining, Autologous group; center of the defect, perpendicular to the mandible; animal 23.04, right mandible, mesial defect. Defect is closed; membrane visible as translucent slope-ladder-structure on lingual cortex and on defect (M), interrupted, no full coverage of defect; moderate periosteal outgrowth reaction of buccal cortex (PO), slight reaction of lingual cortex; defect volume conserved; in the defect areas with bone of lamellar quality (B), woven bone inbetween; root of canine tooth (C); soft tissue (ST), bone marrow (BM)

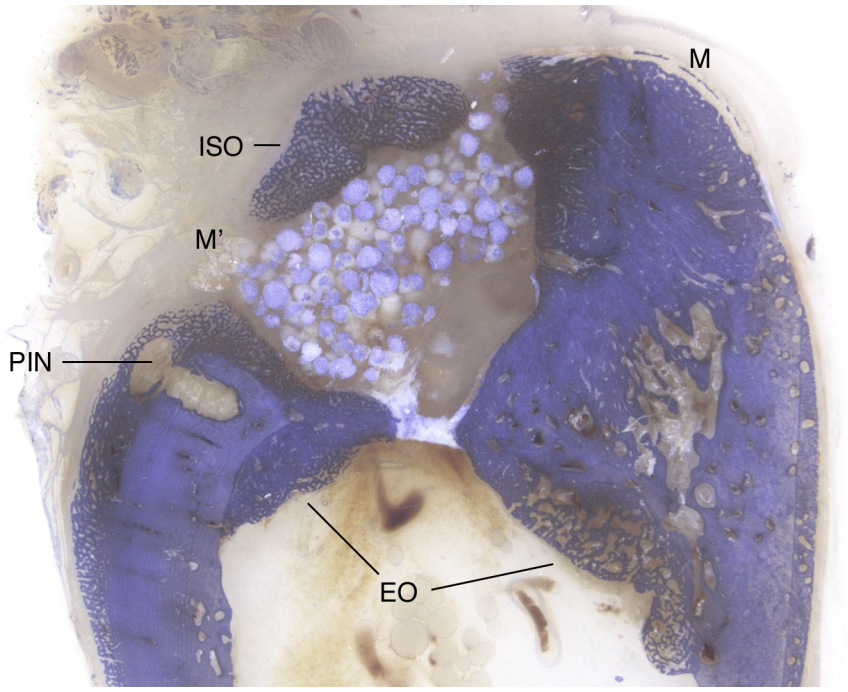

Figure 49: Histologic thick section, toluidine blue surface staining, Unmodified group

Histologic PMMA-thick section, toluidine blue surface staining, Unmodified group; center of the defect, perpendicular to the mandible; animal 23.04, right mandible, distal defect. Isolated structure of woven bone quality above defect (ISO); membrane visible as translucent slope-ladder-structure (M, M'); Inion GTR™ tack (PIN); moderate periosteal outgrowth reaction of buccal cortex, prominent endosteal reaction near defect (EO)

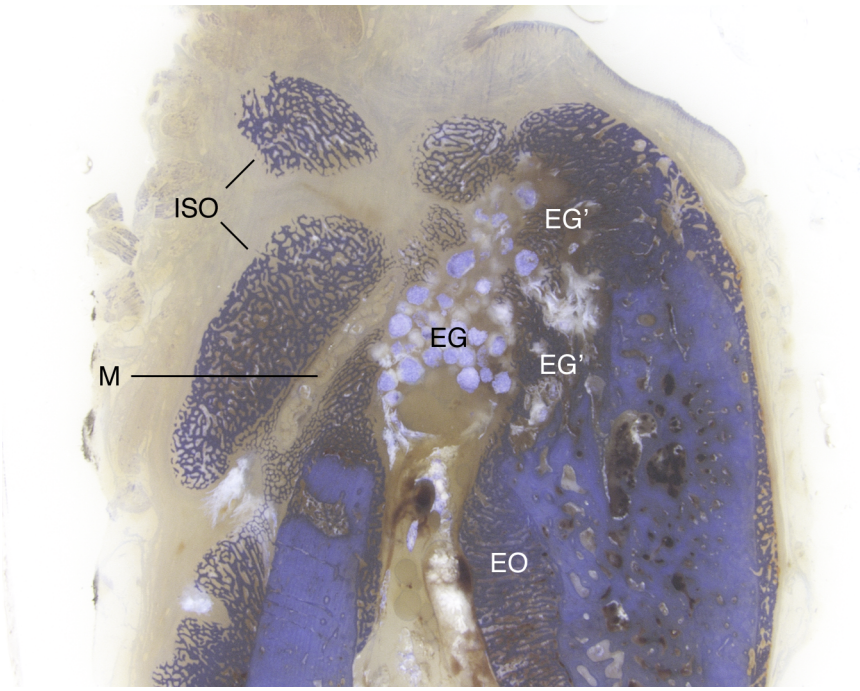

Figure 50: Histologic thick section, toluidine blue surface staining, Unmodified group

Histologic PMMA-thick section, toluidine blue surface staining, Unmodified group; center of the defect, perpendicular to the mandible; animal 23.13, right mandible, mesial defect. Defect is closed; biomaterial residues visible in defect (EG), partly and fully engulfed residues at margin of defect (EG'); membrane as translucent slope-ladder-structure visible at buccal side of defect (M), overgrown by isolated bone structures (ISO); prominent endosteal growth reaction (EO)

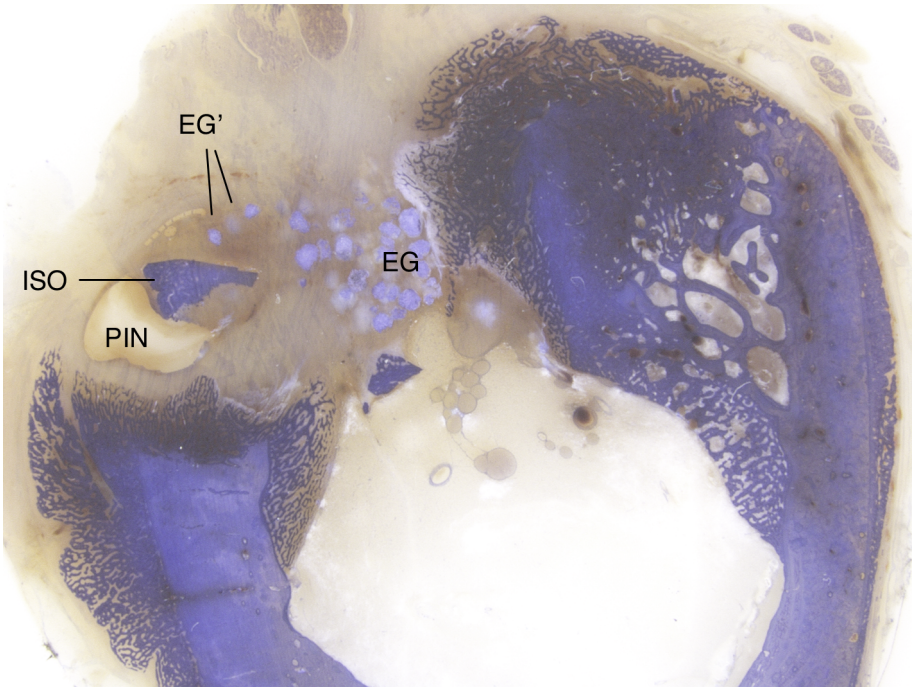

Figure 51: Histologic thick section, toluidine blue surface staining, Montelukast group

Histologic PMMA-thick section, toluidine blue surface staining, Montelukast group; center of the defect, perpendicular to the mandible; animal 23.06, right mandible, distal defect. Residues are visible in the center of the defect (EG) and in the surrounding tissue (EG'); translucent, fungi-shaped structure at buccal osteotomy site identified as Inion GTR™ tack (PIN), next to bony structure of lamellar quality (ISO)

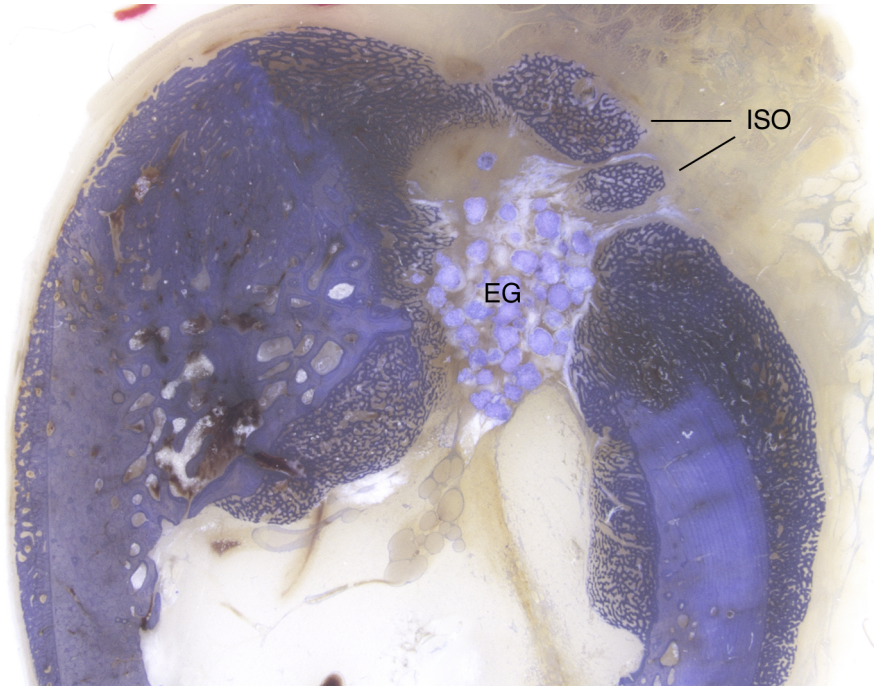

Figure 52: Histologic thick section, toluidine blue surface staining, Montelukast group

Histologic PMMA-thick section, toluidine blue surface staining, Montelukast group; center of the defect, perpendicular to the mandible; animal 23.04, left mandible, distal defect. Defect partly closed at periosteal closure site by two, isolated bony structures of woven bone quality (ISO); defect partly filled with residues in matrix, no bone ingrowth (EG); membrane not visible; prominent periosteal and endosteal reaction

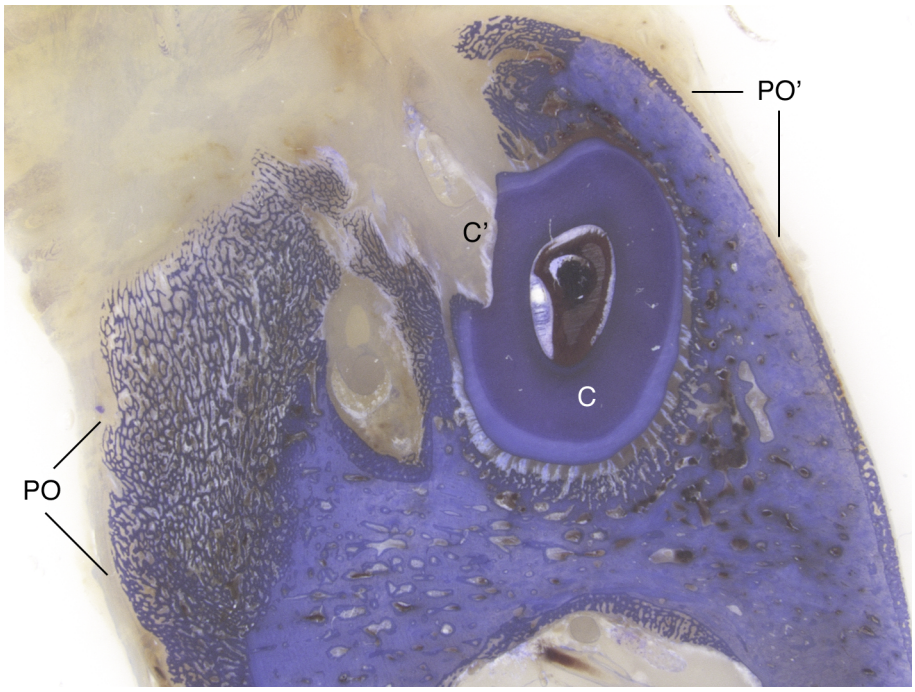

Figure 53: Histologic thick section, toluidine blue surface staining, Simvastatin group

Histologic PMMA-thick section, toluidine blue surface staining, Simvastatin group; center of the defect, perpendicular to the mandible; animal 23.09, right mandible, mesial defect. Canine root (C) with osteotomy site (C'), no new bone formation is seen in this part of the defect; endosteal reaction adjacent to the defect; periosteal outgrowth reaction more prominent at buccal cortex (PO) than lingual (PO'); no visible biomaterial residues; no visible membrane

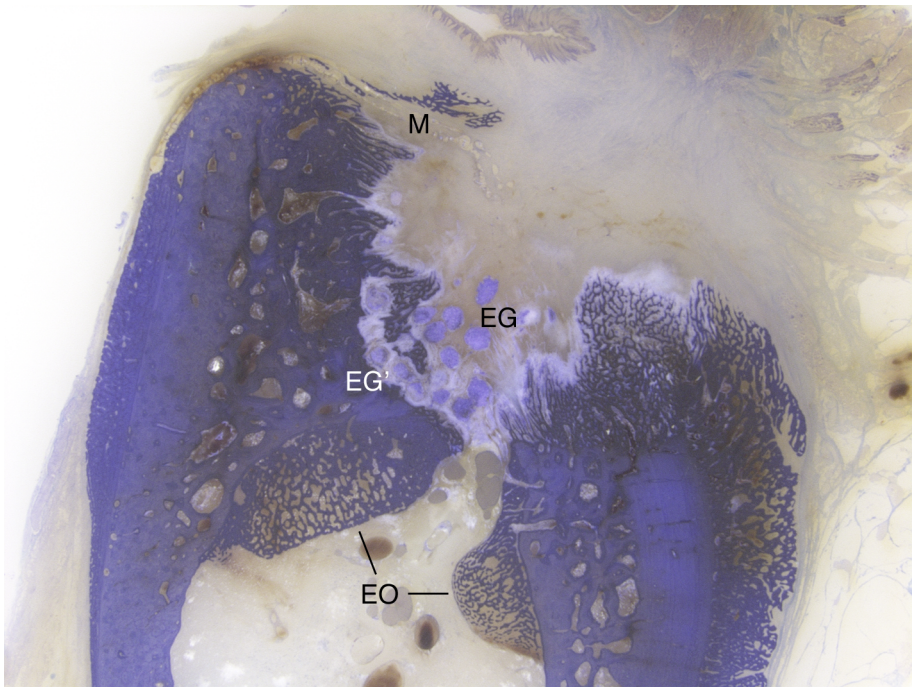

Figure 54: Histologic thick section, toluidine blue surface staining, Simvastatin group

Histologic PMMA-thick section, toluidine blue surface staining, Simvastatin group; center of the defect, perpendicular to the mandible; animal 23.07, left mandible, distal defect. Membrane visible as translucent, rope-ladder-shaped structure coming from lingual cortex to defect center, partly degraded, showing bone in- and overgrowth; biomaterial residues surrounded by matrix in the defect center (EG), partly engulfed by bone near lingual defect wall (EG'); membrane as translucent slope-ladder-structure (M); prominent endosteal reaction with bone growth near defect (EO)

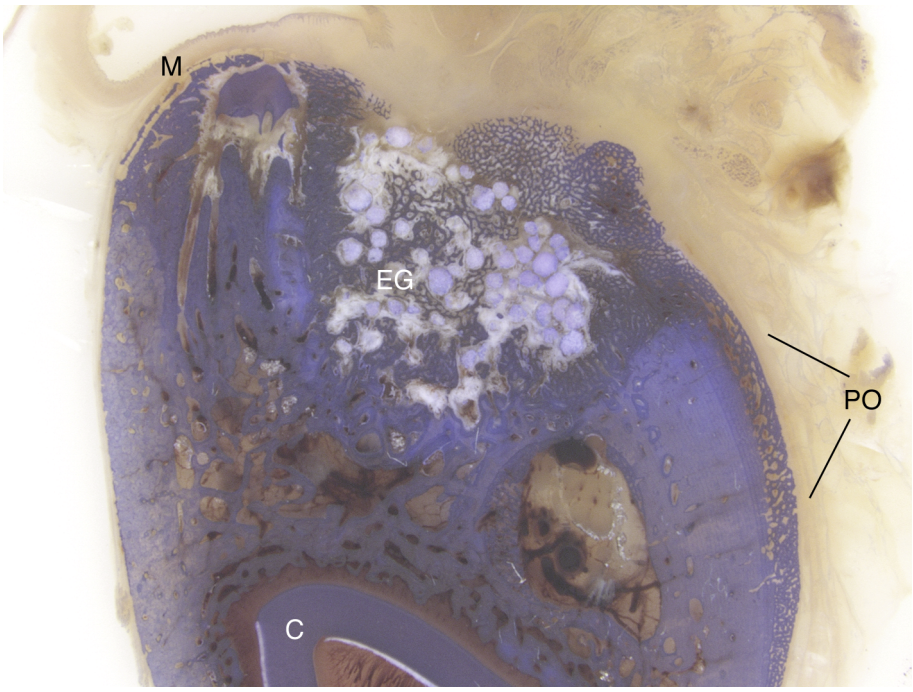

Figure 55: Histologic thick section, toluidine blue surface staining, Teriparatide group

Histologic PMMA-thick section, toluidine blue surface staining, Teriparatide group; center of the defect, perpendicular to the mandible; animal 23.11, left mandible, distal defect. Defect filled with residues, partly or fully engulfed with bone (EG); slight periosteal outgrowth reaction of buccal cortex (PO); translucent slope-ladder-shape of membrane visible at lingual cortex with bone ingrowth (M), but no coverage and none on buccal cortex; canine tooth (C)

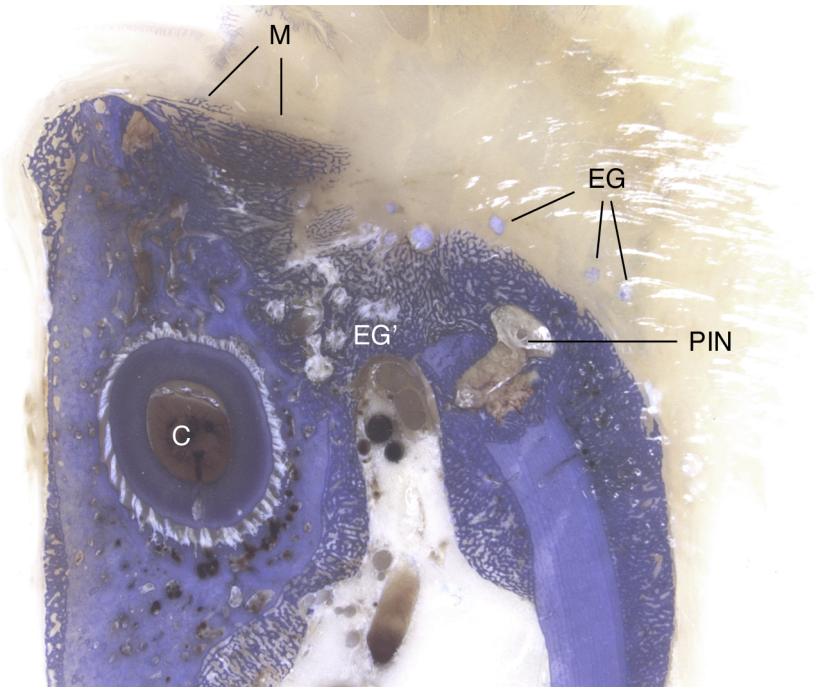

Figure 56: Histologic thick section, toluidine blue surface staining, Teriparatide group

Histologic PMMA-thick section, toluidine blue surface staining, Teriparatide group; center of the defect, perpendicular to the mandible; animal 23.03, left mandible, mesial defect. Residues in soft tissue (EG), in defect base partially and fully engulfed (EG'); Inion GTR™ tack surrounded by new bone growth (PIN); translucent slope-ladder-structure of membrane (M) but no defect coverage; prominent periosteal outgrowth reaction of buccal and lingual cortex; prominent endosteal reaction with bone growth near defect; root of canine tooth (C)

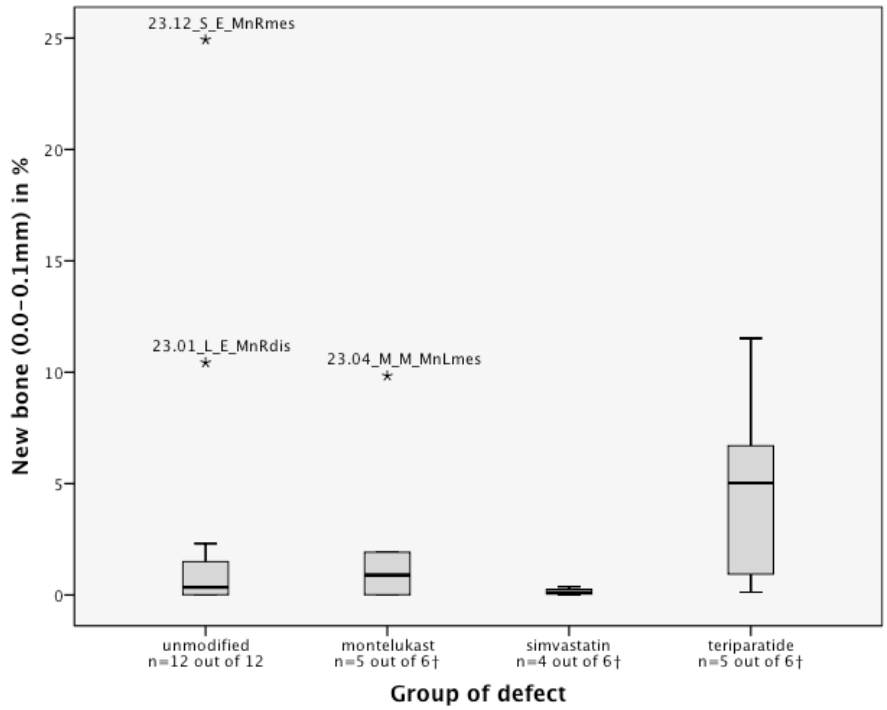

Figure 57: Histomorphometry - New bone formation in 0.0 - 0.1 mm perimeter around biomaterial residues in %

23.12_S_E_MnRmes: animal 23.12, right mandible, mesial defect, defect group Unmodified, animal group Simvastatin;
23.01_L_E_MnRdis: animal 23.01, right mandible, distal defect, defect group Unmodified, animal group Empty;
23.04_M_M_MnLmes: animal 23.04, left mandible, mesial defect, defect group Montelukast, animal group Montelukast
*: far outliers (extreme values outside of tripled interquartile range)
†: see 3.6 Histomorphometry and Table 10 for exclusion criteria

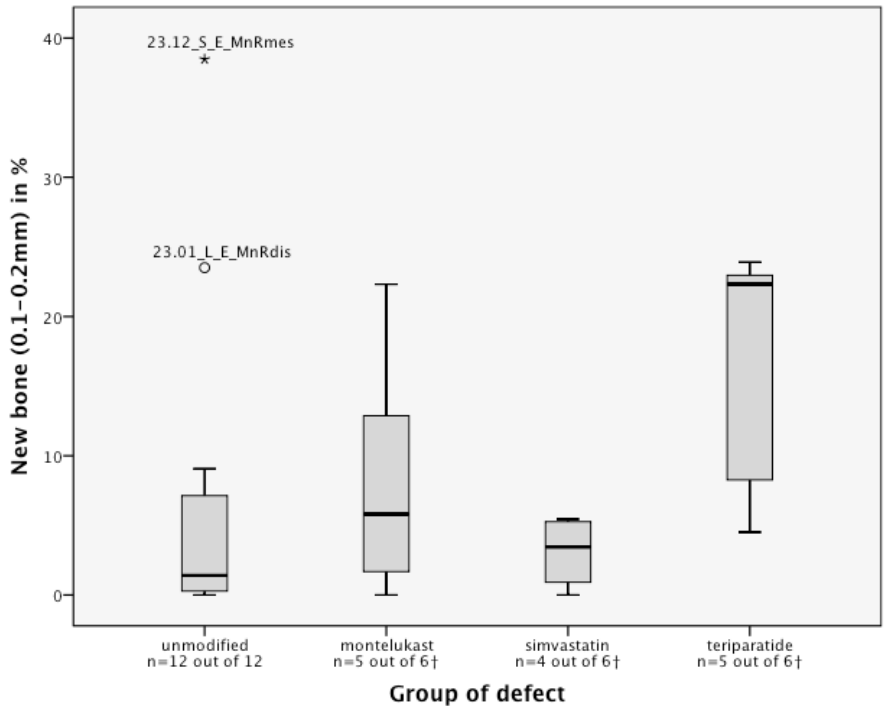

Figure 58: Histomorphometry - New bone formation in 0.1 - 0.2 mm perimeter around biomaterial residues in %

23.12_S_E_MnRmes: animal 23.12, right mandible, mesial defect, defect group Unmodified, animal group Simvastatin;
23.01_L_E_MnRdis: animal 23.01, right mandible, distal defect, defect group Unmodified, animal group Empty
o: outlier (within 1.5x interquartile range); *: far outlier (extreme value outside of tripled interquartile range)
†: see 3.6 Histomorphometry and Table 10 for exclusion criteria

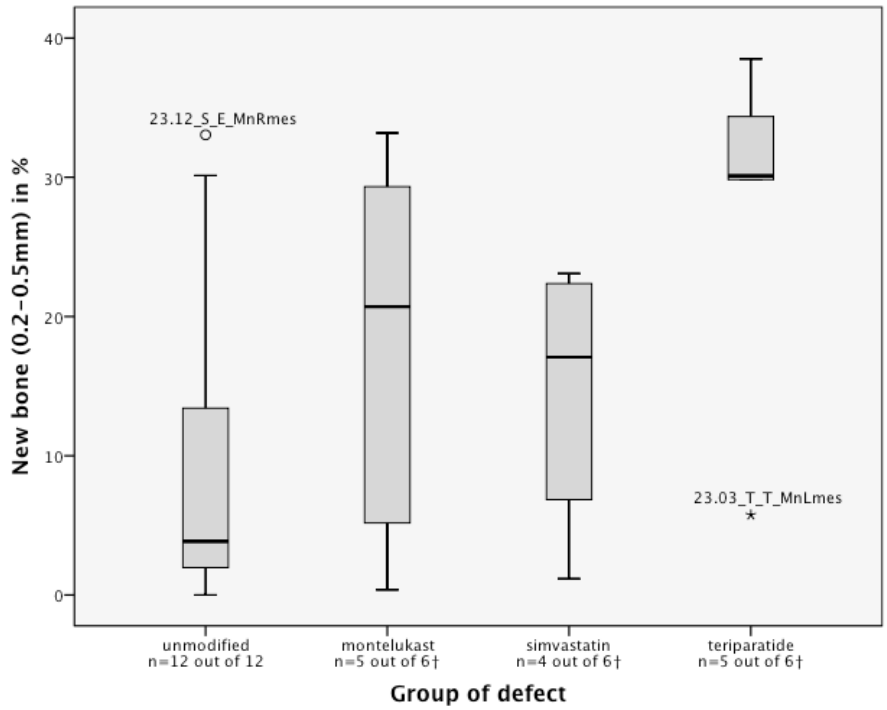

Figure 59: Histomorphometry - New bone formation in 0.2 - 0.5 mm perimeter around biomaterial residues in %

23.12_S_E_MnRmes: animal 23.12, right mandible, mesial defect, defect group Unmodified, animal group Simvastatin;
23.03_T_T_MnLmes: animal 23.03, left mandible, mesial defect, defect group Teriparatide, animal group Teriparatide
o: outlier (within 1.5x interquartile range); *: far outlier (extreme value outside of tripled interquartile range)
†: see 3.6 Histomorphometry and Table 10 for exclusion criteria

Acknowledgement

I gratefully thank Prof. Dr. med. vet. Brigitte von Rechenberg for being a role model and for her constant help and support, PD Dr. med. dent. Stefan Stübinger for his excellent supervision and scientific reasoning. Their impact shall accompany me for the rest of my life.

Prof. Dr. V. Luginbühl for the co-supervision and useful feedback. S. Pfundstein, L. Gegner, L. Müller, A. Solecki, V. Reichle, M. Stempel-Estelmann, M. Benn, S. Schöberl, M. Sidler, A. Drechsler, J. Plihal, N. Saddedine, A. Karol and others which worked with me at MSRU for the camaraderie and everyday help. L. Gegner additionally for her kind introduction to the MSRU life and doctoral work in general. L. Ettinger, K. Kämpf, K. Zlinsky, A. Waddington and S. Wunderlin for their great work and support on the histology. K. Kämpf additionally for her constant effort to keep things running smoothly. A. Grob for her work in histomorphometry and beyond. P. Kronen, I. Iff and their team for anesthesia and competent postoperative care. E. Bürgi for medical supervision of the animals. S. Koch and I. Wüthrich for educating and continuous working with me on principles of Good Labaratory Practice. K. Klein, K. Nuss and F. Clement Frey for their support and scientific supervision during daily work life. S. Darwiche for proof-reading and improving my command of the English language. P. Hänseler, M. Köhli, R. Schneebeli and L. Pfister for managing the project on the industrial side. M. Bless, R. Kissling and J. Nauer for their perioperative help. G. Schmid and N. Kramer for keeping things running on the backside of MSRU.

And last and not least but foremost, the 14 minipigs which gave their life as experimental animals and S. Ressegatti which always took such great care of them.

Curriculum Vitae

Name	Ramon Bucher
Birthdate	07.08.1982
Birthplace	Sursee, Luzern
Nationality	Swiss
Hometown	Escholzmatt-Marbach, Luzern

1989 - 1995	Primary schools Gunzwil and St. Erhard
1995 - 2002	Kantonsschule Sursee, Matura type Economy
2002 - 2004	University of Luzern, Bachelor of Law (no degree)
2004 - 2012	University of Veterinary Medicine Vienna, Austria, Mag. med. vet.
2005 - 2006	Universidad de Zaragoza, Spain, Erasmus exchange
2012 - 2014	University of Zürich, Musculoskeletal Research Unit, Dr. med. vet.